

Beyond Standard Model Physics

New Technicolor Models

Master Thesis

Sven Bjarke Gudnason

Academic Advisor:
Francesco Sannino

The Niels Bohr Institute
Blegdamsvej 17
DK-2100 Copenhagen Ø

University of Copenhagen

September 10, 2006

Abstract

In this master thesis we consider the problems of beyond standard model physics, especially the electroweak symmetry breaking and the naturalness problem of the standard model. We motivate that experiments (e.g. the LHC) will find new physics if unitarity in the partial wave amplitudes of WW scattering holds. We then consider technicolor models and in depth the case of the techniquarks transforming under higher dimensional representations of the gauge group, in particular the two-index symmetric representation of $SU(2)$. Effective theories are constructed and signatures are considered. Next considerations on cosmological implications for the model is made and a dark matter candidate, which is a technibaryon and a Goldstone boson with a conserved (techni)baryon number, is expected to contribute a relic abundance. By applying earth based direct search limits we are able to tell what percentage of dark matter the candidate can constitute. Finally the topic unification is considered and it is found that the model in question unifies far better than the standard model per se. We conclude by suggesting future directions.

Resumé

I dette speciale kigger vi på problemerne i udvidelserne af standard modellen, specielt det elektrosvage symmetribrud og naturlighedsproblemet i standard modellen. Vi motiverer, at hvis unitaritet i delvise bølge amplituder i WW stød holder, så vil eksperimenter (fx. LHC) finde ny fysik. Vi undersøger technicolor modeller og tilfældet, hvor techniquarkene transformerer under højere dimensionale repræsentationer af gauge gruppen, specielt den to-index symmetriske repræsentation af $SU(2)$, i dybden. Effektive teorier bliver konstrueret og signaturer bliver undersøgt. Derefter undersøges implikationerne af mørkt stof for modellen og en mørk stof kandidat, som er en technibaryon og samtidig en Goldstone boson med et bevaret (techni)baryon nummer, konstrueres og vi forventer at den bidrager til det oprindelige overskud. Ved at anvende grænser fra jordbaserede direkte undersøgelseseksperimenter er vi i stand til at forudsige hvad procentdelen af det mørke stof, som vores kandidat partikel vil udgøre, ville være. Endeligt bliver emnet *forening af gauge kræfter* undersøgt og vi finder ud af at modellen forener sine kræfter langt bedre end standard modellen alene. Vi afslutter derefter ved at forslå hvad de fremtidige emner kunne være.

Preface

This thesis is a final dissertation for my master degree at the Niels Bohr Institute, University of Copenhagen with Francesco Sannino as academic advisor. Part of the thesis is reviewing beyond standard model physics and cosmological implications, and part of the thesis is describing new work, done in collaboration with Chris Kouvaris and Francesco Sannino, which is also presented in the following articles [1, 2]. The published parts include the effective theories for the $SU(2)$ -Adj. model and the dark matter computations.

Acknowledgements

I would first of all like to thank my advisor Francesco Sannino for helpful and enlightening discussions, guidance and fruitful collaboration; also Chris Kouvaris for helpful discussions and collaboration. Someone else I especially would like to thank is Stefano Bolognesi, who has been helpful with his great theoretical insight and for many inspiring discussions. In general, I would like to thank the whole group of phenomenology and also Konstantin Petrov for always giving great critique for everything and my talks. Somebody who is also closely connected to the group is Dennis Dietrich. Thanks to him for useful discussions, help and also for careful corrections of drafts in general. Also thanks to my office mates Mads T. Frandsen, Victoria Mazo and Thomas Rytov for discussions and cheering me up. Finally I would like to thank my family and friends for great support.

Sven Bjarke Gudnason

Copenhagen Ø, August 2006.

Contents

Abstract	i
Resumé	ii
Preface	iii
Acknowledgements	iii
List of Figures	vii
List of Tables	xi
1 Introduction	1
1.1 Electroweak Symmetry Breaking	2
1.2 The Naturalness Problem	3
1.3 Triviality	4
1.4 Fermion Masses	5
2 Technicolor	7
2.1 Introduction	7
2.1.1 Fermion Masses and Flavor Symmetry Breaking	10
2.1.2 Oblique Parameters	13
2.1.3 Walking Technicolor	16
2.1.4 The Problems with Technicolor	18
2.2 The Sannino-Tuominen Model	18
2.2.1 The Composite Higgs Mass	21
2.3 The $SU(2)$ -Adj. Model	22
2.3.1 Spectrum	27
2.3.2 EWPD	27
2.3.3 Effective Theories	27
2.3.4 Feynman Rules	32
2.3.5 Minimal Coupling to Fermions	34
2.3.6 Signatures	36
3 Dark Matter	37
3.1 Introduction	37
3.2 Computing the LTB Relic Density.	42
3.2.1 2nd Order Phase Transition	48
3.2.2 1st Order Phase Transition	50
3.3 Detection of the Neutral Technibaryon	50

3.4	Check of Thermal Equilibrium	55
4	Unification	59
4.1	One Loop β -function Computation	59
5	Competing Models	65
6	Conclusions and Outlook	67
A	Conventions and Identities	I
A.1	Identities for the Weinberg Angle	I
A.2	Properties for Unitary Groups	II
A.3	Measured Electroweak Data	II
B	Generators	III
C	Feynman Rules for the $SU(2)$-Adj. Model	V
	Bibliography	XIX

List of Figures

1.1	Diagram of $W_L W_L$ scattering (fusion) which is an interesting probe of <i>new</i> physics at the electroweak scale.	3
2.1	Technicolor condensation by techni-gluon exchange in the spin zero, isospin zero channel.	9
2.2	(a) ETC diagram with gauge boson interacting with both techniquarks and SM fermions. (b) Diagram giving masses to SM fermions when technicolor condenses.	10
2.3	Breaking of the “toy” ETC group in 3 stages down to the TC gauge group providing three different mass scales.	11
2.4	Diagram contributing to mass of pseudo Goldstone bosons via an exchange of an ETC gauge boson inside the fermion loop.	13
2.5	Result of fit of electroweak precision data. The contour curve is the 68% CL in the (S,T)-plane with central value (0.07,0.13). The bands are ± 1 sigma on the measurements of Γ_U, M_W and $\sin^2 \theta_{\text{eff}}^{\text{lepton}}$. The banana shaped region corresponds to the SM prediction with a top mass $m_t = 178 \pm 4.3$ GeV and Higgs mass $m_h = 300_{-186}^{+700}$ GeV. The plot is taken from Ref. [3].	15
2.6	Rainbow approximation for the technifermion self energy function. The boson is a technigluon.	16
2.7	Phase diagram of number of Dirac flavors N_f vs. number of technicolors N_{TC} for two-index symmetric (a) and antisymmetric (b) representations of the gauge group. The graphs are taken from Ref. [4]	20
2.8	Important diagrams that need to be considered in order to write down an anomaly free theory. In (a) the $U(1)$ hypercharge gauge boson and two technigluons are connected via a triangle of fermions. In (b) the $U(1)$ meets two electroweak gauge bosons and in (c) it is just three $U(1)$ gauge bosons. Finally (d) is the triangle with two gravitons and a single $U(1)$ gauge boson.	24
2.9	(S, T) diagram showing the regions the $SU(2)$ -Adj. model can span with the masses of the new leptons ν_ζ and ζ taking on values from M_Z to $10M_Z$. The ellipsis represent the one sigma contour of the global fit to the EWPD with a reference Higgs mass of 150 GeV. The figure is taken from Ref. [5].	28
2.10	Diagrams showing possible production of a charged technibaryon, e.g. the UD state in a pp experiment like the LHC. In (a) WW fusion creates a Z which decays to a technibaryon and an anti-technibaryon. In (b) two photons couple to a technibaryon.	36

3.1	Synthetic rotation curve for galaxies with $\langle M_I \rangle = -21.2$, where $\langle M_I \rangle$ is a measure for the luminosity, R/R_{opt} is the distance measured from the center of the galaxy normalized by the optical radius and V is the velocity. The figure is taken from Ref. [6].	38
3.2	Power in the CMB anisotropy spectrum measured by WMAP and others. The figure is taken from Ref. [7].	39
3.3	Phase space of $(\Omega_m, \Omega_\Lambda)$ with WMAP and additional data. The figure is taken from Ref. [8].	41
3.4	Triangle diagram giving rise to the anomaly that breaks e.g. the baryon number or the lepton number for $i = B, L$ respectively. The two bosons are the gauge bosons of the $SU(2)_L$ group. The particles looping in the triangle are left-handed particles with charge i	43
3.5	Plot representing the region of the parameters according to which the fraction of technibaryon matter density over the baryonic one takes on the values [3.23, 5.55]. We consider here a second order phase transition. The parameters in the plot are the mass of the LTB dark matter particle and ξ of Eq. (3.49). The plot includes various values of T^* . The dotted line separates areas of abundant particles and anti-particles.	49
3.6	Amount of LTB dark matter as function of the mass of the LTB particle. The plot is shown for $L' = 0$ and $L = B$, for second order (SO) phase transitions with various temperatures T^* and a for first order (FO) phase transition as well.	51
3.7	Plot representing the region of the parameters according to which the fraction of technibaryon matter density over the baryonic one takes on the values [3.23, 5.55]. Here we consider the case of a first order phase transition. The parameters in the plot are the mass of the LTB dark matter particle and ξ of Eq. (3.52). The dotted line separates areas of abundant particles and anti-particles.	51
3.8	<i>Top Panel:</i> The maximal fraction of local DM density allowed by the 90% experimental constraint as function of the local DM density and the parameter ξ of Eq. (3.49). <i>Bottom Panel:</i> For the corresponding maximal fraction of local DM density currently allowed by the 90% experimental constraint as function of the local DM density and ξ , we plot the associated LTB mass. Both plots are presented with a second order phase transition with $T^* = 250$ GeV and a recoil energy $T = 50$ keV.	54
3.9	<i>Top Panel:</i> The maximal fraction of local DM density allowed by the 90% experimental constraint as function of the recoil energy measurable by the detector and the parameter ξ of Eq. (3.49). <i>Bottom Panel:</i> For the corresponding maximal fraction of local DM density currently allowed by the 90% experimental constraint as function of the recoil energy measurable by the detector and ξ , we plot the associated LTB mass. Both plots are presented with a second order phase transition with $T^* = 250$ GeV, a recoil energy $T = 50$ keV and $\rho_{DM} = 0.3$ GeV/cm ³	56
3.10	Freeze out temperature for the LTB particle as function of its mass. The filled area corresponds to the particles out of equilibrium.	57
4.1	Extrapolation of the gauge couplings in the SM. A trend of unification is observed, but it is far from exact.	64

-
- 4.2 Extrapolation of the gauge couplings in the $SU(2)$ -Adj. model. It is seen that the gauge couplings of the SM do almost unify (but as calculated above, it is still not exact, but far better than in the pure SM case). The gauge coupling value of the techniforce at the Z mass is taken to be the critical coupling of Eq. (2.46). 64

List of Tables

2.1	Quantum numbers for a “toy” ETC model.	11
2.2	Summary of the properties of the $SU(2)$ -Adj. model.	22
2.3	Quantum numbers for the $SU(2)$ -Adj. model.	25
3.1	Fitted parameters from WMAP data [8].	40

CHAPTER 1

Introduction

The Standard Model (SM) that up to now successfully describes most of all experiments in high energy particle physics to great precision (e.g. LEP II at CERN) is the following gauge theory

$$SU(3)_c \times SU(2)_L \times U(1)_Y , \quad (1.1)$$

which is the direct product of the gauge groups of the color force, the weak force and the hypercharge, respectively.

Phenomenologically it is known that the low energy gauge symmetry is just

$$SU(3)_c \times U(1)_{em} , \quad (1.2)$$

where only the strong force and electromagnetism are present. So a symmetry breaking has to occur at some energy scale (the electroweak scale $\Lambda_{ew} \sim 246$ GeV).

In the SM the Higgs mechanism is used to spontaneously break the electroweak symmetry down to that of electromagnetism and at the same time provide mass terms for the fermions through Yukawa couplings to the neutral Higgs field. An introduction to the Higgs mechanism can be found in many places in the literature, e.g. in Peskin and Schroeder [9] and in Ref. [10].

First we will motivate the study of the electroweak symmetry breaking by general arguments that model independently states, why we can expect to gain knowledge on this field by imminent experiments such as the Large Hadron Collider (LHC) at CERN and the International Linear Collider (ILC). Then we will motivate why the SM is theoretically unsatisfactory and how this leads to e.g. technicolor. This includes the naturalness problem and the triviality problem, which we will explain shortly.

In the next chapter we will briefly introduce technicolor and its extension, extended technicolor (ETC) and then explain, what are the problems with the traditional QCD-like technicolor and finally how we can resolve some of the problems via higher dimensional representations of the technicolor gauge group. We will then make effective theories of the technicolor model which will be, in a phenomenological sense, the most attractive (in the class we will consider) and these effective theories can then be used for computations at low energy. Then we will compute the associated Feynman rules for the linearly realized effective theory.

In Chapter 3, we will first make a brief introduction to dark matter and then make the calculation of the relic density of a specific dark matter candidate from the technicolor model we investigate in depth. Using that we have a conserved technibaryon number and that the particle is only weakly interacting, together with the experimental

limits from earth based dark matter search experiments, we can predict what is the relic abundance, in percent of the measured dark matter density, and what is the mass of our particle.

In Chapter 4, we consider the interesting topic of unification of the SM gauge forces and investigate what is the impact of the new technicolor gauge force on the SM gauge forces.

In Chapter 5, we briefly mention the ongoing research in competing models in technicolor theories, but also refer to the literature for other types of models, e.g. supersymmetric models and little Higgs models.

Finally, we conclude by a summary and present an outlook of where to go next.

1.1 Electroweak Symmetry Breaking

It is possible to estimate at what scale *new physics* has to set in, using unitarity. In the literature there are several ways to do this.

One way to go is to use the equivalence theorem [11, 12, 13]. In words it says that the Higgs mechanism transmutes the Goldstone bosons, coming from the electroweak symmetry breaking ($SU(2)_L \times U(1)_Y \rightarrow U(1)_{em}$), which we here will denote by Π^\pm and Π^0 , into the longitudinal gauge boson modes W_L^\pm and Z_L .¹ This is seen by performing a gauge transformation into the unitary gauge. In equations it relates the physical S-matrix amplitudes involving W_L^\pm and Z_L to amplitudes with Π^\pm and Π^0

$$M(W_L^\pm(p_1), W_L^\pm(p_2), \dots) = M(\Pi^\pm(p_1), \Pi^\pm(p_2), \dots)_{R_\xi} + \mathcal{O}\left(\frac{M_W}{E}\right), \quad (1.3)$$

where E is the center-of-mass energy and the right-hand-side (rhs) of the above equation is in the generalized R_ξ gauge and does in general depend on the ξ gauge parameter to order M_W/E .

Analogously to the pion scattering low-energy theorems, where it is known that

$$M(\pi^+\pi^- \rightarrow \pi^0\pi^0) = \frac{s}{F_\pi^2}, \quad (1.4)$$

it can be shown by a method similar to the current-algebra derivation of the pion amplitude that [14]

$$M(\Pi^+\Pi^- \rightarrow \Pi^0\Pi^0) = \frac{s}{\rho v_{\text{weak}}^2}, \quad (1.5)$$

where

$$\rho \equiv \frac{M_W^2}{M_Z^2 \cos^2 \theta_w}, \quad (1.6)$$

is equal to one in the minimal Higgs model and is preserved at tree-level, if the ‘‘Higgs sector’’ has custodial symmetry (where it is understood that by Higgs sector is meant whatever theory is underlying/replacing the Higgs mechanism). Using Eq. (1.3) yields

$$M(W_L^+W_L^- \rightarrow Z_L Z_L) = \frac{s}{\rho v_{\text{weak}}^2}. \quad (1.7)$$

By considering the partial-wave projection $J = 0$ of the amplitude (1.7) one finds

$$|a_0(W_L^+W_L^- \rightarrow Z_L Z_L)| = \frac{s}{16\pi v_{\text{weak}}^2} = \frac{sG_F}{8\sqrt{2}\pi}, \quad (1.8)$$

¹The index L denotes the longitudinal mode

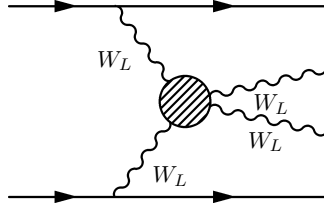


Figure 1.1: Diagram of $W_L W_L$ scattering (fusion) which is an interesting probe of *new* physics at the electroweak scale.

where G_F is the Fermi constant. By the condition of partial-wave unitarity

$$|a_J(s)| \leq 1, \quad (1.9)$$

the scale for which unitarity is violated, is

$$\Lambda_{SB}^2 \leq \frac{8\sqrt{2}\pi}{G_F} \approx (1.7\text{TeV})^2. \quad (1.10)$$

A more careful analysis has been performed in the literature by Lee, Quigg, and Thacker [15, 16] where partial-wave unitarity in the four-channel system, consisting of $W_L^+ W_L^-$, $\frac{1}{\sqrt{2}} Z_L Z_L$, $\frac{1}{\sqrt{2}} H H$, and $H Z_L$, has to be obeyed. The result is

$$\Lambda_{SB}^2 \leq \frac{8\sqrt{2}\pi}{3G_F} \approx (1.0\text{TeV})^2. \quad (1.11)$$

It is interesting to note, that information about the symmetry breaking sector is to be found by considering $W_L W_L$ -scattering (see Fig. 1.1) because the longitudinal modes of the gauge bosons are exactly part of the new physics which breaks the electroweak symmetry.

It is quite motivating, that the symmetry breaking mechanism can be probed with collider machines, such as the LHC and the ILC which can reach the TeV scale.

1.2 The Naturalness Problem

The hierarchy problem can be stated as the theoretical mystery that there are seventeen orders of magnitudes between the electroweak scale Λ_{ew} and the Planck scale Λ_{Planck} . This is no problem in the SM per se. The problem comes in via the naturalness of the Higgs boson.

There are various ways to define the naturalness problem. If we start by taking a look at the SM Higgs boson, its mass will acquire quantum corrections

$$\delta m_h^2 \propto \Lambda^2, \quad (1.12)$$

where Λ is the cut-off scale to which the theory is valid. Insisting that the SM holds until some large scale, e.g. some Grand Unified (GUT) Scale Λ_{GUT} or the Planck scale Λ_{Planck} , the correction of the mass is unnaturally large compared to the mass of the Higgs boson and the electroweak scale.

The fact that the Higgs boson is a fundamental scalar leads to, that there is no symmetry to “protect” the mass from these *additive* corrections. Setting the bare Higgs boson mass to zero will not eliminate the large corrections as it is the case with *multiplicative* corrections. Taking e.g. quantum electrodynamics (QED), the electron mass is protected by the chiral symmetry ($U(1)_L \times U(1)_R$) which will forbid the non-zero corrections. Such a symmetry is called a “custodial symmetry”.

It is interesting to note, that quantum chromodynamics (QCD) is natural per se, as the scale Λ_{QCD} is an intrinsic scale and the chiral symmetry of the fermions acts as custodial symmetry.

There are in general (at least) three exceptions where the Higgs boson is protected.

- 1 Composite scalars which first forms when the theory becomes strongly coupled and thus only would receive corrections of order of that scale.
- 2 Goldstone bosons which can have low masses due to the spontaneous broken chiral symmetry.
- 3 Supersymmetric scalars have fermionic partners that are protected by chiral symmetry. They are thus protected via their partners. Another way to see this naturalness is by computing the corrections for the Higgs boson and for its fermionic partner, the higgsino. One then finds, that the quadratic corrections cancel out and only logarithmic corrections are left. This is, however, only true in the case of unbroken supersymmetry which is not observed at low energy. The so-called soft breaking of supersymmetry is then required to be of the order of the electroweak scale in order to retain the naturalness.²

Models of type 2 (from above) are e.g. the Little Higgs models. Supersymmetric theories e.g. the minimal supersymmetric standard model (MSSM) are examples of type 3. Technicolor belongs to the solution of type 1 and will be further motivated in the next chapter.

The theories not of technicolor type will briefly be discussed/compared with technicolor in chapter 5.

1.3 Triviality

Another problem with the elementary Higgs boson is that the model is *trivial* [18, 19, 20]. The Higgs self-coupling $\lambda(\mu)$ of the minimal one-doublet Higgs boson model (i.e. used in the SM) at the energy μ is

$$\lambda(\mu) \sim \frac{\lambda(\Lambda_{\text{cutoff}})}{1 + \frac{24}{16\pi^2} \lambda(\mu) \log\left(\frac{\Lambda_{\text{cutoff}}}{\mu}\right)}, \quad (1.13)$$

where Λ_{cutoff} is the cutoff scale. The problem here is that the self-coupling vanishes for all μ when $\Lambda_{\text{cutoff}} \rightarrow \infty$ and thus the description of the Higgs boson is trivial. That has also been shown to hold for two-doublet Higgs models [21]. This triviality problem of the elementary Higgs boson means that it has to be considered an effective description valid at low energy (i.e. at scales lower than where *new physics* sets in). The larger the Higgs coupling is, the lower the scale Λ_{cutoff} has to be. This leads to

²Split Supersymmetry [17] claims to have much larger breaking scale but do also give up on the naturalness problem.

the so-called triviality bounds on the Higgs mass. For the minimal one-doublet Higgs model the bound is computed in Ref. [19] to be $m_h \lesssim 640\text{GeV}$.

This is another hint that the elementary Higgs boson is not the whole story, but might as well be a low energy effective description. The search for the underlying theory is then again motivated by the fact that new physics should be within the reach of the TeV scale and thus one of the next collider machines (LHC or ILC).

1.4 Fermion Masses

Compared to the symmetry breaking scale on which an upper limit can be put, it is not so easy to put constraints on where the mechanisms for generating fermion masses appear. Flavor physics is also a very interesting problem and solutions have been proposed in the context of extended technicolor, tumbling gauge theories. By flavor physics, we mean the problem of generating the mass textures and mixing angles etc. of the SM particles, as well as producing viable masses for all the new particles, introduced to the theory. This area of beyond-SM physics will not be the main emphasis in this thesis, though, and we will refer to the literature (see e.g. [22]). It is interesting to note that there is no explanation of the flavor symmetry breaking in the SM where only the top quark has an $\mathcal{O}(1)$ Yukawa coupling. Neither is there any enlightening information to gain on the flavor symmetry breaking in the popular supersymmetric models such as the MSSM.

CHAPTER 2

Technicolor

2.1 Introduction

Here we will only give a brief introduction to technicolor theories. There are many great reviews of technicolor in the literature e.g. that by Hill and Simmons [22] and Refs. [23, 24, 25, 26, 27]. Also interesting is the paper by Weinberg [28].

Following the basic idea of Farhi and Susskind [24] it is instructive to consider the SM without a Higgs sector. Naively one would think that the vector gauge bosons would remain massless and the gauge symmetry $SU(2)_L \times U(1)_Y$ unbroken. This is, however, not true as for the fact that quantum chromodynamics (QCD) will break the electroweak symmetry down to that of electromagnetism, $U(1)_{em}$ via spontaneous symmetry breaking of chiral symmetry. The symmetry breaking vacuum condensate is the scalar quark bilinear (considering here two-flavor QCD)

$$\langle \bar{u}_L u_R + \bar{d}_L d_R \rangle \neq 0 . \quad (2.1)$$

This happens due to the attractive exchange of gluons in the spin zero, isospin zero channel which causes condensation.

The result of the Higgs mechanism is this. The Higgs mechanism occurs and the pions are in the unitary gauge the longitudinal modes of the W^\pm and Z bosons. The masses would be

$$M_W = \frac{gF_\pi}{2} \sim 29\text{MeV} , \quad M_Z = \frac{M_W}{\cos \theta_W} , \quad (2.2)$$

which holds because of the isospin symmetry (which works as custodial symmetry).

We will now briefly show how the Higgs mechanism works. It can be understood via the vacuum polarization tensor

$$\Pi^{\mu\nu}(p) = - \int d^4x e^{-ipx} \langle T J_L^{+\mu}(x) J_L^{-\mu}(0) \rangle_0 , \quad (2.3)$$

where

$$J_L^{i\mu}(x) = \bar{\psi}_L(x) \frac{\tau^i}{2} \gamma^\mu \psi_L(x) , \quad (2.4)$$

is the weak current and

$$\psi_L = \begin{pmatrix} u \\ d \end{pmatrix}_L , \quad (2.5)$$

and τ the Pauli matrices and $\tau^+ = (\tau^-)^\dagger = \tau^1 + i\tau^2$.

The pion decay constant is defined by

$$\langle 0 | J_L^{+\mu} | \pi^-(p) \rangle = \frac{i}{\sqrt{2}} F_\pi p^\mu . \quad (2.6)$$

The pion pole contribution to Eq. (2.3) is

$$\Pi^{\mu\nu}(p) = -\frac{i}{p^2} p^\mu p^\nu \frac{F_\pi^2}{2} + \dots . \quad (2.7)$$

Gauge invariance of the polarization tensor implies that it can be written in terms of a single Lorentz scalar

$$\Pi^{\mu\nu}(p) = i(p^2 g^{\mu\nu} - p^\mu p^\nu) \Pi(p^2) , \quad (2.8)$$

and the Lorentz scalar then reads

$$\Pi(p^2) = \frac{F_\pi^2}{2p^2} + \dots . \quad (2.9)$$

The W propagator to leading order in Landau gauge is

$$D_0^{\mu\nu} = -i \left(g^{\mu\nu} - \frac{p^\mu p^\nu}{p^2} \right) \frac{1}{p^2} , \quad (2.10)$$

where the 0 refers to the propagator being leading order. To higher orders we need to sum the geometric series

$$D^{\mu\nu} = D_0^{\mu\nu} + \frac{1}{2} g^2 D_0^{\mu\alpha} \Pi_{\alpha\beta} D_0^{\beta\nu} + \frac{1}{2} g^2 D_0^{\mu\alpha} \Pi_{\alpha\beta} D_0^{\beta\gamma} \Pi_{\gamma\delta} D_0^{\delta\nu} + \dots \quad (2.11)$$

$$= -i \left(g^{\mu\nu} - \frac{p^\mu p^\nu}{p^2} \right) \frac{1}{p^2 \left(1 - \frac{1}{2} g^2 \Pi(p^2) \right)} . \quad (2.12)$$

Inserting Eq. (2.9) the full propagator reads

$$D^{\mu\nu} = -i \left(g^{\mu\nu} - \frac{p^\mu p^\nu}{p^2} \right) \frac{1}{p^2 - \frac{1}{4} g^2 F_\pi^2} , \quad (2.13)$$

and it is easily seen that the W -boson now has acquired a mass

$$M_W = \frac{1}{2} g F_\pi . \quad (2.14)$$

What we have shown is the Higgs mechanism: When a massless spin-zero particle couples to the gauge current a mass is generated for the associated gauge boson.

In QCD chiral symmetry breaking (CSB) is driven by this quark bilinear condensate and good high-energy behavior is assured by the $I = J = 0$ quark-antiquark continuum [29].

Comparing with the SM with one Higgs doublet the W mass is $\frac{1}{2} g v_{\text{weak}}$, where v_{weak} is the vacuum expectation value (VEV) of the Higgs boson. To make the theory produce the correct W mass consider an asymptotic free (confining) gauge theory with symmetry $SU(2)_L \times SU(2)_R$ which is broken down to $SU(2)_{L+R}$ by the bilinear

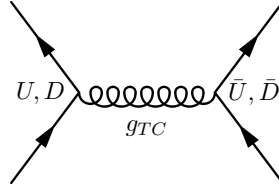


Figure 2.1: Technicolor condensation by techni-gluon exchange in the spin zero, isospin zero channel.

(techni-)quark condensate, see Fig. 2.1. We here imagine a theory which is the direct product of another $SU(N)$ gauge group (of technicolor) and the SM gauge groups

$$SU(N_{TC})_{TC} \times SU(3)_c \times SU(2)_L \times U(1)_Y . \quad (2.15)$$

If we force the gauge current which couples to the particle, equivalent to the pion, to be

$$F_\pi^{TC} = v_{\text{weak}} = 246 \text{ GeV} , \quad (2.16)$$

then the gauge bosons will acquire the correct (measured) masses. This is a very simple example of a technicolor model. It is simply a scaled-up version of QCD where the condensate equivalent to the QCD CSB condensate is used to break the electroweak symmetry at the correct scale.

In this type of QCD-like technicolor QCD results can be used to make estimates in the technicolor sector. These results are most reliable, though, if one considers the gauge group of type $SU(N_{TC})$ in the fundamental representation. In the large N_{TC} limit we can naively estimate masses of technimesons. The technicolor scale is estimated to be

$$\Lambda_{TC} \sim \sqrt{\frac{3}{N_{TC}} \frac{F_\pi^{TC}}{F_\pi}} \Lambda_{\text{QCD}} . \quad (2.17)$$

The reason why the ratio of number of colors from technicolor to QCD is reciprocal lies in the fact that the pion decay constant is proportional to the square root of “colors”

$$F \sim \sqrt{N_c} \Lambda . \quad (2.18)$$

From this, one can deduce that the meson masses from the QCD spectrum would scale like

$$M_{\text{technimeson}} \sim \sqrt{\frac{3}{N_{TC}} \frac{F_\pi^{TC}}{F_\pi}} M_{\text{QCD-meson}} , \quad (2.19)$$

where an example could be the techni- ρ from the QCD ρ meson.

The previous example of a QCD-like technicolor is just the simplest case. It is straightforward to generalize to a more complicated model. In fact, any strongly interacting gauge theory which has a chiral symmetry pattern $G \rightarrow H$, where G contains $SU(2)_L \times U(1)_Y$ and H contains $SU(2)_V \times U(1)_{em}$ and *not* $SU(2)_L \times U(1)_Y$, will break the electroweak interactions down to the electromagnetic one [27]. The reason why H should contain $SU(2)_V$, i.e. the custodial symmetry, is to satisfy the following relation for the ρ parameter at tree-level

$$\rho = \frac{M_W^2}{M_Z^2 \cos^2 \theta_w} = 1 . \quad (2.20)$$

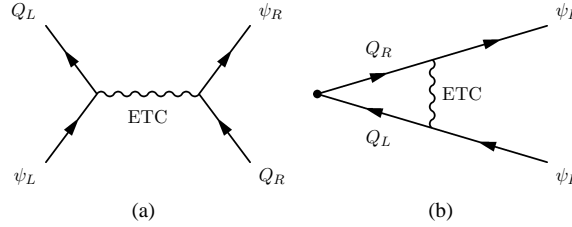


Figure 2.2: (a) ETC diagram with gauge boson interacting with both techniquarks and SM fermions. (b) Diagram giving masses to SM fermions when technicolor condenses.

2.1.1 Fermion Masses and Flavor Symmetry Breaking

In a sense the minimal Higgs model of the SM is very economical as it also provides fermion masses through Yukawa couplings of the type

$$-\Gamma_d^{ij} \bar{\Psi}_L^i \phi d_R^j, \quad (2.21)$$

where Γ is the Yukawa coupling constant, Ψ is the left-handed Dirac spinor of quarks, ϕ the Higgs doublet and finally d the right-handed Weyl spinor for the down-type quark.

This coupling is, however, not possible in technicolor theories per se, as it requires four-fermion interactions which are described by unrenormalizable dimension-6 operators. The most popular way to deal with this issue is to introduce another gauge interaction called extended technicolor (ETC) [30, 31].

ETC theories are not the main focus of this thesis and will thus not be discussed in depth and we will refer to the literature. However, the issue of mass generation, flavor physics and problems with ETC models are quite important in the context of technicolor theories so we will here briefly explain the concepts.

The ETC gauge interactions must connect the chiral symmetries of the techniquarks to those of the SM fermions. This is done via an interaction like the one shown in Fig. 2.2a. After technicolor chiral symmetry breaking and the formation of the technicolor condensate, the diagram can be drawn as the one in Fig. 2.2b.

In order to set up the scene we want to introduce just a ‘‘toy’’ ETC-model. Consider a model composed by a gauge group $SU(N_{ETC})$, where

$$N_{ETC} = N_{TC} + N_g, \quad (2.22)$$

and N_g is the number of SM generations. The model transforms as shown in Table 2.1. The ETC gauge group will now be broken N_g times down to $SU(N_{TC})$ as shown in Fig. 2.3. This provides three different mass scales such that each SM family can have different masses. This type of technicolor with associated ETC is called a *one family model* [32]. Notice that the heavy masses are provided by the breaking at low energy and the light masses are provided by breaking at higher energy scales. The estimate of the masses generated at a certain scale will be explained shortly. This model does not, per se, explain how the gauge group is broken several times, neither is the breaking of isospin symmetry accounted for.

With an idea of how an ETC model could be constructed we now turn to some of the ETC induced (dimension-6) operators which are the following

$$\alpha_{ab} \frac{\bar{Q} \gamma_\mu T^a Q \bar{\psi} \gamma^\mu T^b \psi}{\Lambda_{ETC}^2} + \beta_{ab} \frac{\bar{Q} \gamma_\mu T^a Q \bar{Q} \gamma^\mu T^b Q}{\Lambda_{ETC}^2} + \gamma_{ab} \frac{\bar{\psi} \gamma_\mu T^a \psi \bar{\psi} \gamma^\mu T^b \psi}{\Lambda_{ETC}^2}, \quad (2.23)$$

Table 2.1: Quantum numbers for a “toy” ETC model.

	$SU(N_{ETC})_{ETC}$	$SU(3)_c$	$SU(2)_L$	$U(1)_Y$
U_L, D_L	\square	\square	\square	1/6
U_R	\square	\square	1	2/3
D_R	\square	\square	1	-1/3
N_L, E_L	\square	1	\square	-1/2
N_R	\square	1	1	0
E_R	\square	1	1	-1

$$\begin{aligned}
& SU(N_{TC} + 3) \\
\Lambda_1 \downarrow \quad m_1 & \sim \frac{4\pi(F_\pi^{TC})^3}{\Lambda_1^2} \\
& SU(N_{TC} + 2) \\
\Lambda_2 \downarrow \quad m_2 & \sim \frac{4\pi(F_\pi^{TC})^3}{\Lambda_2^2} \\
& SU(N_{TC} + 1) \\
\Lambda_3 \downarrow \quad m_3 & \sim \frac{4\pi(F_\pi^{TC})^3}{\Lambda_3^2} \\
& SU(N_{TC})
\end{aligned}$$

Figure 2.3: Breaking of the “toy” ETC group in 3 stages down to the TC gauge group providing three different mass scales.

where we denote by Q the techniquarks and by ψ the SM fermions. Performing a Fierz rearrangement, following terms are the most interesting phenomenologically

$$\alpha_{ab} \frac{\bar{Q}T^a Q \bar{\psi}T^b \psi}{\Lambda_{ETC}^2} + \beta_{ab} \frac{\bar{Q}T^a Q \bar{Q}T^b Q}{\Lambda_{ETC}^2} + \gamma_{ab} \frac{\bar{\psi}T^a \psi \bar{\psi}T^b \psi}{\Lambda_{ETC}^2} + \dots, \quad (2.24)$$

The α -terms lead to the wanted mass terms for SM fermions

$$m_q \approx \frac{g_{ETC}^2}{M_{ETC}^2} \langle \bar{Q}Q \rangle_{ETC}, \quad (2.25)$$

where m_q is the mass of e.g. a SM quark, g_{ETC} is the ETC coupling constant evaluated at the ETC scale, M_{ETC} is the mass of an ETC gauge boson and $\langle \bar{Q}Q \rangle_{ETC}$ is the technicolor condensate where the operator is renormalized at the ETC scale. The condensate can be related to the condensate renormalized at the technicolor scale via following relation

$$\langle \bar{Q}Q_{ETC} \rangle = \exp \left(\int_{\Lambda_{TC}}^{\Lambda_{ETC}} d(\ln \mu) \gamma_m(\alpha(\mu)) \right) \langle \bar{Q}Q_{TC} \rangle, \quad (2.26)$$

where γ_m is the anomalous dimension of the operator and the integration of the operator is from the ETC scale down to the TC scale. For QCD-like technicolor theories the coupling

$$\alpha(\mu) \propto \frac{1}{\ln \mu}, \quad \text{for } \mu > \Lambda_{TC}, \quad (2.27)$$

which implies that the anomalous dimension $\gamma_m \propto \alpha(\mu)$ so the integral is

$$\langle \bar{Q}Q_{ETC} \rangle \sim \ln \left(\frac{\Lambda_{ETC}}{\Lambda_{TC}} \right)^{\gamma_m} \langle \bar{Q}Q_{TC} \rangle, \quad (2.28)$$

which is not a big enhancement of the operator (as compared to that of a walking type of theory as we will see later). Therefore the mass term yields

$$m_q \approx \frac{g_{ETC}^2}{M_{ETC}^2} N_{TC} \Lambda_{TC}^3, \quad (2.29)$$

as the condensate is proportional to the number of technicolors

$$\langle \bar{Q}Q \rangle_{TC} \sim N_{TC} \Lambda_{TC}^3. \quad (2.30)$$

By dimensional analysis we get [33]

$$m_q \approx 4\pi \frac{g_{ETC}^2}{M_{ETC}^2} (F_\pi^{TC})^3. \quad (2.31)$$

The β -terms of Eq. (2.24) provide masses for pseudo Goldstone bosons via a diagram like that of Fig. 2.4 and also provide masses for techniaxions [22]. This provides masses for the unwanted massless particles that still can be problematic phenomenologically. We will later see that walking technicolor will further enhance these mass terms.

The last class of terms, namely the γ -terms of Eq. (2.24), is the point where the trouble comes in. Generally following terms will be induced

$$\frac{1}{\Lambda_{ETC}^2} (\bar{s}\gamma^5 d)(\bar{s}\gamma^5 d) + \frac{1}{\Lambda_{ETC}^2} (\bar{\mu}\gamma^5 e)(\bar{e}\gamma^5 e) + \dots, \quad (2.32)$$

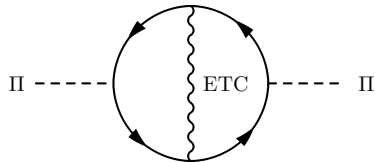


Figure 2.4: Diagram contributing to mass of pseudo Goldstone bosons via an exchange of an ETC gauge boson inside the fermion loop.

where s, d, μ, e denote the strange quark, the down quark, the muon and the electron, respectively. The first term is a $\Delta S = 2$ flavor-changing neutral current interaction which would contribute to a $K_L K_S$ mass difference which is quite well-known experimentally. This constrains the ETC scale to be larger than 10^3 TeV [30] which in turn puts an upper limit on how large masses can be generated, i.e. less than around 100 MeV (for a small coupling and number of technicolors as well as the choice of the fundamental representation of the gauge group). Even the mass for the charm quark will be difficult to generate with the classical ETC model. As we will see later the problem is ameliorated by walking technicolor.

The second term of Eq. (2.32) will induce flavor changing processes in the leptonic sector such as $\mu \rightarrow e\bar{e}e, e\gamma$ which are not observed.

2.1.2 Oblique Parameters

An important notion is the oblique parameters (also called Peskin-Takeuchi parameters) which are computed from the quantum corrections to the self energy of the gauge bosons [34, 35]. They are important, because with those at hand it is an easy way, to compare the effect of the quantum corrections, of the new particles in the theory, to the experiments.

The idea is that they span a basis of the quantum corrections contributed by new physics. The approximation is then, that the dominant effects of the new physics resides in the gauge boson propagators. Because almost all electroweak observable contain gauge boson propagators, the contributions of the new physics is then accounted for when the contributions to the propagators are considered. A priori it is not known if this method works for a specific model, but there are many models for which it does work out well.

There are general arguments to why it is universal to consider the contributions to the self energy of the gauge bosons. The gauge bosons couple to all the particles charged under the given gauge group so their self energies are enhanced by the multiplicity of the new particles. Contrarily, process specific quantum corrections are fixed by flavor quantum numbers on the external legs. Experts on electroweak precision data and data analysis then make fits and provide the experimental preferred values for these three parameters which the model builder then, by relatively simple computations, can

compare with. The definitions of the parameters are the following

$$\hat{\alpha}(M_Z) T \equiv \frac{\Pi_{WW}^{\text{new}}(0)}{M_W^2} - \frac{\Pi_{ZZ}^{\text{new}}(0)}{M_Z^2}, \quad (2.33)$$

$$\frac{\hat{\alpha}(M_Z)}{4\hat{s}_Z^2\hat{c}_Z^2} S \equiv \frac{\Pi_{ZZ}^{\text{new}}(M_Z^2) - \Pi_{ZZ}^{\text{new}}(0)}{M_Z^2}, \quad (2.34)$$

$$\frac{\hat{\alpha}(M_Z)}{4\hat{s}_Z^2} (S + U) \equiv \frac{\Pi_{WW}^{\text{new}}(M_W^2) - \Pi_{WW}^{\text{new}}(0)}{M_W^2}, \quad (2.35)$$

where $\hat{\alpha}$ is the fine structure constant in the \overline{MS} -scheme, $\hat{s}_Z = \sin \hat{\theta}_w(M_Z)$, $\hat{c}_Z = \cos \hat{\theta}_w(M_Z)$ and Π_{ii} are the self energies with respect to the gauge boson i .

The result of the current fit [3] is shown in Fig. 2.5. The SM reference point, at which all the S, T, U parameters vanish, is

$$\begin{aligned} \Delta\alpha_{\text{had}}^{(5)}(M_Z^2) &= 0.02758, & \alpha_s(M_Z^2) &= 0.118, \\ M_Z &= 91.1875\text{GeV}, & m_t &= 175\text{GeV}, \\ m_h &= 150\text{GeV}, & & \end{aligned} \quad (2.36)$$

where $\Delta\alpha_{\text{had}}^{(5)}$ is the hadronic vacuum polarization, α_s is the coupling constant of QCD and M_Z, m_t, m_h are the Z mass, the top mass and the Higgs mass, respectively. The central point of the fit is

$$\begin{aligned} S &= 0.07 \pm 0.10, \\ T &= 0.13 \pm 0.10, \end{aligned} \quad (2.37)$$

where $U = 0$ is imposed [3]. It is seen from the Fig. 2.5 that a low Higgs mass is preferred by the electroweak precision data (EWPd). However, an important point is that the S parameter can have positive corrections if also the T parameter has a positive correction.

A perturbative computation of one $SU(2)_L$ doublet, say $(N, E)_L$, contributes the following to the S parameter [34]

$$S = \frac{1}{6\pi} \left[1 - Y \ln \left(\frac{m_N^2}{m_E^2} \right) \right], \quad (2.38)$$

$$T = \frac{1}{16\pi s^2 c^2 M_Z^2} \left[m_N^2 + m_E^2 - \frac{2m_N^2 m_E^2}{m_N^2 - m_E^2} \ln \left(\frac{m_N^2}{m_E^2} \right) \right], \quad (2.39)$$

where Y is the hypercharge. If there is no isospin breaking in the doublet under consideration then the S parameter is simply $\frac{1}{6\pi}$. The T parameter is approximately $\frac{1}{12\pi s^2 c^2} \frac{(\Delta m)^2}{m_Z^2}$ where $\Delta m \equiv |m_N - m_E|$. The U parameters can be looked up in Ref. [34] but it is in general the S parameter which is problematic in technicolor theories and hence emphasized here.

Considering the simple example of Section 2.1.1 the contribution to the S parameter would be

$$S = \frac{1}{6\pi} (N_{TC}(N_c = 3) + N_{TC}) = \frac{2}{3\pi} N_{TC}, \quad (2.40)$$

where the first term originates from the techniquarks which carry technicolor and QCD color and the second term is for the technileptons which carry only technicolor.

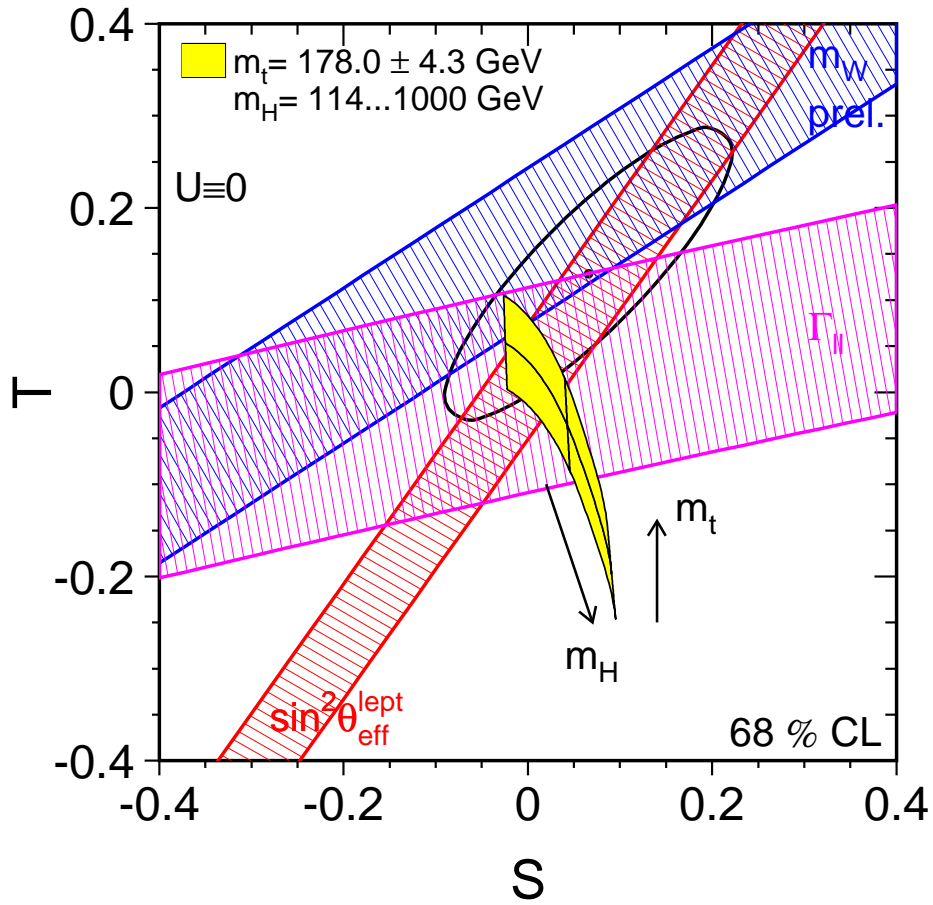


Figure 2.5: Result of fit of electroweak precision data. The contour curve is the 68% CL in the (S, T) -plane with central value $(0.07, 0.13)$. The bands are ± 1 sigma on the measurements of Γ_H , M_W and $\sin^2 \theta_{\text{eff}}^{\text{lepton}}$. The banana shaped region corresponds to the SM prediction with a top mass $m_t = 178 \pm 4.3$ GeV and Higgs mass $m_h = 300^{+700}_{-186}$ GeV. The plot is taken from Ref. [3].

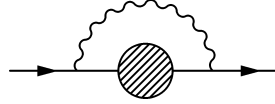


Figure 2.6: Rainbow approximation for the technifermion self energy function. The boson is a technigluon.

In general a techniquark doublet (transforming under the fundamental representation of the technicolor gauge group) will contribute $N_{TC}/(6\pi)$ to the S parameter and $N_c N_{TC}/(6\pi)$ if it also carries QCD color.

The lesson to learn here is that the more matter the model prescribes, the larger the S parameter will be¹.

2.1.3 Walking Technicolor

A way to circumvent FCNCs and still have sufficiently large mass terms for the SM fermions and, equally important, sufficiently large mass terms for the pseudo Goldstone bosons and techniaxions of the theory, is to achieve walking.

Computing the quantum correction to the $\langle \bar{Q}Q \rangle$ operator from the ETC scale down to the technicolor scale (i.e. Eq. (2.26)) the contribution of the QCD-like technicolor theory is that of Eq. (2.28). This contribution is small because the anomalous dimension of the operator is small in the energy range $\Lambda_{TC} < \mu < \Lambda_{ETC}$. However, if the theory exists approximately at a conformal fixed point i.e.

$$\alpha(\mu) = \alpha^* \neq 0, \quad \text{where} \quad \beta(\alpha^*) = 0, \quad (2.41)$$

then the radiative corrections will change into the following form (recalling that $\gamma_m \propto \alpha(\mu)$ which is now $\gamma_m \propto \alpha^*$ independent of μ in the energy range $\Lambda_{TC} < \mu < \Lambda_{ETC}$)

$$\langle \bar{Q}Q_{ETC} \rangle \sim \left(\frac{\Lambda_{ETC}}{\Lambda_{TC}} \right)^{\gamma_m(\alpha^*)} \langle \bar{Q}Q_{TC} \rangle, \quad (2.42)$$

which is a considerably larger contribution [36, 37, 38, 39]. If e.g. $\Lambda_{ETC} \sim 10^3 \Lambda_{TC}$ this factor is quite big. The fact that $\beta = 0$ implies that the technicolor coupling does not run, but instead runs very slowly, i.e. it “walks”. Thus the name *walking technicolor*.

An interesting twist to this point is that walking can also be achieved with only an *approximate* fixed point or a *near conformal* fixed point. It is not possible to show this within perturbation theory, so one way to go is to use a nonperturbative approximation for γ_m and chiral symmetry breaking based on the *rainbow* approximation (also called the ladder approximation) to the Schwinger-Dyson equation [40], see Fig. 2.6. The full nonperturbative fermion propagator in momentum space reads

$$iS^{-1}(p) = Z(p) (\not{p} - \Sigma(p)), \quad (2.43)$$

and the Euclidianized gap equation in Landau gauge is given by

$$\Sigma(p) = 3C_2(R) \int \frac{d^4k}{(2\pi)^4} \frac{\alpha((k-p)^2)}{(k-p)^2} \frac{\Sigma(k^2)}{Z(k^2)k^2 + \Sigma^2(k^2)}, \quad (2.44)$$

¹Before the data analysis done in [3] the central value of the S parameters has always been negative which was unobtainable in technicolor models.

where $Z(k^2) = 1$ in the *rainbow* approximation and we linearize the equation by neglecting $\Sigma^2(k^2)$ in the denominator. By converting to a differential equation and assuming that the coupling $\alpha(\mu) \approx \alpha_c$ is slowly varying ($\beta(\alpha) \simeq 0$), following approximate (WKB) solutions are then found [41]

$$\Sigma(p) \propto p^{-\gamma_m(\mu)}, \quad \Sigma(p) \propto p^{\gamma_m(\mu)-2}, \quad (2.45)$$

where the critical coupling is given in terms of the quadratic Casimir of the representation of the technifermions

$$\alpha_c \equiv \frac{\pi}{3C_2(R)}. \quad (2.46)$$

The anomalous dimension of the fermion mass operator then reads

$$\gamma_m(\mu) = 1 - \sqrt{1 - \frac{\alpha(\mu)}{\alpha_c}} \sim \frac{3C_2(R)\alpha(\mu)}{2\pi}. \quad (2.47)$$

The two different solutions can be understood in terms of physics in the following way. The solution is proportional to two terms. The first one corresponds to the running of a normal mass term of nondynamical origin and the second term corresponds to a “soft” mass dynamically generated and with a $1/p^2$ behavior in the limit of large momentum.

The rainbow approximation indicates that spontaneous symmetry breaking will only occur if α reaches the critical coupling α_c of Eq. (2.46). From Eq. (2.47) the following equivalence is seen

$$\alpha(\Lambda_{TC}) = \alpha_c \Leftrightarrow \gamma_m(\Lambda_{TC}) = 1. \quad (2.48)$$

This defines the symmetry breaking scale Λ_{TC} and it is believed that beyond the rainbow approximation, $\gamma_m = 1$ at the critical coupling [42, 43]. In the rainbow approximation the symmetry breaking occurs when the “soft mass” term and the “hard” non-dynamical mass scales in the same way.

In QCD the coupling drops quickly and the anomalous dimension gets small. So the crucial assumption is that the beta function

$$\beta(\alpha(\mu)) \simeq 0, \quad \text{for } \Lambda_{TC} < \mu < \Lambda_{ETC}, \quad (2.49)$$

which in turn keeps $\alpha \approx \alpha_c$ and finally γ_m large. Then the result of the computation of the radiative correction from the ETC scale down to the ETC scale of the operator $\langle \bar{Q}Q \rangle$ is exactly that of Eq. (2.42).

The reason why walking can ameliorate the problem of FCNCs in technicolor models is that with a large enhancement of the $\langle \bar{Q}Q \rangle$ condensate, the terms generating masses for SM fermions and technicolor pseudo Goldstone bosons are enhanced by a factor of $\Lambda_{ETC}/\Lambda_{TC}$ while the “ γ ” terms in Eq. (2.24) do not include any techniquarks and thus no enhancement. Then one can crank up the ETC scale and suppress the FCNCs. Before one gets too pleased about that, it should be noted that in order to have sufficiently low rates of FCNCs the largest mass the walking technicolor model can account for is ~ 1 GeV [36]. By tuning a model one can perhaps account for the bottom mass, but it is certain that something has to happen in order to account for the large top mass.

The question of walking is essentially of nonperturbative nature so it is a subtle point of the theory. If the β -function is kept small to finite order in the perturbative expansion, one is still not assured that no higher order terms ruin the walking.

A final important point is how to make a technicolor theory a walking theory. For technifermions transforming with respect to the fundamental representation of the gauge group, the number of flavors, N_f , has to be close to $4N_{TC} \pm 20\%$ [44].

2.1.4 The Problems with Technicolor

In order to have a realistic extended technicolor model, at least the following criteria has to be fulfilled

- It must be asymptotically free and cannot have gauge anomalies.
- It cannot be at odds with electroweak precision measurements i.e. it has to have reasonable S, T (and U) parameters.
- It must account for the mass hierarchies and at the same time generate the very small neutrino masses.
- It must generate sufficiently large masses for its gauge bosons and Goldstone bosons etc.
- It must generate weak CP-violation without too much strong CP-violation.
- It must generate isospin breaking in order to account for the top-bottom, charm-strange and up-down mass differences without being at odds with the EWPD fit to the T parameter.
- It must account for the large top mass and in the same time only contribute sufficiently little to $Z \rightarrow \bar{b}b$ and $b \rightarrow s\gamma$ [45].
- It should also have a candidate for dark matter which is not yet excluded by dark matter search experiments such as the CDMS.
- It must unify at some large scale in order to explain the quantization of electric charge.

Some of the problems have been revealed in the course of this chapter e.g. the problem with the large S parameter which is typical in technicolor theories. This can be cured by putting as little matter into the model as possible e.g. one doublet of techniquarks transforming under the fundamental representation of $SU(2)$ or $SU(3)$ which gives an S parameter of 0.11 and 0.16, respectively. This is within one sigma.

Another problem already introduced is the large FCNCs which can be ameliorated via walking technicolor. Having the techniquarks transform under the fundamental representation of the technicolor gauge group, a minimum of colors (2) and the requirement of walking would imply $N_f = 8$, meaning 4 doublets. That corresponds to $S \sim 0.42$ i.e. quite big.

Theoretically there are several ways to circumvent this phenomenological dilemma; either we have too large S or no walking: One way is to make a negative contribution to S by having a sufficiently large mass splitting in the (one or more) doublets (and hypercharge different from zero). Another way is to choose different representations of the technicolor gauge group. This is the idea of the model which we will present in the next section.

2.2 The Sannino-Tuominen Model

The idea of having quarks (or techniquarks) transforming under a higher dimensional representations² of the gauge group is not a new idea. An early attempt of having

²We use the name higher dimensional representations, because $d(\mathcal{R}) > d(\square)$ with $\mathcal{R} \neq \square$ and it is understood that it is representations of $SU(N)$.

quarks transforming under a higher dimensional representation of the gauge group is done by Ma [46]. The quarks in higher dimensional representations carry “more color” than those of the fundamental representation and thus have different characteristics. The use of higher dimensional representations for quarks in the context of dynamical symmetry breaking is considered by Marciano [47] where exotic quarks belong to **6**, **8**, **10** of $SU(3)_c$. Higher dimensional representations of technicolor-like theories has been considered by Eichten and Lane in Ref. [30].

We will now consider a technicolor extension of the SM with quarks in higher dimensional representations starting by the simple case of two-index symmetric and two-index antisymmetric representations of $SU(N_{TC})$. This class of models has been considered by Sannino and Tuominen in Ref. [4] and also later by Refs. [48, 49, 50]. In this line of research a prototype ETC has been constructed in Ref. [51] and effective theories and considerations on dark matter has been made in Ref. [1] and finally more aspects of a possible relic abundance and experimental limits on dark matter has been considered in Ref. [2].

The motivation for choosing this class of higher dimensional representations is due to a map by Armoni, Shifman and Veneziano [52, 53], which states an equivalence between Yang Mills theories with a Dirac fermion in two-index symmetric or antisymmetric tensor representation of $SU(N_{TC})$ and supersymmetric Yang Mills (SYM) with large N_{TC} . This makes exact solutions from SYM usable in this class of technicolor models (with two-index symmetric and antisymmetric representations).

Another motivation is that we will show that it is possible to make a walking technicolor model with less matter than that of the minimal model in the fundamental representation.

Considering $N_f = N_D/2$ Dirac flavors (where N_D is number of electroweak doublets) in the two-index symmetric (S-type) representation and two-index antisymmetric (A-type) representation. The perturbative β -function reads

$$\beta = -\beta_0 \frac{g^3}{(4\pi)^2} - \beta_1 \frac{g^5}{(4\pi)^4} + \dots, \quad (2.50)$$

where the coefficients are given in terms of number of technicolors and number of flavors by [4]

$$\begin{aligned} \beta_0 &= \frac{11}{3}N_{TC} - \frac{2}{3}N_f(N_{TC} \pm 2), \\ \beta_1 &= \frac{34}{3}N_{TC}^2 - N_f(N_{TC} \pm 2) \left(\frac{10}{3}N_{TC} + \frac{2}{N_{TC}}(N_{TC} \mp 1)(N_{TC} \pm 1) \right), \end{aligned} \quad (2.51)$$

where the upper sign is for the S-type and the lower sign the A-type case. It is interesting to note that in the limit of infinite N_{TC} , the β -function is that of SYM and the S-type and A-type models coincide.

Asymptotical freedom is intact when

$$N_f \leq \frac{11}{2} \frac{N_{TC}}{N_{TC} \pm 2}. \quad (2.52)$$

The next important value for the number of flavors is where the theory enters the conformal window. Considering the Banks Zaks fixed point i.e. the β -function truncated to the first two terms (Eq. (2.50)) and set equal to zero, the coupling constant is

$$\alpha^* = -4\pi \frac{\beta_0}{\beta_1}. \quad (2.53)$$

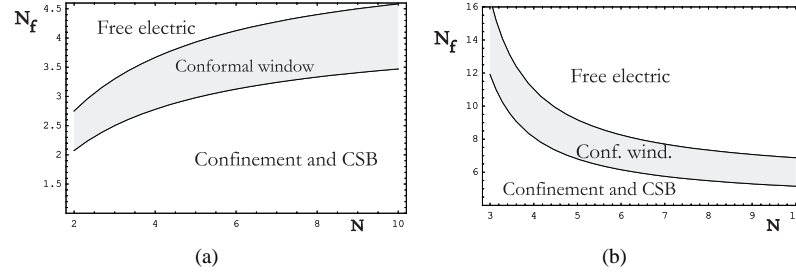


Figure 2.7: Phase diagram of number of Dirac flavors N_f vs. number of technicolors N_{TC} for two-index symmetric (a) and antisymmetric (b) representations of the gauge group. The graphs are taken from Ref. [4]

From Eq. (2.46) we have the critical coupling, above which the gap equation in the rainbow approximation has a non-trivial solution. Recalling that the quadratic Casimir for the two-index symmetric (S-type) and antisymmetric (A-type) representation is, respectively

$$C_2(\square\square) = \frac{(N_{TC} + 2)(N_{TC} - 1)}{N_{TC}}, \quad (2.54)$$

$$C_2(\square) = \frac{(N_{TC} - 2)(N_{TC} + 1)}{N_{TC}}, \quad (2.55)$$

we set α^* of Eq. (2.53) equal to the value of the critical coupling of Eq. (2.46) and obtain a critical number of flavors for which chiral symmetry is restored when

$$N_f > N_f^c \simeq \frac{83N_{TC}^3 \pm 66N_{TC}^2 - 132N_{TC}}{20N_{TC}^3 \pm 55N_{TC}^2 \mp 60}, \quad (2.56)$$

where the upper sign is S-type and the lower sign is A-type. With these two boundaries at hand one can plot the phase diagram, see Fig. 2.7.

It is seen from Fig. 2.7a that with an S-type model with two technicolors and two techniflavors it is very close to the conformal window. In fact the critical number of flavors for two technicolors is ~ 2.075 . In the A-type case, one has to go to four technicolors in order to have less techniflavors than in the QCD-like technicolor case and still have a prototype walking model.

The models have built-in custodial symmetry so the T, U parameters are no problem, if the mass splitting in the doublet(s) of technifermions is small. The S parameter which usually plagues technicolor theories is

$$S_{\text{perturbative}} = \frac{1}{6\pi} \frac{N_f}{2} \frac{N_{TC}(N_{TC} \pm 1)}{2}, \quad (2.57)$$

where the upper sign is for S-type and the lower for A-type models and the last factor is the dimension of the representation i.e. the number of doublets as seen from the electroweak point-of-view.

It should be noted that the near conformal dynamics will reduce the S parameter from the perturbative value [54, 55]. In the estimate made in Ref. [54] taking into account the nonperturbative part gives a reduction of around 30%.

Considering first the S-type models: With two technicolors, two flavors are needed and for the minimal model with only one electroweak doublet $S = 1/(2\pi) \sim 0.16$. This specific case, though, adds three electroweak doublets to the SM and the full theory would suffer from the Witten anomaly [56] unless still an odd number of electroweak doublets are added. For simplicity one could add a fourth family of leptons. This specific case is considered much more in detail in later sections of this thesis. The flavor symmetry would be $SU(4)$ breaking to $SO(4)$ because the two-index symmetric representation (i.e. the same as the adjoint representation of $SU(2)$ is real). More on this in the next section. Having instead three technicolors would render the extra leptons superfluous but on the downside the $S = 1/\pi \sim 0.32$. The flavor symmetry would be just $SU(2)_L \times SU(2)_R$ breaking to $SU(2)_V$.

With the A-type models one needs four techniflavors in order to be better off than ordinary QCD-like walking technicolor. Here extra electroweak doublets are not needed as it is six times four doublets which are added to the SM (i.e. an even number). Compared to the S-type models it is a whole lot of matter which is needed. Namely four technicolors and eight techniflavors which makes $S = 4/\pi \sim 1.27$, which is quite off with respect to the EWPD.

2.2.1 The Composite Higgs Mass

A final point which is quite interesting in the Sannino-Tuominen class of models is that it is possible to obtain a light Higgs boson as we only briefly will point out and otherwise refer to the literature. This is in sharp contrast with QCD-like technicolor as the scaled up result from the QCD σ meson would estimate the Higgs boson mass to be $4\pi F_\pi^{TC} = 4\pi v_{\text{weak}}$ which is quite big.

First it should be noted that it is not possible to scale up QCD in order to obtain results in a walking/near conformal technicolor theory. So other tools have to be used. There are two obvious ones. The large- N expansion and lattice computing. Lattice computing might be the most precise but also the most involved and expensive in flops and computer time.

The large- N expansion associated to estimating the Higgs mass has been done in Ref. [48]. The S-type model is used with the limit $N_{TC} \rightarrow \infty$ and the number of flavors N_f is set to one (which is considered a good approximation to two). The Higgs boson is identified with the scalar fermion-antifermion state whose pseudoscalar partner in QCD is known as η' . The model is mapped into SYM using the mentioned map due to Armoni, Shifman and Veneziano [52]. The bosonic sector contains a low mass scalar and pseudoscalar meson. In this limit, the masses can be related to the fermion condensate $\langle \tilde{q}q \rangle \equiv \langle \tilde{q}^{\{i,j\}} q_{\{i,j\}} \rangle$ [57]

$$M = \frac{2}{3}\alpha \left(\frac{3\langle \tilde{q}q \rangle}{32\pi^2 N_{TC}} \right)^{\frac{1}{3}} = \frac{2}{3}\hat{\alpha}\Lambda, \quad (2.58)$$

with

$$\langle \tilde{q}q \rangle = 3N_{TC}\Lambda^3, \quad (2.59)$$

$$\hat{\alpha} \equiv \alpha \left(\frac{9}{32\pi^2} \right)^{\frac{1}{3}}, \quad (2.60)$$

where Λ is the one loop large- N -invariant scale of the theory. It has been argued in Ref. [48] that $\hat{\alpha}$ is of order 1 – 3 and an example connected to QCD is illustrating

Table 2.2: Summary of the properties of the $SU(2)$ -Adj. model.

upper limit of asymptotic freedom, N_f	2.75
lower limit of the conformal window, N_f^c	2.075
critical coupling for chiral symmetry breaking, α_c	$\pi/6 \sim 0.52$
S	$1/(2\pi) \sim 0.16$

this point. This gives the first estimate of the composite Higgs boson mass, namely $m_h \approx M$, where M is that of Eq. (2.58). $1/N_{TC}$ corrections are found to be

$$\frac{m_h}{M} = 1 \mp \frac{4}{9N_{TC}} + \frac{1}{8N_{TC}} \frac{\langle G_{\mu\nu}^a G^{a\mu\nu} \rangle}{\hat{\alpha}\Lambda^4} + \mathcal{O}\left(\frac{1}{N_{TC}^2}\right), \quad (2.61)$$

where $\langle G_{\mu\nu}^a G^{a\mu\nu} \rangle \sim \Lambda^4$ is the technigluon condensate and the upper sign is for S-type models and the lower for A-type models. As the second term is dominating, the S-type models have a lowered Higgs mass compared to QCD-like walking technicolor theories and the A-type models have an increased Higgs mass.

2.3 The $SU(2)$ -Adj. Model

For phenomenological reasons the specific model with the two-index symmetric (S-type) representation of $SU(2)$ in the Sannino-Tuominen class is the most interesting, as was illustrated in the previous section by the low value of the S parameter. The corresponding model with three technicolors has larger S parameter, but on the other hand it does not need to be cured by an extra family of leptons. It also has a slightly larger Higgs mass than the one with two technicolors. Another interesting thing is that it has flavor symmetry $SU(2)_L \times SU(2)_R$ breaking to $SU(2)_V$ giving three Goldstone bosons which are all eaten and become the longitudinal modes of the electroweak gauge bosons. In that sense there is not so much to explore as in the minimal model that is preferred by EWPD. Therefore we choose to investigate the model with two technicolors in depth.

This section and most of the rest of the thesis is devoted to the investigation of the S-type $SU(2)$ model with only one electroweak doublet.

The two-index symmetric representation of $SU(2)$ is real and it is equal to the adjoint representation of $SU(2)$ and we will from now on just call the model the $SU(2)$ -Adj. model.

Some of the results obtained in the previous sections are summarized for this model in Table 2.2.

Since we consider adjoint Dirac fermions, the critical number of flavors is independent of the number of colors [51]. We expect that the theory will enter a conformal regime unless the coupling rises above the critical value, triggering the formation of a fermion condensate. Hence a $N_f = 2$ theory is sufficiently close to the critical number of flavors $N_f^c = 2.075$. This makes it a perfect candidate for a walking technicolor theory.

The technifermions are

$$\left(\begin{array}{c} U^{\{\alpha,\beta\}} \\ D^{\{\alpha,\beta\}} \end{array} \right)_L, \quad U_R^{\{\alpha,\beta\}}, \quad D_R^{\{\alpha,\beta\}}, \quad \text{with } \alpha, \beta = 1, 2. \quad (2.62)$$

Since the two fermions can equivalently be written as adjoint fermions we have

$$Q_L^a = \begin{pmatrix} U^a \\ D^a \end{pmatrix}_L, \quad U_R^a, \quad D_R^a, \quad a = 1, 2, 3, \quad (2.63)$$

with a the adjoint technicolor index of $SU(2)$. The left fields are arranged in three doublets of the $SU(2)_L$ weak interactions in the standard fashion. The condensate is $\langle \bar{U}U + \bar{D}D \rangle$ which correctly breaks the electroweak symmetry.

As mentioned in the last section this model, as described so far, suffers from the Witten topological anomaly [56]. An $SU(2)$ gauge theory must have an even number of fermion doublets to avoid this anomaly. Here there are three extra electroweak doublets added to the SM and we need to add an odd number of doublets. The simplest thing to do is to add one more doublet. Since we do not wish to disturb the walking nature of the technicolor dynamics, the doublet must be a technicolor singlet (and in order to keep the S parameter small).

Our additional matter content is essentially a copy of a standard model fermion family with quarks (here transforming under the adjoint representation of $SU(2)$) and the following lepton doublet³

$$\mathcal{L}_L = \begin{pmatrix} \nu_\zeta \\ \zeta \end{pmatrix}_L, \quad \nu_{\zeta R}, \quad \zeta_R. \quad (2.64)$$

Now we need to assign hypercharge to the new fermions in such a way that there will be no anomalies. Following the analysis done in Peskin and Schroeder [9] we can write down constraints on the hypercharge. The exhausted list of diagrams giving rise to anomalies is shown in Ref. [9]. However, not all of them are non-vanishing or lead to new constraints. It will suffice to consider the diagrams of Fig. 2.8.

Let us be generic and assign $y/2$ to the left-handed techniquarks and $z/2$ to the left-handed new leptons. In order to have the correct electric charge for the right-handed fermions, the hypercharges for the new particles are now

$$Y(Q_L) = \frac{y}{2}, \quad Y(U_R, D_R) = \left(\frac{y+1}{2}, \frac{y-1}{2} \right), \quad (2.65)$$

$$Y(\mathcal{L}_L) = \frac{z}{2}, \quad Y(N_R, E_R) = \left(\frac{z+1}{2}, \frac{z-1}{2} \right), \quad (2.66)$$

where $y, z \in \mathbb{R}$.

First the diagram (a) of Fig. 2.8, which is two technigluons and a $U(1)$ hypercharge gauge boson, will lead to the following constraint (we use the convention of Peskin and Schroeder to add the left-handed particles with a factor of -1)

$$\sum Y_{TC} = -2 \left(\frac{y}{2} \right) + \left(\frac{y+1}{2} \right) + \left(\frac{y-1}{2} \right) = 0. \quad (2.67)$$

The diagram (b) with two $SU(2)$ electroweak gauge bosons gives rise to

$$\sum Y_L = -3 \left(\frac{y}{2} \right) - \left(\frac{z}{2} \right) = 0 \quad \Rightarrow \quad \boxed{z = -3y}. \quad (2.68)$$

³It is interesting to note that our technicolor sector has the same fermionic matter content as that of $\mathcal{N} = 4$ super Yang-Mills.

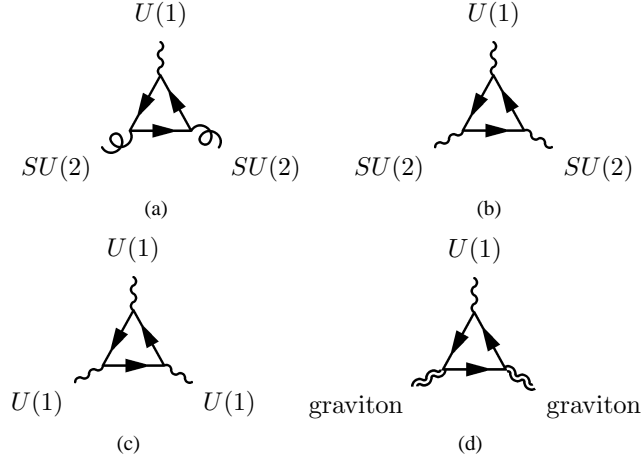


Figure 2.8: Important diagrams that need to be considered in order to write down an anomaly free theory. In (a) the $U(1)$ hypercharge gauge boson and two techniglucos are connected via a triangle of fermions. In (b) the $U(1)$ meets two electroweak gauge bosons and in (c) it is just three $U(1)$ gauge bosons. Finally (d) is the triangle with two gravitons and a single $U(1)$ gauge boson.

The diagrams (c) and (d) give the following constraints

$$\begin{aligned} \sum Y^3 = & -2 \left(\frac{-3y}{2} \right)^3 + \left(\frac{-3y+1}{2} \right)^3 + \left(\frac{-3y-1}{2} \right)^3 \\ & - 6 \left(\frac{y}{2} \right)^3 + 3 \left(\frac{y+1}{2} \right)^3 + 3 \left(\frac{y-1}{2} \right)^3 = 0, \end{aligned} \quad (2.69)$$

$$\begin{aligned} \sum Y = & -2 \left(\frac{-3y}{2} \right) + \left(\frac{-3y+1}{2} \right) + \left(\frac{-3y-1}{2} \right) \\ & - 6 \left(\frac{y}{2} \right) + 3 \left(\frac{y+1}{2} \right) + 3 \left(\frac{y-1}{2} \right) = 0. \end{aligned} \quad (2.70)$$

The cancellation in the sum of cubed hypercharges is not trivial as the techniquarks contribute $9y/4$ and the new leptons contribute the same with opposite sign. The sum of hypercharges is trivial as it is obeyed even within the techniquarks and the new leptons separately.

Thus the generic gauge anomaly free hypercharge assignment reads

$$Y(Q_L) = \frac{y}{2}, \quad Y(U_R, D_R) = \left(\frac{y+1}{2}, \frac{y-1}{2} \right), \quad (2.71)$$

$$Y(\mathcal{L}_L) = -3\frac{y}{2}, \quad Y(\nu_{\zeta R}, \zeta_R) = \left(\frac{-3y+1}{2}, \frac{-3y-1}{2} \right), \quad (2.72)$$

In our notation the electric charge is $Q = T_3 + Y$, where T_3 is the weak isospin generator. We summarize the charges in Table 2.3. One recovers the SM hypercharge assignment for $y = 1/3$. In Ref. [51], the SM hypercharge has been investigated in the context of an extended technicolor theory. Another interesting choice of the

Table 2.3: Quantum numbers for the $SU(2)$ -Adj. model.

	$SU(2)_{TC}$	$SU(3)_c$	$SU(2)_L$	$U(1)_Y$
U_L, D_L	\square	1	\square	$y/2$
U_R	\square	1	1	$\frac{y+1}{2}$
D_R	\square	1	1	$\frac{y-1}{2}$
$\nu_{\zeta L}, \zeta_L$	1	1	\square	$-3y/2$
$\nu_{\zeta R}$	1	1	1	$\frac{-3y+1}{2}$
ζ_R	1	1	1	$\frac{-3y-1}{2}$

hypercharge is $y = 1$, which has been investigated, from the point of view of the electroweak precision measurements, in Refs. [49, 50]. In this case

$$\begin{aligned} Q(U) &= 1, & Q(D) &= 0, \\ Q(\nu_\zeta) &= -1, & Q(\zeta) &= -2, \quad \text{with } y = 1. \end{aligned} \quad (2.73)$$

Notice that with this particular hypercharge assignment, the D techni-down is electrically neutral.

Since we have two Dirac fermions in the adjoint representation of the gauge group, the global symmetry is $SU(4)_{\text{flavor}}$.

It is a simple exercise to show that the flavor symmetry of fermions in real representations of the gauge group is exactly $SU(2N_f)$ instead of $SU(N_f)_L \times SU(N_f)_R$. In the case of a real (real-positive) representation there exists a symmetric matrix S such

$$T^{*a}[\mathcal{R}] = -ST^a[\mathcal{R}]S^{-1}, \quad \forall a, \quad (2.74)$$

where T^a are the generator matrices belonging to the representation \mathcal{R} . Performing a gauge symmetry transformation

$$\Psi = \begin{pmatrix} \psi_L \\ \psi_R \end{pmatrix} \rightarrow e^{ie^a T^a} \Psi, \quad (2.75)$$

and thus

$$\Psi^* \rightarrow e^{-ie^a (T^a)^*} \Psi^* = e^{ie^a ST^a S^{-1}} \Psi^*. \quad (2.76)$$

Multiplying by the inverse matrix S^{-1} we have

$$S^{-1}\Psi^* \rightarrow e^{ie^a T^a} S^{-1}\Psi^*, \quad (2.77)$$

and we can thus write down the vector

$$\begin{pmatrix} \psi_L^a \\ (S^{-1}\psi_R^*)^a \end{pmatrix}, \quad (2.78)$$

where all the elements transform equally under gauge transformations.

In particular, for the adjoint representation, we have the generators [9]

$$(T^b[G])_{ac} = if^{abc}, \quad (2.79)$$

where G is for the adjoint representation, a, c are matrix indices, and f^{abc} are the structure constants for the group in question. Because the structure constants are real and antisymmetric, we have

$$T^{*a}[G] = -T^a[G], \quad (2.80)$$

and thus that S in Eq. (2.78) equals one in the case of adjoint representations.

To discuss the symmetry properties of the theory it is convenient to use the Weyl base for the fermions and arrange them in the following vector, transforming according to the fundamental representation of $SU(4)$

$$Q = \begin{pmatrix} U_L \\ D_L \\ -i\sigma^2 U_R^* \\ -i\sigma^2 D_R^* \end{pmatrix}, \quad (2.81)$$

where U_L and D_L are the left handed techni-up and techni-down respectively and U_R and D_R are the corresponding right handed particles. Assuming the standard breaking to the maximal diagonal subgroup, the $SU(4)$ symmetry breaks spontaneously down to $SO(4)$. Such a breaking is driven by the following condensate

$$\langle Q_i^\alpha Q_j^\beta \epsilon_{\alpha\beta} E^{ij} \rangle = -2 \langle \bar{U}_R U_L + \bar{D}_R D_L \rangle, \quad (2.82)$$

where the indices $i, j = 1, \dots, 4$ denote the components of the tetraplet of Q , and the Greek indices indicate the ordinary spin. The matrix E is a 4×4 matrix defined in terms of the 2-dimensional unit matrix as

$$E = \begin{pmatrix} 0 & \mathbb{1} \\ \mathbb{1} & 0 \end{pmatrix}. \quad (2.83)$$

Following the notation of Wess and Bagger [58] $\epsilon_{\alpha\beta} = -i\sigma_{\alpha\beta}^2$ and

$$\langle U_L^\alpha U_R^{*\beta} \epsilon_{\alpha\beta} \rangle = -\langle \bar{U}_R U_L \rangle. \quad (2.84)$$

A similar expression holds for the D techniquark. The above condensate is invariant under an $SO(4)$ symmetry. The easiest way to check that an $SO(4)$ symmetry remains intact is by going to the following base

$$U_L = \frac{\lambda_1 + i\lambda_2}{\sqrt{2}}, \quad \epsilon U_R^* = \frac{\lambda_1 - i\lambda_2}{\sqrt{2}}, \quad D_L = \frac{\lambda_3 + i\lambda_4}{\sqrt{2}}, \quad \epsilon D_R^* = \frac{\lambda_3 - i\lambda_4}{\sqrt{2}}, \quad (2.85)$$

where the λ s are four independent two-component spinors. In this base, our condensate becomes simply

$$\langle \lambda_1^2 + \lambda_2^2 + \lambda_3^2 + \lambda_4^2 \rangle, \quad (2.86)$$

which clearly is an $SO(4)$ invariant. We are left with nine broken generators of the original $SU(4)$ global symmetry and to the generators are associated Goldstone bosons.

In terms of the underlying degrees of freedom, and focusing only on the techniflavor symmetries, the nine Goldstone bosons transform like

$$\bar{D}_R U_L, \quad \bar{U}_R D_L, \quad \frac{1}{\sqrt{2}}(\bar{U}_R U_L - \bar{D}_R D_L), \quad (2.87)$$

for the three which will be eaten by the longitudinal components of the massive electroweak gauge bosons. The electric charge is respectively one, minus one and zero. For the other six Goldstone bosons we have

$$U_L U_L, \quad D_L D_L, \quad U_L D_L, \quad (2.88)$$

with the following electric charges

$$y + 1, \quad y - 1, \quad y, \quad (2.89)$$

together with the associated anti-particles. The last six Goldstone bosons (Eq. (2.88)) are di-technibaryons with opposite baryonic charge, one and minus one, respectively. The baryon number is a diagonal generator of $SU(4)$. As we already mentioned the choice of $y = 1$ makes one of the Goldstone bosons (namely the DD) electrically neutral.

2.3.1 Spectrum

We have previously described the Goldstone bosons of the model. These are mesons but an interesting fact is that they are also baryons. The flavor symmetry is $SU(4)$ and it is recognized that there is a $U(1)$ of technibaryon number which is conserved unless broken by ETC interactions. The fact that the model has particles which almost only receive mass from ETC interactions and have a conserved quantum number is welcomed and can be exploited in the context of constructing a cold dark matter component which is a di-technibaryon, see Chapter 3.

The simplest low lying technibaryons are constructed in the following way

$$\mathcal{B}_{\{f, \tilde{f}\}} = Q_{L; \alpha, f}^{\{c_1, c_2\}} Q_{L; \beta, \tilde{f}}^{\{c_3, c_4\}} \epsilon^{\beta\alpha} \epsilon_{c_1, c_3} \epsilon_{c_2, c_4}, \quad (2.90)$$

where $f, \tilde{f} = U, D$, $c_i = 1, 2$, and $\alpha, \beta = 1, 2$ are the spin indices. These states correspond to an $SU(2)$ triplet of scalar states. In a similar fashion one can construct states out of only right-handed fields. An $SU(2)_L$ singlet, though, has to have spin one in order to also have antisymmetric flavor indices.

2.3.2 EWPD

We already presented the value of the S parameter for the pure technicolor part of the model. Adding the leptons though will change this picture. Depending on the masses and especially the mass gap of the leptons, the model can actually be within one sigma of what the EWPD prescribes with a convenient choice of lepton masses, see Fig. 2.9. It is seen from Eq. (2.38) that the left wing of the parabola shape is for the case where the logarithm is positive and thus the ν_ζ neutrino mass greater than the ζ mass and oppositely for the right wing.

2.3.3 Effective Theories

While the leptonic sector can be described within perturbation theory since it interacts only via electroweak interactions, the situation for the techniquarks is more involved since they combine into composite objects interacting strongly among themselves. It is therefore useful to construct low energy effective theories encoding the basic symmetry features of the underlying theory. We construct the linearly and non-linearly realized low energy effective theories for our underlying theory. The theories we will present can be used to investigate relevant processes of interest at LHC and ILC. It would be interesting to perform the analysis in Ref. [59] with these specific theories.

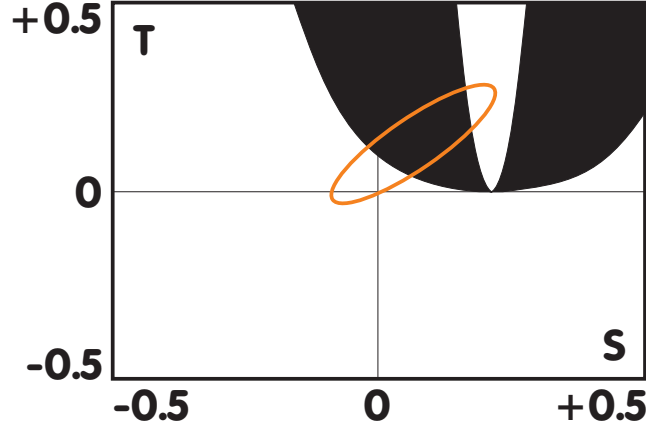


Figure 2.9: (S, T) diagram showing the regions the $SU(2)$ -Adj. model can span with the masses of the new leptons ν_ζ and ζ taking on values from M_Z to $10M_Z$. The ellipsis represent the one sigma contour of the global fit to the EWPd with a reference Higgs mass of 150 GeV. The figure is taken from Ref. [5].

The Linear Realization

The relevant effective theory for the Higgs sector at the electroweak scale consists, in our model, of a light composite Higgs and nine Goldstone bosons. These can be assembled in the matrix

$$M = \left(\frac{\sigma}{2} + i\sqrt{2}\Pi^a X^a \right) E, \quad (2.91)$$

which transforms under the full $SU(4)$ group according to

$$M \rightarrow uMu^T, \quad \text{with } u \in SU(4), \quad (2.92)$$

and X^a are the generators of the $SU(4)$ group which do not leave invariant the vacuum expectation value of M , see Appendix B

$$\langle M \rangle = \frac{v}{2} E. \quad (2.93)$$

We will now show that the Goldstone bosons transform like those of Eqs. (2.87-2.88). Multiplying by another generator X^b on the rhs. of Eq. (2.91), taking the trace and using that $E^2 = \mathbb{1}$ we get

$$\text{Tr} \{ MEX^b \} = i\sqrt{2}\Pi^a \text{Tr} \{ X^a X^b \} = i\frac{1}{\sqrt{2}}\Pi^a \delta^{ab} = i\frac{1}{\sqrt{2}}\Pi^b. \quad (2.94)$$

A point which might seem subtle at first sight is that, in order to eliminate the scalars, we need to take the imaginary part of the equation which will leave us with the pseudoscalars

$$\Pi^a = \sqrt{2}\Im \text{Tr} \{ MEX^a \}. \quad (2.95)$$

The matrix M is connected to the quark content via

$$M_{ij} = Q_i Q_j, \quad \text{with } i, j = 1, \dots, 4. \quad (2.96)$$

This reveals that the eaten Goldstone bosons which are real transform like

$$\Pi^1 = \Im \frac{\overline{DU} + \overline{UD}}{\sqrt{2}}, \quad \Pi^2 = \Re \frac{\overline{DU} - \overline{UD}}{\sqrt{2}}, \quad \Pi^3 = \Im \frac{\overline{UU} - \overline{DD}}{\sqrt{2}}, \quad (2.97)$$

while the baryonic sector transforms like

$$\begin{aligned} \Pi^4 &= \Im \frac{UD + \overline{UD}}{\sqrt{2}}, & \Pi^5 &= \Re \frac{\overline{UD} - UD}{\sqrt{2}}, & (2.98) \\ \Pi^{8/6} &= \Im \frac{UU \pm DD + \overline{UU} \pm \overline{DD}}{2}, & \Pi^{7/9} &= \Re \frac{\overline{UU} \mp \overline{DD} - UU \pm DD}{2}, & (2.99) \end{aligned}$$

where the real Goldstone bosons are written in terms of their underlying degrees of freedom which at the same time represents the charge eigenstates of the model.

One should note our short-hand notation for the states. We are using the conventions of Wess and Bagger [58] and the spin contracted states are defined as follows

$$UD \equiv U_L^\alpha D_{L;\alpha}, \quad (2.100)$$

$$\overline{DU} \equiv (D_R^*)^\alpha U_{L;\alpha}, \quad (2.101)$$

$$\overline{DD} \equiv (D_R^*)^\alpha (D_R^*)_\alpha. \quad (2.102)$$

It is convenient to separate the fifteen generators of $SU(4)$ into the six that leave the vacuum invariant $\{S^a\}$ and the other nine that do not $\{X^a\}$.

It is easy to show that the generators $\{S^a\}$ of the $SO(4)$ subgroup that leave the vacuum invariant satisfy following relation

$$S^a E + E S^{aT} = 0, \quad \text{with } a = 1, \dots, 6. \quad (2.103)$$

The proof goes like this. The vacuum is left invariant by the generators so we can write

$$\frac{v}{2} E = e^{i\alpha^a S^a} \frac{v}{2} E \left(e^{i\alpha^a S^a} \right)^T \Rightarrow 0 = i\alpha^a S^a E + iE\alpha^a S^{aT}. \quad (2.104)$$

Because the α s are arbitrary we get

$$S^a E + E S^{aT} = 0. \quad (2.105)$$

□

An explicit realization of the generators is shown in Appendix B.

The electroweak subgroup can be embedded in $SU(4)$, as explained in detail in Ref. [60]. The main difference here is that we have a more general definition of the hypercharge. The electroweak covariant derivative is

$$D_\mu M = \partial_\mu M - ig [G_\mu M + M G_\mu^T], \quad (2.106)$$

with

$$G_\mu = \begin{pmatrix} W_\mu & 0 \\ 0 & -\frac{g'}{g} \tilde{B}_\mu^T \end{pmatrix} + \frac{y}{2} \frac{g'}{g} B_\mu \begin{pmatrix} \mathbb{1} & 0 \\ 0 & -\mathbb{1} \end{pmatrix}. \quad (2.107)$$

We also have

$$W_\mu = W_\mu^a \frac{\tau^a}{2}, \quad \tilde{B}_\mu^T = B_\mu \frac{\tau^{3T}}{2} = B_\mu \frac{\tau^3}{2}, \quad (2.108)$$

where τ^a are the Pauli matrices. It is convenient to rewrite the gauge bosons in a more compact form

$$G = W^a L^a - \frac{g'}{g} B_\mu R^{3T} + \sqrt{2} y \frac{g'}{g} B_\mu S^4, \quad (2.109)$$

with

$$L^a = \frac{S^a + X^a}{\sqrt{2}}, \quad R^{aT} = \frac{X^a - S^a}{\sqrt{2}}, \quad \text{and } a = 1, 2, 3. \quad (2.110)$$

With this gauging we are ensuring the correct pattern of electroweak symmetry breaking. In fact, we can rewrite

$$G = G_S + G_X, \quad (2.111)$$

with

$$G_S = \frac{1}{\sqrt{2}} \sum_{a=1}^3 S^a \left[W^a + \frac{g'}{g} B \delta_a^3 \right] + \sqrt{2} y \frac{g'}{g} B S^4, \quad (2.112)$$

$$G_X = \frac{1}{\sqrt{2}} \sum_{a=1}^3 X^a \left[W^a - \frac{g'}{g} B \delta_a^3 \right]. \quad (2.113)$$

The generators satisfy the normalization conditions $\text{Tr}[X^a X^b] = \delta^{ab}/2$, $\text{Tr}[S^a S^b] = \delta^{ab}/2$ and $\text{Tr}[SX] = 0$. In the unitary gauge, three of the Goldstone bosons are absorbed into the longitudinal degrees of freedom of the massive weak gauge bosons while the extra six Goldstone bosons will acquire masses due to extended technicolor interactions (see the Fig. 2.4) as well as the electroweak interactions per se.

Assuming a bottom up approach we will introduce by hand a mass term for the Goldstone bosons. The new Higgs Lagrangian is then

$$\begin{aligned} \mathcal{L} &= \frac{1}{2} \text{Tr} [D_\mu M D^\mu M^\dagger] + \frac{m^2}{2} \text{Tr} [M M^\dagger] \\ &- \frac{\lambda}{4} \text{Tr} [M M^\dagger]^2 - \tilde{\lambda} \text{Tr} [M M^\dagger M M^\dagger] - \frac{1}{2} \Pi_a (M_{\text{ETC}}^2)^{ab} \Pi_b, \end{aligned} \quad (2.114)$$

with $m^2 > 0$ and a and b running over the six uneaten Goldstone bosons. The matrix M_{ETC}^2 is dynamically generated and parametrizes our ignorance about the underlying extended technicolor model yielding the specific mass texture. The pseudo Goldstone bosons are expected to acquire masses of the order of a TeV. Direct and computable contributions from the electroweak corrections break $SU(4)$ explicitly down to $SU(2)_L \times SU(2)_R$ yielding an extra contribution to the uneaten Goldstone bosons. However the main contribution comes from the ETC interactions.

The relation between the vacuum expectation value of the Higgs and the parameters of the present theory is

$$v^2 = \langle \sigma \rangle^2 = \frac{m^2}{\lambda + \tilde{\lambda}}. \quad (2.115)$$

In our theory we expect a light composite Higgs whose mass (in the broken phase)⁴ is $2m^2$. This corresponds to a small overall self coupling. In Ref. [49] a Higgs mass in

⁴Note that if one assumes a strongly coupled linear sigma model the relation between the physical mass and the mass parameter in the theory is no longer linear and important modifications are expected [49].

the range $M_H \simeq 90 - 150$ GeV is predicted, see also Subsection 2.2.1. By choosing the fiducial value 125 GeV and recalling that in our conventions we have $M_W = vg/2$, we then find

$$\lambda + \tilde{\lambda} \approx \frac{1}{8}, \quad \text{with} \quad v \approx 250 \text{ GeV}. \quad (2.116)$$

$\lambda + \tilde{\lambda}$ corresponds to the Higgs self coupling in the SM. It turns out that due to the presence of a light Higgs the associated sector can be treated perturbatively. We stress that the expectation of a light composite Higgs relies on the assumption that the quantum chiral phase transition as function of number of flavors near the nontrivial infrared fixed point is smooth and possibly of second order⁵. The composite Higgs Lagrangian is a low energy effective theory and higher dimensional operators will also be phenomenologically relevant.

The Non-Linearly Realized Effective Theory

One can always organize the low energy effective theory in a derivative expansion. The best way is to make use of the exponential map

$$U = \exp\left(i \frac{\Pi^a X^a}{F_\pi^{TC}}\right) E, \quad (2.117)$$

where Π^a represent the nine Goldstone bosons and X^a are the nine generators of $SU(4)$ that do not leave the vacuum invariant (see Appendix B for an explicit realization of the group generators). To introduce the electroweak interactions, one simply adopts the same covariant derivative used for the linearly realized effective theory, see Eqs. (2.106-2.113).

The associated non-linear effective Lagrangian reads

$$\mathcal{L} = \frac{(F_\pi^{TC})^2}{2} \text{Tr} [D_\mu U D^\mu U^\dagger] - \frac{1}{2} \Pi_a (M_{\text{ETC}}^2)^{ab} \Pi_b. \quad (2.118)$$

Still the mass squared matrix parametrizes our ignorance about the underlying ETC dynamics.

A common ETC mass for all the pseudo Goldstone bosons carrying baryon number can be provided by adding the following term to the previous Lagrangian

$$2C \text{Tr} [UBU^\dagger B] + C = \frac{C}{4(F_\pi^{TC})^2} \sum_{i=1}^6 \Pi_B^i \Pi_B^i, \quad (2.119)$$

with

$$B = \frac{1}{2\sqrt{2}} \begin{pmatrix} \mathbb{1} & 0 \\ 0 & -\mathbb{1} \end{pmatrix}. \quad (2.120)$$

Dimensional analysis requires $C \propto \Lambda_{TC}^6 / \Lambda_{ETC}^2$. A similar term can be added to the linearly realized version of our theory.

It is straightforward to add the vector meson sector to these theories, which would then allow to repeat the analysis performed in Ref. [59].

⁵There are provided supporting arguments for this picture in Ref. [49] where the reader will find also a more general discussion of this issue and possible pitfalls.

2.3.4 Feynman Rules

Here we will explain the steps to derive the Feynman rules which are presented in Appendix C. We will use the linearly realized theory up to dimension four operators. First the covariant derivative is rewritten using the mass diagonalized vectors fields

$$igG = ig [T^-W^+ + T^+W^-] + i \frac{g}{\cos \theta_w} Z [T^3 - \sin^2 \theta_w Q] + ieAQ, \quad (2.121)$$

with

$$T^\pm = \frac{T^1 \pm iT^2}{\sqrt{2}}, \quad T^i = \frac{S^i + X^i}{\sqrt{2}}, \quad i = 1, 2, 3, \quad (2.122)$$

$$Q = \sqrt{2} (S^3 + yS^4). \quad (2.123)$$

The electric charge eigenstates of the Goldstone bosons are given by Eqs. (2.97-2.99). Expanding now the kinetic term of the linear realization of the effective theory (Eq. 2.91) there will arise trilinear and quartic couplings.

A note on the notation is that we here use Π^{DD} instead of DD in order to emphasize that derivatives act on the state and not on the first D quark.

Here we will work in the unbroken phase, i.e. the electroweak symmetry is still unbroken, but it is straightforward to make the shift in the VEV of the neutral Higgs field.

Trilinear Couplings

$$\begin{aligned} & -\frac{ig}{2} \sec \theta_w \left[\Pi^{\overline{DD}} \overleftrightarrow{\partial}_\mu \Pi^{DD} - \Pi^{\overline{UU}} \overleftrightarrow{\partial}_\mu \Pi^{UU} + \Pi^{\overline{UD}} \overleftrightarrow{\partial}_\mu \Pi^{\overline{UD}} - i\sigma \overleftrightarrow{\partial}_\mu \Pi^0 \right. \\ & \quad - i2 \sin^2 \theta_w \left((1-y) \Pi^{\overline{DD}} \overleftrightarrow{\partial}_\mu \Pi^{DD} + (1+y) \Pi^{\overline{UU}} \overleftrightarrow{\partial}_\mu \Pi^{\overline{UU}} \right. \\ & \quad \left. \left. + \Pi^{\overline{UD}} \overleftrightarrow{\partial}_\mu \Pi^{\overline{UD}} - y \Pi^{\overline{UD}} \overleftrightarrow{\partial}_\mu \Pi^{UD} \right) \right] Z^\mu \quad (2.124) \end{aligned}$$

$$\begin{aligned} & -ie \left[(1-y) \Pi^{\overline{DD}} \overleftrightarrow{\partial}_\mu \Pi^{DD} + (1+y) \Pi^{\overline{UU}} \overleftrightarrow{\partial}_\mu \Pi^{\overline{UU}} \right. \\ & \quad \left. + \Pi^{\overline{UD}} \overleftrightarrow{\partial}_\mu \Pi^{\overline{UD}} - y \Pi^{\overline{UD}} \overleftrightarrow{\partial}_\mu \Pi^{UD} \right] A^\mu \quad (2.125) \end{aligned}$$

$$-\frac{ig}{2} \left[\Pi^{DD} \overleftrightarrow{\partial}_\mu \Pi^{\overline{UD}} + \Pi^{UD} \overleftrightarrow{\partial}_\mu \Pi^{\overline{UU}} + \Pi^{\overline{UD}} \overleftrightarrow{\partial}_\mu (\Pi^0 + i\sigma) \right] W^{+\mu} \quad (2.126)$$

$$\frac{ig}{2} \left[\Pi^{\overline{DD}} \overleftrightarrow{\partial}_\mu \Pi^{UD} + \Pi^{\overline{UD}} \overleftrightarrow{\partial}_\mu \Pi^{UU} + (i\sigma - \Pi^0) \overleftrightarrow{\partial}_\mu \Pi^{U\overline{D}} \right] W^{-\mu} \quad (2.127)$$

Quartic Couplings

In order to get the terms into this form, the identities of Appendix A.1 have been used.

$$g^2 \Pi^{DD} \Pi^{\overline{UU}} (W^+)^2 \quad (2.128)$$

$$g^2 \Pi^{\overline{DD}} \Pi^{UU} (W^-)^2 \quad (2.129)$$

$$\begin{aligned} & \frac{1}{4} g^2 \left[2 \left(\Pi^{\overline{DD}} \Pi^{DD} + \Pi^{\overline{UD}} \Pi^{U\overline{D}} + \Pi^{\overline{UU}} \Pi^{UU} \right) \right. \\ & \left. + 4 \Pi^{\overline{UD}} \Pi^{UD} + \sigma^2 + (\Pi^0)^2 \right] W_\mu^+ W^{-\mu} \end{aligned} \quad (2.130)$$

$$\begin{aligned} & (g^2 + g'^2) \left[4 \left(\Pi^{\overline{DD}} \Pi^{DD} + \Pi^{\overline{UU}} \Pi^{UU} \right) + 2 \Pi^{\overline{UD}} \Pi^{U\overline{D}} + \sigma^2 + (\Pi^0)^2 \right. \\ & - \frac{1}{2} \sin^2 \theta_w \left\{ 3 \left(\sigma^2 + (\Pi^0)^2 \right) + 10 \Pi^{\overline{UD}} \Pi^{U\overline{D}} \right. \\ & \quad \left. + \Pi^{\overline{DD}} \Pi^{DD} (4 - y) + \Pi^{\overline{UU}} \Pi^{UU} (4 + y) \right\} \\ & + \sin^4 \theta_w \left\{ \frac{3}{2} \left(\sigma^2 + (\Pi^0)^2 \right) + 5 \Pi^{\overline{UD}} \Pi^{U\overline{D}} + 8 y^2 \Pi^{\overline{UD}} \Pi^{UD} \right. \\ & \quad \left. + 2 \left(\Pi^{\overline{DD}} \Pi^{DD} (4 - 5y + 4y^2) + \Pi^{\overline{UU}} \Pi^{UU} (4 + 5y + 4y^2) \right) \right\} \Big] Z^2 \end{aligned} \quad (2.131)$$

$$\begin{aligned} & e^2 \left[\frac{3}{2} \left(\sigma^2 + (\Pi^0)^2 \right) + 5 \Pi^{\overline{UD}} \Pi^{U\overline{D}} + 8 y^2 \Pi^{\overline{UD}} \Pi^{UD} \right. \\ & \left. + 2 \left(\Pi^{\overline{DD}} \Pi^{DD} (4 - 5y + 4y^2) + \Pi^{\overline{UU}} \Pi^{UU} (4 + 5y + 4y^2) \right) \right] A^2 \end{aligned} \quad (2.132)$$

$$\begin{aligned} & g^2 \sec \theta_w \left[\Pi^{\overline{UU}} \Pi^{UD} - \Pi^{DD} \Pi^{\overline{UD}} \right. \\ & + \sin^2 \theta_w \left\{ - \Pi^{\overline{UU}} \Pi^{UD} (y + 1) - \Pi^{\overline{UD}} \Pi^{DD} (y - 1) \right. \\ & \quad \left. + \frac{1}{2} \Pi^{\overline{UD}} (\Pi^0 + i\sigma) \right\} \Big] W_\mu^+ Z^\mu \end{aligned} \quad (2.133)$$

$$\begin{aligned} & g^2 \sec \theta_w \left[\Pi^{UU} \Pi^{\overline{UD}} - \Pi^{\overline{DD}} \Pi^{UD} \right. \\ & + \sin^2 \theta_w \left\{ - \Pi^{UU} \Pi^{\overline{UD}} (y + 1) - \Pi^{UD} \Pi^{\overline{DD}} (y - 1) \right. \\ & \quad \left. + \frac{1}{2} \Pi^{UD} (\Pi^0 - i\sigma) \right\} \Big] W_\mu^- Z^\mu \end{aligned} \quad (2.134)$$

$$\frac{1}{2} e g \left[2 \left(\Pi^{DD} \Pi^{\overline{UD}} (y - 1) + \Pi^{UD} \Pi^{\overline{UU}} (y + 1) \right) - \Pi^{\overline{UD}} (\Pi^0 + i\sigma) \right] W_\mu^+ A^\mu \quad (2.135)$$

$$\frac{1}{2} e g \left[2 \left(\Pi^{\overline{DD}} \Pi^{UD} (y - 1) + \Pi^{\overline{UD}} \Pi^{UU} (y + 1) \right) - \Pi^{UD} (\Pi^0 - i\sigma) \right] W_\mu^- A^\mu \quad (2.136)$$

$$\begin{aligned}
& \frac{1}{4} eg \sec \theta_w \left[\sigma^2 + (\Pi^0)^2 + 6\Pi \bar{U}^D \Pi^{U\bar{D}} + 4 \left(\Pi \bar{D}^D \Pi^{DD} (2-y) + \Pi \bar{U}^U \Pi^{UU} (2+y) \right) \right. \\
& \quad - 2 \sin^2 \theta_w \left\{ \sigma^2 + (\Pi^0)^2 + 6\Pi \bar{U}^D \Pi^{U\bar{D}} + 8y^2 \Pi \bar{U}^D \Pi^{UD} \right. \\
& \quad \quad + 4 \left(\Pi \bar{D}^D \Pi^{DD} (2-3y+2y^2) \right. \\
& \quad \quad \left. \left. \left. + \Pi \bar{U}^U \Pi^{UU} (2+3y+2y^2) \right) \right\} \right] Z_\mu A^\mu \tag{2.137}
\end{aligned}$$

2.3.5 Minimal Coupling to Fermions

We now wish to give masses to ordinary fermions. There are a number of logical possibilities. The traditional way is to assume that Yukawa terms emerge as four fermion interactions generated by ETC at higher energies. We will consider a minimal approach and write down the simplest Yukawa couplings between our Higgs sector and the SM fermions. Experimental deviations from our predictions in this sector will teach us about the underlying theory providing mass to all of the ordinary fermions. Starting with the leptonic sector one can define the following column vector

$$L = \begin{pmatrix} \nu_L \\ e_L \\ -i\sigma^2 \nu_R^* \\ -i\sigma^2 e_R^* \end{pmatrix}. \tag{2.138}$$

Imagine L to transform under the same full $SU(4)$ flavor symmetry under which M of Eq. (2.91) also transforms

$$L \rightarrow g L. \tag{2.139}$$

When gauging the $SU(2)_L$ subgroup we find the correct weak transformation of the left-handed leptons. There is a subtle point to the hypercharge invariance which will be discussed in a moment.

Now it is easy to construct an $SU(4)$ invariant term

$$\mathcal{L}_{\text{lepton-sym}} = Y_{\text{lepton}} L_\alpha^T M^* L_\beta \epsilon^{\alpha\beta} + \text{h.c.}, \tag{2.140}$$

where α, β are spin indices and M is the matrix of Eq. (2.91). When the theory condenses, the following mass term is obtained

$$-v_{\text{weak}} Y_{\text{lepton}} (\bar{\nu}_R \nu_L + \bar{e}_R e_L) + \text{h.c.}. \tag{2.141}$$

Because we have used a larger symmetry than is really observed experimentally, the electron and neutrino masses are degenerate. Such large symmetry is not present in the SM and we need to break the $SU(2)_R$ subgroup of $SU(4)$

$$\begin{aligned}
\mathcal{L}_{\text{lepton-asym}} &= Y_{\text{lepton-D}} L_\alpha^T P_D M^* P_D L_\beta \epsilon^{\alpha\beta} \\
&+ Y_{\text{lepton-U}} L_\alpha^T P_U M^* P_U L_\beta \epsilon^{\alpha\beta} + \text{h.c.}, \tag{2.142}
\end{aligned}$$

where

$$P_{D/U} = \begin{pmatrix} \mathbb{1} & 0 \\ 0 & \frac{\mathbb{1} \mp \tau^3}{2} \end{pmatrix}. \tag{2.143}$$

If we were interested only in the mass terms this would have completed our analysis. In order to extract also interaction terms, one must be sure that the hypercharge is conserved by our Yukawa terms. Now the situation is a little more delicate. Considering still just the leptonic sector, one finds the following transformations

$$\begin{aligned} M &\rightarrow e^{i\alpha(-R^{3T}+\sqrt{2}yS^4)}Me^{i\alpha(-R^3+\sqrt{2}yS^{4T})} \\ &= e^{i\alpha(-R^3+\sqrt{2}yS^4)}Me^{i\alpha(-R^3+\sqrt{2}yS^4)}, \\ L &\rightarrow e^{i\alpha(-R^3-\sqrt{2}S^4)}L. \end{aligned} \quad (2.144)$$

The simplest possible Yukawa term will then transform like

$$L^T M^* L \rightarrow L^T e^{-i\alpha\sqrt{2}(y+1)S^4} M^* e^{-i\sqrt{2}(y+1)S^4} L, \quad (2.145)$$

and we see that the hypercharge parameter y has to be -1 in order to make the Yukawa invariant under hypercharge transformations. One can easily convince oneself that this is still true even when inserting the projection operators $P_{D/U}$ since they commute with the hypercharge generator.

Following the same line for the quarks we obtain

$$Q = \begin{pmatrix} u_L \\ d_L \\ -i\sigma^2 u_R^* \\ -i\sigma^2 d_R^* \end{pmatrix}. \quad (2.146)$$

$$\begin{aligned} \mathcal{L}_{\text{quark-asym}} &= Y_{\text{quark-D}} Q_\alpha^T P_D M^* P_D Q_\beta \epsilon^{\alpha\beta} \\ &+ Y_{\text{quark-U}} Q_\alpha^T P_U M^* P_U Q_\beta \epsilon^{\alpha\beta} + \text{h.c.} . \end{aligned} \quad (2.147)$$

The quark vector transforms as follows under a hypercharge transformation

$$Q \rightarrow e^{i\alpha(-R^3+\frac{\sqrt{2}}{3}S^4)} Q. \quad (2.148)$$

So for the quarks, one would need $y = 1/3$ in order to keep the term invariant. This is a priori in conflict with the result found in the leptonic sector. In principle it would be possible to construct two different matrices M and M' for each sector respectively. But that would go beyond the minimal coupling idea we had in mind in the first place.

Observing that the off-diagonal 2×2 blocks in the matrix i.e. the technibaryonic sector are the problem and the diagonal 2×2 blocks are just corresponding to the SM Higgs sector we can strip away the technibaryonic sector, and we find

$$\begin{aligned} \mathcal{L}_{\text{masses}} &= Y_{\text{quark-D}} Q_\alpha^T P_D M_{\text{off}}^* P_D Q_\beta \epsilon^{\alpha\beta} + Y_{\text{quark-U}} Q_\alpha^T P_U M_{\text{off}}^* P_U Q_\beta \epsilon^{\alpha\beta} \\ &+ Y_{\text{lepton-D}} L_\alpha^T P_D M_{\text{off}}^* P_D L_\beta \epsilon^{\alpha\beta} + Y_{\text{lepton-U}} L_\alpha^T P_U M_{\text{off}}^* P_U L_\beta \epsilon^{\alpha\beta} + \text{h.c.} , \end{aligned} \quad (2.149)$$

where

$$M_{\text{off}} = M - P_1 M P_1 - P_2 M P_2, \quad (2.150)$$

$$P_1 = \text{diag}(1, 1, 0, 0), \quad (2.151)$$

$$P_2 = \text{diag}(0, 0, 1, 1). \quad (2.152)$$

Physically this means that the technibaryonic sector of the theory does not couple to ordinary fermions via the Yukawa interactions in a minimal approach.

The Feynman rules for $\mathcal{L}_{\text{masses}}$ can be found in Appendix C.

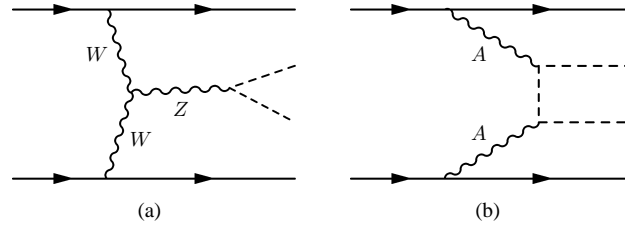


Figure 2.10: Diagrams showing possible production of a charged technibaryon, e.g. the UD state in a pp experiment like the LHC. In (a) WW fusion creates a Z which decays to a technibaryon and an anti-technibaryon. In (b) two photons couple to a technibaryon.

2.3.6 Signatures

It is interesting to consider how the model is significant at the LHC (or later experiments). Will it look exactly like the SM or another extension of the SM or how is it possible to distinguish it from the other extensions.

When modeling, there is always some freedom in choosing the parameters. A crucial choice to make is if the technibaryon number is conserved or if it is broken by some ETC operators. Until now, and for the research done in Chapter 3, we assume it not to be broken. This is essential for the dark matter to survive and be abundant at our late time of the Universe. This choice has consequences for phenomenology at collider experiments, because the initial states in the experiment have no technibaryon number and that will remain so. Pair production is the only option and could be realized like depicted in Fig. 2.10.

Another interesting point to the $SU(2)$ -Adj. model is that it is a vector-like theory with a light (composite) Higgs. This has been investigated by Zerwekh in Ref. [59]. The interesting and somewhat surprising point is that the cross section for Higgs production is enhanced a lot (up to above 100% for a certain mass of the neutral techni- ρ) compared to the SM Higgs cross section, by the presence of the techni- ρ .

A project which is in progress is to implement the model into a computer programme which is called MadGraph [61, 62]. The programme is a tool which computes all possible processes when given some initial states and some final states and makes corresponding programmes which uses HELAS [63] routines. Then a connected programme called MadEvent is used to compute the phase space integrals for the cross sections via a fast Monte Carlo method [61]. As mentioned this is in progress and the model is already implemented, but is still in the testing phase (which is the most time-consuming). The trick with this programme is that it computes *a lot* of diagrams quickly to get cross sections of different processes, but also that the output of the programme is compatible with event simulation software such as PYTHIA. With such software at hand, it would be possible to get an idea of which signatures would drown in e.g. QCD background and which would not.

CHAPTER 3

Dark Matter

3.1 Introduction

The cosmological implications of explaining the dark matter problem and the dark energy problem in particle physics has become a popular tool to further constrain the theory in question. We will here explain briefly what is dark matter and what are the observational evidences for its existence.

Here we consider the standard model of cosmology (with a big bang and inflation) where it is observed that the Universe on large scales is homogeneous and isotropic. Writing down the most generic space-time metric, the Robertson-Walker metric

$$ds^2 = dt^2 - R^2(t) \left[\frac{dr^2}{1 - kr^2} + r^2 (d\theta^2 + \sin^2 \theta d\phi^2) \right], \quad (3.1)$$

two quantities are included, which are the cosmological scale factor $R(t)$ and the curvature constant k . By rescaling r there are three different values k can take on; 1, -1 or 0, which corresponds to a closed, an open and a flat Universe, respectively.

Starting by the Einstein equations

$$R_{\mu\nu} - \frac{1}{2}g_{\mu\nu}\mathcal{R} = 8\pi G_N T_{\mu\nu} + \Lambda g_{\mu\nu}, \quad (3.2)$$

where $R_{\mu\nu}$ is the Ricci tensor, $g_{\mu\nu}$ is the metric, \mathcal{R} is the Ricci scalar, G_N is the Newton constant, $T_{\mu\nu}$ is the energy-momentum tensor and Λ is a cosmological constant. Then it is common to assume that the matter in the Universe can, to good approximation, be described by a perfect fluid which gives the following energy-momentum tensor

$$T_{\mu\nu} = -p g_{\mu\nu} + (p + \rho) u_\mu u_\nu, \quad (3.3)$$

where p is the pressure, ρ the energy density and u the velocity in co-moving coordinates. This leads to the Friedmann-Lemaître equations

$$H^2 = \frac{\dot{R}^2}{R^2} = \frac{8\pi G_N \rho}{3} - \frac{k}{R^2} + \frac{\Lambda}{3} \quad \text{and} \quad \frac{\ddot{R}}{R} = \frac{\Lambda}{3} - \frac{4\pi G_N}{3}(\rho + 3p), \quad (3.4)$$

where $H(t)$ is the Hubble parameter. The Friedmann equation can then be rewritten into the following form

$$(\Omega - 1)H^2 = \frac{k}{R^2}, \quad (3.5)$$

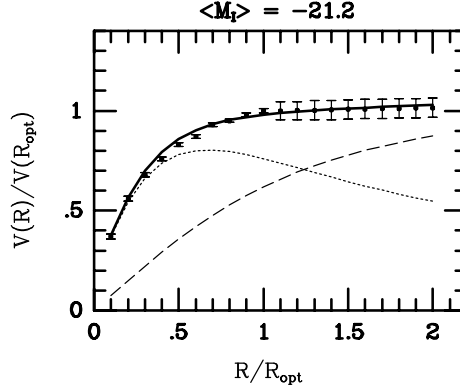


Figure 3.1: Synthetic rotation curve for galaxies with $\langle M_I \rangle = -21.2$, where $\langle M_I \rangle$ is a measure for the luminosity, R/R_{opt} is the distance measured from the center of the galaxy normalized by the optical radius and V is the velocity. The figure is taken from Ref. [6].

where Ω is the total “energy” i.e. matter plus vacuum energy or cosmological constant and it is defined via the critical density

$$\Omega \equiv \frac{\rho}{\rho_{\text{critical}}}, \quad (3.6)$$

where the critical density ρ_{critical} would render the Universe geometrically flat. We can write

$$\Omega = \Omega_m + \Omega_\Lambda = \Omega_B + \Omega_{dm} + \Omega_\Lambda, \quad (3.7)$$

where $\Omega = \Omega_{\text{tot}}$ is the total energy density, Ω_m is the matter density, Ω_Λ is the density associated with the cosmological constant term, Ω_B is the density of the baryons, Ω_{dm} is the density of the dark matter, and all the energy densities are in units of the critical density. As it is seen from the equation, the matter density is a sum of the baryon density and the dark matter density, which we will argue next.

One of the direct observational evidences of dark matter is found on the scale of galactic halos where there is observed flatness in the rotation curves of the spiral galaxies, see Fig. 3.1. On these large scales one would expect that the gravitational field is undisturbed by the small masses far apart and thus Newtonian gravity would hold, giving

$$M(r) \propto v^2 r / G_N, \quad (3.8)$$

where M is the mass of the galaxy (in the center), v is the velocity, r the distance measured from the center of the galaxy and G_N is Newton’s constant. This of course assumes that the galaxies are in virial equilibrium. The figure shows a compilation of almost 1000 rotation curves of spiral galaxies restricted to a narrow range in brightness characteristic for a lot of spiral galaxies. Eq. (3.8) implies that outside the bulk of the galaxy the velocity should go as

$$v \propto 1/\sqrt{r}, \quad (3.9)$$

which is not what is seen in Fig. 3.1. On the contrary $v \sim \text{constant}$ outside the bulk, which implies that $M \propto r$, outside where there is no light. Dark matter has also been confirmed in elliptical galaxies, see Refs. [64, 65].

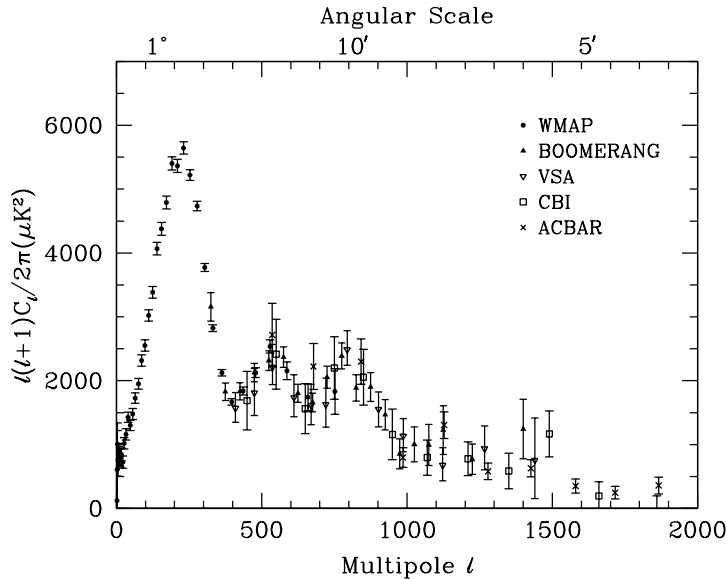


Figure 3.2: Power in the CMB anisotropy spectrum measured by WMAP and others. The figure is taken from Ref. [7].

There has also been great development in the determination of the matter and cosmological densities. One of the tools are the Cosmic Microwave Background (CMB) anisotropy experiments which have made estimates of the curvature with uncertainties down to the few percent level. In fact, the CMB was a prediction of the big bang nucleosynthesis (BBN). The argument goes like this. The minimum temperature for which the BBN can function, relates via the standard model time-temperature relation, to the maximum time scale. Together with the typical cross section for the first link in the nucleosynthesis chain one can compute the necessary density. Knowing the density of baryonic matter and that the density scales like $R^{-3} \sim T^3$, the temperature today is found to be ~ 10 K.

A lot of information is encoded into the angular expansion of the CMB temperature

$$T(\theta, \phi) = \sum_{lm} a_{lm} Y_{lm}(\theta, \phi), \quad (3.10)$$

where the monopole term characterizes the mean temperature of the CMB. It has been determined by the COBE satellite to be 2.725 ± 0.002 K [66]. The dipole term can be found from the Doppler shift produced by our peculiar motion with respect to the CMB. Higher order multipoles contain information about the energy density perturbations in the early Universe. The power spectrum has been measured up to $l \sim 2000$, see Fig. 3.2. The values from a fit of the WMAP data to the Λ CDM model¹ [8] are shown in Table 3.1. The fit of Ω_Λ from the WMAP data gives $0.758^{+0.035}_{-0.058}$ which renders the total energy budget close to one [8]. In fact, the fits are so close to one, that it is not possible to tell whether the curvature constant k is negative or positive. It is seen from

¹The Λ CDM model means a model with a cold dark matter candidate and a cosmological constant, on top of the standard inflationary scenario.

Table 3.1: Fitted parameters from WMAP data [8].

	WMAP three year mean
$100\Omega_B h^2$	2.23 ± 0.08
$\Omega_m h^2$	0.126 ± 0.009
H_0	74 ± 3
τ	0.093 ± 0.029
n_s	0.961 ± 0.017

Fig. 3.3 that the WMAP data prefers an almost flat Universe. Combining the WMAP data with the data from supernovae (SNe) observations (the middle panel in Fig. 3.3) it is seen that the matter density is ~ 0.3 and the total density is ~ 1 (the black straight line is $\Omega = 1$). It is also noticed that the matter density is far greater than ~ 0.04 which is shown in Table 3.1. This is one of the indications that there is more matter than is visible. A notion commonly used, is the following measure for red-shift

$$1 + z \equiv \frac{\lambda_0}{\lambda_1}, \quad (3.11)$$

where λ_0 is the detected wavelength and λ_1 is the emitted wavelength. One of the advantages with the SNe measurements are the high- z analysis which leads to a good test of the cosmological geometry, thus Ω and k [67].

Theoretically there is support for the fact that more energy is present in the Universe than what is observed as baryonic matter. The inflationary scenario suggests that $\Omega_{\text{tot}} \simeq 1$ [68]. The following simple solution to the curvature problem shows why Ω_{tot} is expected to be so close to unity. At present point we do not know if Ω_{tot} is smaller or greater than one and thus not the sign of the curvature constant. This is because that the curvature term in Eq. (3.4) is subdominant. For a radiation dominated gas we have $R \sim T^{-1}$. Assuming now an adiabatically expanding Universe, the quantity

$$\hat{k} \equiv \frac{k}{R^2 T^2} = (\Omega_0 - 1) \frac{H_0^2}{T_0^2} < 2 \times 10^{-58}, \quad (3.12)$$

is dimensionless and a constant (and the subscripts refer to the present-day values). This constant would be expected to be of order one, but it is quite far off, which is a kind of a hierarchy problem. This problem is called the curvature problem and one way to deal with this is by inflation. Denote by $R = R_i$, $T = T_i$ the initial values and $R_i \sim T_i^{-1}$. During inflation, we have $R \sim e^{Ht}$, with H constant. After the inflation $R \gg R_i$ and $T = T_R \lesssim T_i$ with T_R the reheating temperature. This implies RT and \hat{k} are not constants and $\hat{k} \rightarrow 0$. But if $\hat{k} \rightarrow 0 \Rightarrow \Omega_{\text{tot}} \rightarrow 1$. As the inflation is exponential, Ω_{tot} becomes exponentially close to unity.

By the use of BBN calculations it is possible to determine Ω_B from the abundances of D, ${}^4\text{He}$, and ${}^7\text{Li}$, and not surprisingly it gives values comparable to those of the CMB anisotropy analysis.

Finally evidence for dark matter is found from gravitational lensing [69]. Systematic lensing of about 150,000 galaxies per degree at redshifts $z = 1 - 3$ makes it possible to estimate the matter distribution in the foreground cluster. The lensing is usually categorized into strong lensing and weak lensing and both seem consistent with the existence of dark matter.

The problem left is to predict what constitutes this dark matter, what type of particles/objects they are and how do they behave? There are quite a number of candidates;

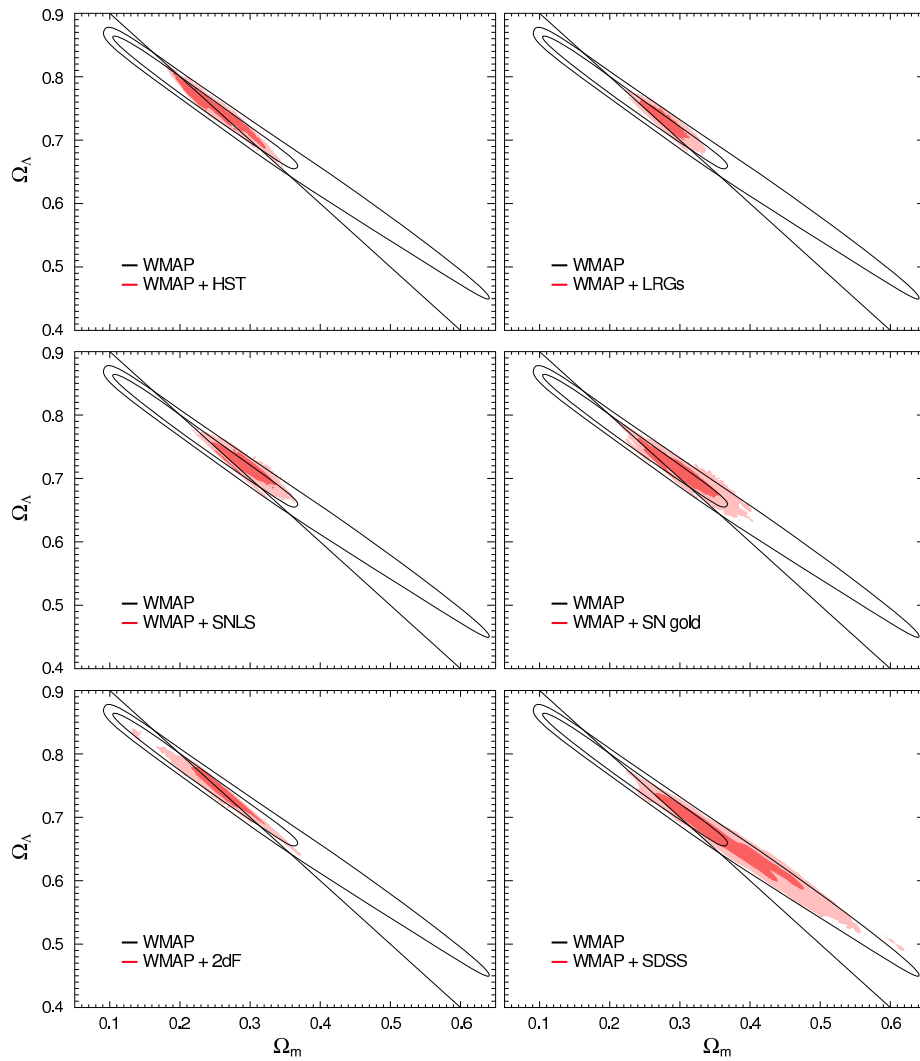


Figure 3.3: Phase space of $(\Omega_m, \Omega_\Lambda)$ with WMAP and additional data. The figure is taken from Ref. [8].

baryonic particles, hydrogen, Jupiter-like objects which also are called massive compact halo objects (MACHOs), remnants of massive stars, black holes, neutrinos, heavy neutrino-like objects which are in the class of weakly interacting massive particles (WIMPs), axions, and finally also technibaryonic types which we will consider in the next section.

It is quite involved to consider all of the candidates for dark matter in depth and we will thus refer to the literature. It is however useful to know that strong limits are coming up on the different types of dark matter (we will later consider some detection limits for WIMPs). For example the MACHOs are testable via gravitational lensing of stars in a neighboring galaxy e.g. the LMC. This puts constraints on the amount of MACHO the Universe can have and it is found that MACHOs cannot take up the whole dark matter amount but only a fraction. Neutrinos have limits coming from supernovae type Ia data and the HST Key project data as well as from BBN. The mass is restricted to be either very small or quite heavy in order to be a viable dark matter candidate. If the mass is small it is a so-called hot dark matter candidate. The problem with the hot dark matter is that it reacts too much and will smear out the structure formation at large scales [70]. Thus cold dark matter (CDM) candidates who are assumed to cluster are considered more viable.

For further reading we refer to Refs. [71, 72, 73, 68].

3.2 Computing the LTB Relic Density.

We are now considering the $SU(2)$ -Adj. technicolor model of Section 2.3 and then explicitly compute the DD -type boson relic density in the case where it is neutral and stable (i.e. $y = 1$). We will use in the computations, the assumption of thermal equilibrium and overall electric neutrality, as well as the conserved technibaryon quantum number.

In the next section we will take into account the experimental limits from earth based dark matter search experiments and figure out what is the relic density, in percent of the measured dark matter density, and what the mass of the particle will be.

Finally, we will in the last section of this chapter speculate how good is the assumption of thermal equilibrium.

We impose thermal equilibrium and overall electric neutrality for the matter in the Universe. Imposing overall electrical neutrality avoids the huge energetic Coulomb costs due to electric fields of the otherwise uncanceled charges in the Universe. In addition to the theoretical reasons, observations confirm an overall neutrality. Thermal equilibrium occurs among different particles as long as their rate of interaction Γ is much larger than the expansion rate of the Universe H , where H is the Hubble constant. If $H > \Gamma$ at a given time, the particles decouple from each other and hence can no longer be in thermal equilibrium.

At some energy scale higher than the electroweak one, following the work of Nussinov [74], we assume the existence of a mechanism leading to a technibaryon asymmetry in the Universe. Given that the technibaryon and baryon number have a very similar nature such an asymmetry is very plausible and can have a common origin. Here we will not speculate further on the origin of the (techni)baryon asymmetry, but will relate it to the observed baryon asymmetry as done by Nussinov as well as in Ref. [75].

Even if one is able to produce an asymmetry above or around the electroweak scale, the (techni)baryon number is spoiled by quantum anomalies. Fortunately, although the baryon (B), technibaryon (TB), lepton (L) number and the new lepton number for the

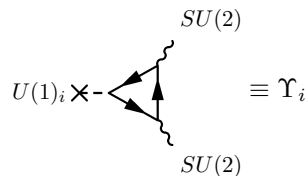


Figure 3.4: Triangle diagram giving rise to the anomaly that breaks e.g. the baryon number or the lepton number for $i = B, L$ respectively. The two bosons are the gauge bosons of the $SU(2)_L$ group. The particles looping in the triangle are left-handed particles with charge i .

new lepton family (L'), are not conserved individually, their differences, e.g. $B - L$ and $3TB - L$ are preserved.

This is seen from the contributions of the triangle diagrams of the type shown in Fig. 3.4. For the $U(1)_B$ of the baryon number the diagram is proportional to

$$\Upsilon_B \sim \frac{1}{3} N_g N_c, \quad (3.13)$$

where the fraction $1/3$ is the baryon number of a single quark, N_g is number of number of generations in the SM and N_c is the number of colors. For the leptons we have

$$\Upsilon_L \sim N_g, \quad (3.14)$$

where the lepton number is unity. In order to construct a conserved current, one simply subtracts the two anomalous currents

$$\partial_\mu (J_B^\mu - J_L^\mu) = 0, \quad (3.15)$$

and the conserved quantum number is $B - L$, where $B = B_1 + B_2 + B_3$ and $L = L_e + L_\mu + L_\tau$.

This is all well known, but it is useful to see explicitly when constructing the new conserved quantum numbers. For the technibaryons, the anomaly contribution reads

$$\Upsilon_{TB} \sim \frac{1}{3} \frac{N_{tc}(N_{tc} + 1)}{2} = 1 \quad \text{for } N_{tc} = 2, \quad (3.16)$$

where N_{tc} is the number of technicolors, $1/3$ is the technibaryon number per techniquark and the remaining factor is the number of colors in the $SU(2)$ -Adj. model. For the new lepton family we assign the quantum number L' and the anomaly contribution is

$$\Upsilon_{L'} \sim 1, \quad (3.17)$$

where unity has been assigned to a single new lepton. By constructing conserved currents with the new constituents in the model we can make a series of “good” quantum numbers (for $N_g = 3$)

$$B - L, \quad 3TB - L, \quad 3L' - L, \quad (3.18)$$

$$TB - L', \quad B - 3L', \quad 3TB - B. \quad (3.19)$$

These quantum numbers are very useful to have in mind when constructing the sphaleron process later.

The fact that both $B - L$ and $3TB - L$ are conserved allows for a nonzero (techni)-baryonic asymmetry to survive. The process leading to a violation of $B + L$ and $3TB + L$, but conservation of the above quantum numbers, is termed a ‘‘sphaleron’’ process and is at the present time negligible. However this process was active during the time the Universe had a temperature above or at the scale of the electroweak symmetry breaking (~ 250 GeV). Indeed this process was rapid enough to thermalize baryons, leptons and technibaryons. At some point as the Universe expands and its temperature falls, the baryon-lepton-technibaryon number violating process ceases to be significant. The precise value of this temperature T^* depends on the underlying theory driving electroweak symmetry breaking. Within the SM framework and assuming the validity of the semi-classical calculation of the tunneling effect [76], T^* has been estimated by equating the rate of the sphaleron process to H . According to Ref. [76], T^* satisfies the following equation

$$T^* = \frac{2M_W(T^*)}{\alpha_w \ln\left(\frac{M_{Pl}}{T^*}\right)} B\left(\frac{\lambda}{\alpha_w}\right), \quad (3.20)$$

where M_W is the mass of the W bosons, M_{Pl} is the Planck scale, α_w is the weak coupling constant, λ is the self coupling of the Higgs boson and $B(\lambda/\alpha_w)$ is a function that takes on values from 1.5 to 2.7 as the ratio λ/α_w goes from zero to infinity [76, 77]. As we already mentioned, this formula is an approximation and it depends on the not very well known ratio of λ/α_w . According to what is the value of this ratio, T^* can vary within the 150 – 250 GeV range. In technicolor theories, since the Higgs is a composite object, the self-coupling λ is in principle calculable. An estimation $\lambda = 1/8$ for our specific model was given in Ref. [49]. Since $\alpha_w = 1/29$ (or a bit smaller at the electroweak scale), the ratio λ/α_w gives a T^* around 200 GeV.

Now it is time to introduce the chemical potentials for the relevant particle species. We here follow Ref. [78]

$$\begin{array}{llll} \mu_W & \text{for } W^- & \mu_{dL} & \text{for } d_L, s_L, b_L \\ \mu_0 & \text{for } \phi^0 & \mu_{dR} & \text{for } d_R, s_R, b_R \\ \mu_- & \text{for } \phi^- & \mu_{iL} & \text{for } e_L, \mu_L, \tau_L \\ \mu_{uL} & \text{for } u_L, c_L, t_L & \mu_{iR} & \text{for } e_R, \mu_R, \tau_R \\ \mu_{uR} & \text{for } u_R, c_R, t_R & \mu_{\nu iR} & \text{for } \nu_{eR}, \nu_{\mu R}, \nu_{\tau R} \\ \mu_{\nu iL} & \text{for } \nu_{eL}, \nu_{\mu L}, \nu_{\tau L} & & \end{array}$$

where the indices L and R denote chirality. We have a common chemical potential for the up, charm and top quarks, and a different one for the other triplet of down, strange and bottom. A common chemical potential has to do with the fact that at the scale of interest, QCD interactions put quarks of the same charge on equal footing. We introduce a different chemical potential for all of the leptons. Also in order to be as general as possible we have assumed the existence of right handed neutrinos and introduced different chemical potentials for the left and the right handed particles. The

thermal equilibrium conditions associated to the weak interactions read

$$\mu_W = \mu_- + \mu_0 \quad (W^- \leftrightarrow \phi^- + \phi^0), \quad (3.21)$$

$$\mu_{dL} = \mu_{uL} + \mu_W \quad (W^- \leftrightarrow \bar{u}_L + d_L), \quad (3.22)$$

$$\mu_{iL} = \mu_{\nu iL} + \mu_W \quad (W^- \leftrightarrow \bar{\nu}_{iL} + e_{iL}), \quad (3.23)$$

$$\mu_{\nu iR} = \mu_{\nu iL} + \mu_0 \quad (\phi^0 \leftrightarrow \bar{\nu}_{iL} + \nu_{iR}), \quad (3.24)$$

$$\mu_{uR} = \mu_0 + \mu_{uL} \quad (\phi^0 \leftrightarrow \bar{u}_L + u_R), \quad (3.25)$$

$$\mu_{dR} = -\mu_0 + \mu_W + \mu_{uL} \quad (\phi^0 \leftrightarrow d_L + \bar{d}_R), \quad (3.26)$$

$$\mu_{iR} = -\mu_0 + \mu_W + \mu_{\nu iL} \quad (\phi^0 \leftrightarrow e_{iL} + \bar{e}_{iR}), \quad (3.27)$$

where it is understood that the Higgs is a composite of two techniquarks. The Goldstone bosons of Eq. (2.88) are gauged under the weak symmetry and hence we introduce the following chemical potential for these Goldstone bosons and the new lepton family of Eq. (2.64)

$$\begin{array}{llll} \mu_{\zeta L} & \text{for } \zeta_L & \mu_{UU} & \text{for } UU \\ \mu_{\zeta R} & \text{for } \zeta_R & \mu_{UD} & \text{for } UD \\ \mu_{\nu' L} & \text{for } \nu_{\zeta L} & \mu_{DD} & \text{for } DD \\ \mu_{\nu' R} & \text{for } \nu_{\zeta R} & & \end{array}$$

The corresponding thermal equilibrium equations for the extra particles introduced by the technicolor theory per se are

$$\mu_{\zeta L} = \mu_W + \mu_{\nu' L} \quad (\zeta_L \leftrightarrow W^- + \nu_{\zeta L}), \quad (3.28)$$

$$\mu_{UD} = \mu_{DD} - \mu_W \quad (DD \leftrightarrow UD + W^-), \quad (3.29)$$

$$\mu_{UU} = \mu_{UD} - \mu_W = \mu_{DD} - 2\mu_W \quad (UD \leftrightarrow UU + W^-), \quad (3.30)$$

$$\mu_{\zeta R} = -\mu_0 + \mu_{\zeta L} \quad (\phi^0 \leftrightarrow \zeta_L + \bar{\zeta}_R), \quad (3.31)$$

$$\mu_{\nu' R} = \mu_0 + \mu_{\nu' L} \quad (\phi^0 \leftrightarrow \bar{\nu}_{\zeta L} + \nu_{\zeta R}), \quad (3.32)$$

where Eq. (3.29) has been used in Eq. (3.30).

Each classical gauge and scalar field configuration with a given topological number leads to a simultaneous jump for *all* of the anomalous charges. Hence each quark-doublet generation, lepton-doublet generation, the new lepton family number as well as techniquark number are violated by the same classical field configuration. The one loop anomalous coefficient dictates the relative amount of the jump for each anomalous charge when turning on a given classical field configuration.

With the normalization of 1/3 for the technibaryonic charge for our techniquarks and 1/3 for the ordinary quark-baryonic charge of the quarks, 1 for all of the leptons, the simplest classical configuration with one unit of topological charge will induce a transition from the vacuum of the theory to a state containing three baryons (per each generation), one lepton (for each generation), a technibaryon-like object with three technibaryons and one new lepton. The explicit construction of the sphaleron process is

Vacuum \Rightarrow

$$\prod_{i=1}^3 \left(\epsilon^{f\bar{f}} \epsilon^{f'\bar{f}'} \epsilon_{abc} \psi_{i,f}^a \psi_{i,\bar{f}}^b \psi_{i,f'}^c \psi_{i,\bar{f}'} \right) \times \left(\epsilon^{f\bar{f}} \epsilon^{f'\bar{f}'} \epsilon_{ABC} Q_f^A Q_{\bar{f}}^B Q_{f'}^C \mathcal{L}_{\bar{f}'} \right), \quad (3.33)$$

where ψ are SM quarks, l SM leptons, Q techniquarks, \mathcal{L} the new leptons, the product is over the SM generations with i a generation index, f, \bar{f} $SU(2)_L$ indices taking on values which are either the first or the second constituent in an $SU(2)_L$ doublet, a, b, c are QCD-color indices and finally A, B, C are technicolor adjoint indices. We see that it is necessary to have three techniquarks in the sphaleron process in order to have a weak charge neutral and in the same time a electric charge neutral object. Thus the technibaryon number is defined as $1/3$ per techniquark even though the technibaryonic sector will consist of only two techniquarks.

The relation among the chemical potentials emerging from the above is

$$3(\mu_{u_L} + 2\mu_{d_L}) + \mu + \frac{1}{2}\mu_{UU} + \mu_{DD} + \mu_{\nu'} = 0. \quad (3.34)$$

The parameter μ is defined as $\sum_i \mu_{\nu_i L} \equiv \mu$. We have assumed that the difference in the baryon number between two different quark-doublet generations is created identically before the electroweak phase transition. A similar relation will be assumed for the lepton charges. Note that the difference is not affected by the weak anomaly and hence will not be generated later on.

We can now turn to the calculation of number densities. The difference between the number densities of particles and their corresponding antiparticles is given by

$$n = n_+ - n_- = g \int \frac{d^3 k}{(2\pi)^3} \frac{1}{z^{-1} e^{E\beta} - \eta} - g \int \frac{d^3 k}{(2\pi)^3} \frac{1}{z e^{E\beta} - \eta}, \quad (3.35)$$

where n_+ and n_- are the number densities of the particles and antiparticles, respectively. The constant g is the multiplicity of the degrees of freedom (spin for example), $\beta = 1/T$ in units $k_B = 1$, and η takes on the values 1 and -1 for bosons and fermions, respectively. The fugacity $z = e^{\mu\beta}$ and E is the energy. The ratio μ/T is sufficiently small in the Universe, that we can Taylor expand the above relation. The number density now can be written as

$$n = \begin{cases} gT^3 \frac{\mu}{T} \mathcal{F} \left(\frac{\mu}{T} \right) & \text{for fermions,} \\ gT^3 \frac{\mu}{T} \mathcal{G} \left(\frac{\mu}{T} \right) & \text{for bosons,} \end{cases} \quad (3.36)$$

where the functions \mathcal{F} and \mathcal{G} are defined as follows

$$\mathcal{F}(z) = \frac{1}{4\pi^2} \int_0^\infty dx x^2 \cosh^{-2} \left(\frac{1}{2} \sqrt{x^2 + z^2} \right), \quad (3.37)$$

$$\mathcal{G}(z) = \frac{1}{4\pi^2} \int_0^\infty dx x^2 \sinh^{-2} \left(\frac{1}{2} \sqrt{x^2 + z^2} \right). \quad (3.38)$$

We now differentiate two cases according to the order of the electroweak phase transition. In the case of a second order or weak first order electroweak phase transition we expect that the temperature T^* is below the temperature of the phase transition. This means that the baryon, lepton and technibaryon violating process persists after the phase transition. The second possibility is to have a strong first order phase transition where the violating process freezes right at the phase transition. We are going to examine separately the two different cases.

Assuming that the violating process persists even after the phase transition, we need to impose two conditions: Electric neutrality and that $\mu_0 = 0$, since the Higgs boson condenses and the electroweak symmetry breaks spontaneously. Recall that we can

introduce a nonzero chemical potential only for unbroken symmetries whose generators commute with all of the gauge ones. Here the Higgs boson is a composite particle, made of techni-up and techni-down quarks $(\bar{U}U + \bar{D}D)/\sqrt{2}$. Therefore when we refer to μ_0 as the chemical potential, we mean the chemical potential of the composite object.

From Eq. (3.36) we see that the number densities, in the leading approximation, are linear in the chemical potential for small μ/T . For convenience we express the baryon number density as

$$B \equiv \frac{n_B - n_{\bar{B}}}{gT^2/6}. \quad (3.39)$$

We shall use the same normalization (dividing the number density by $gT^2/6$) also for the lepton number, technibaryon number etc. Since in the end we only care for ratios of number densities, the normalization constant cancels out.

We conveniently define the function σ as follows

$$\sigma_i = \begin{cases} 6\mathcal{F}\left(\frac{m_i}{T^*}\right) & \text{for fermions,} \\ 6\mathcal{G}\left(\frac{m_i}{T^*}\right) & \text{for bosons,} \end{cases} \quad (3.40)$$

where \mathcal{F} and \mathcal{G} are those of Eq. (3.37) and (3.38), respectively and the index i refers to the particle in question.

For all of the SM particles, the statistical function is taken to be 1 and 2 for massless fermions and bosons, respectively, except for the top quark which we treat massive, as m_t is of order T^* . The reason why we can take the other SM particles to be massless in the statistical function is that $m \ll T^*$. However, the technibaryons as well as the particles of the new lepton family have masses that cannot be ignored. We should emphasize that we calculate the baryon and lepton numbers at the temperature T^* where the sphaleron dies out.

The baryon density can be written as

$$\begin{aligned} B &= \frac{3}{3} [(2 + \sigma_t)(\mu_{uL} + \mu_{uR}) + 3(\mu_{dL} + \mu_{dR})], \\ &= (10 + 2\sigma_t)\mu_{uL} + 6\mu_W + (\sigma_t - 1)\mu_0, \end{aligned} \quad (3.41)$$

where Eqs. (3.22), (3.25) and (3.26) have been used and the factor in the first line includes number of colors and the baryon number of each quark, which is $1/3$. The factor 3 of the down-type quarks is the number of families and equivalently the factor $2 + \sigma_t$ is the number of families taking into account the top mass effect.

Similarly the lepton number for the SM leptons is

$$\begin{aligned} L &= \sum_i (\mu_{\nu iL} + \mu_{\nu iR} + \mu_{iL} + \mu_{iR}), \\ &= 4\mu + 6\mu_W. \end{aligned} \quad (3.42)$$

For the new lepton family we have

$$\begin{aligned} L' &= \sigma_\zeta(\mu_{\zeta L} + \mu_{\zeta R}) + \sigma_{\nu'}(\mu_{\nu' L} + \mu_{\nu' R}), \\ &= 2(\sigma_{\nu'} + \sigma_\zeta)\mu_{\nu' L} + 2\sigma_\zeta\mu_W + (\sigma_{\nu'} - \sigma_\zeta)\mu_0. \end{aligned} \quad (3.43)$$

Similarly for the technibaryons we get

$$\begin{aligned} TB &= \frac{2}{3}(\sigma_{UU}\mu_{UU} + \sigma_{UD}\mu_{UD} + \sigma_{DD}\mu_{DD}), \\ &= \frac{2}{3}(\sigma_{UU} + \sigma_{UD} + \sigma_{DD})\mu_{DD} - \frac{2}{3}(\sigma_{UD} + 2\sigma_{UU})\mu_W. \end{aligned} \quad (3.44)$$

The charge constraint for all the particles is

$$\begin{aligned}
Q &= \frac{2}{3} \cdot 3(2 + \sigma_t)(\mu_{uL} + \mu_{uR}) - \frac{1}{3} \cdot 3 \cdot 3(\mu_{dL} + \mu_{dR}) \\
&\quad - \sum_i (\mu_{iL} + \mu_{iR}) - 2 \cdot 2\mu_W - 2\mu_- \\
&\quad + 2\sigma_{UU}\mu_{UU} + \sigma_{UD}\mu_{UD} - 2\sigma_\zeta(\mu_{\zeta L} + \mu_{\zeta R}) - \sigma_{\nu'}(\mu_{\nu' L} + \mu_{\nu' R}). \quad (3.45)
\end{aligned}$$

For the first order phase transition we will need also the neutrality with respect to the weak isospin charge which is

$$\begin{aligned}
Q_3 &= \frac{3(2 + \sigma_t)}{2}\mu_{uL} - \frac{3 \cdot 3}{2}\mu_{dL} + \frac{1}{2} \sum_{i=1}^3 (\mu_{\nu i L} - \mu_{iL}) - 4\mu_W - (\mu_0 + \mu_-) \\
&\quad + (\sigma_{UU}\mu_{UU} - \sigma_{DD}\mu_{DD}) + \frac{1}{2}(\sigma_{\nu'}\mu_{\nu' L} - \sigma_\zeta\mu_{\zeta L}). \quad (3.46)
\end{aligned}$$

The need for the isospin neutrality condition, in the first order case, comes from the fact that we are computing our final relic densities above the electroweak phase transition where the weak isospin is unbroken.

Since it is not clear whether the electroweak phase transition is first or second order, we should examine both cases. It is expected as in Ref. [78] that a strong first order phase transition occurs fast enough to “freeze” the baryon and technibaryon violating process just at the transition. In this case one calculates the equilibrium conditions just before the transition. On the other hand, in a second order phase transition we expect the violating process to persist below the phase transition and the equilibrium conditions are imposed after the phase transition. If the phase diagram as function of temperature and density of our technicolor theory would be known, a specific order of the electroweak phase transition would be used.

When the ratio between the number densities of the technibaryons to the baryons is determined, we have

$$\frac{\Omega_{TB}}{\Omega_B} = \frac{3}{2} \frac{TB}{B} \frac{m_{LTB}}{m_p}, \quad (3.47)$$

here m_{LTB} is the mass of the LTB (the m_{DD}) and m_p is the mass of the proton.

Note that a possible mixing between the new family and an ordinary SM family would dilute the relative ν_ζ abundance and eventually annihilate L' .

3.2.1 2nd Order Phase Transition

Here the two conditions we have to impose are: Overall electrical neutrality and $\mu_0 = 0$ for the chemical potential of the Higgs boson. The ratio between the number density of the technibaryons to the baryons can be expressed as function of the L/B and L'/B ratios. In order to provide a simple and compact expression, we consider the limiting case in which the UU and UD technibaryons are substantially heavier than the DD companion, the top is light with respect to the electroweak phase transition temperature and the new lepton family is degenerate, i.e. $\sigma_\zeta = \sigma_{\nu'}$. In this approximation the ratio simplifies to

$$-\frac{TB}{B} = \frac{\sigma_{DD}}{3(18 + \sigma_{\nu'})} \left[(17 + \sigma_{\nu'}) + \frac{(21 + \sigma_{\nu'})}{3} \frac{L}{B} + \frac{2}{3} \frac{(9 + 5\sigma_{\nu'})}{\sigma_{\nu'}} \frac{L'}{B} \right]. \quad (3.48)$$

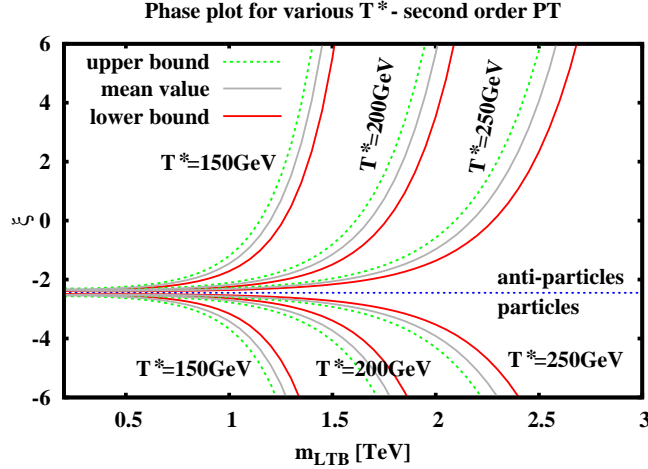


Figure 3.5: Plot representing the region of the parameters according to which the fraction of technibaryon matter density over the baryonic one takes on the values $[3.23, 5.55]$. We consider here a second order phase transition. The parameters in the plot are the mass of the LTB dark matter particle and ξ of Eq. (3.49). The plot includes various values of T^* . The dotted line separates areas of abundant particles and anti-particles.

The results of the calculation are summarized in Fig. 3.5. This figure shows what are the allowed values of the parameter ξ defined below, as a function of the mass of the LTB, for a given T^* , if the LTB accounts for the whole dark matter density of the Universe. The parameter ξ can be considered, roughly speaking, as the total ratio of lepton over baryon number density, with the new lepton family number density L' weighted “appropriately” due to the large mass that ν_ζ and ζ carry.

For convenience, with respect to plotting the results, we define the following parameter

$$\xi \equiv \frac{L}{B} + \frac{2}{\sigma_{\nu'}} \frac{9 + 5\sigma_{\nu'}}{21 + \sigma_{\nu'}} \frac{L'}{B}. \quad (3.49)$$

With this definition at hand the ratio of technibaryons to baryons reads

$$-\frac{TB}{B} = \frac{\sigma_{DD}}{3(18 + \sigma_{\nu'})} \left[(17 + \sigma_{\nu'}) + \frac{(21 + \sigma_{\nu'})}{3} \xi \right]. \quad (3.50)$$

From Fig. 3.5 we see for example that if $L' = 0$ (no new leptons present) while also having $L/B = -4$, we need a mass for the LTB somewhere between 1.1 to 2.2 TeV, according to what is the freeze out temperature T^* . We should emphasize that there are two branches of allowed values for ξ , separated by the dotted horizontal line. The lower branch, as for example the one we just described with $\xi = -4$, corresponds to a relic density made by technibaryons DD . The upper set of allowed values, (as for $\xi = 2$), corresponds to the DD antiparticle.

In Fig. 3.6 we show the dependence of the neutral technibaryon matter density as a function of its mass for a fixed value of the parameter ξ . We see that if the LTB mass is lighter than roughly a TeV, the density of the particles is very large, giving a too large ratio Ω_{TB}/Ω_B . So, for a given value of ξ and T^* , WMAP data put constraints

on the allowed mass of the technibaryon. On the other hand if we increase sufficiently the mass of the technibaryon, we can get a ratio less than 4-5, which means that the technibaryon can be a component of the dark matter density.

3.2.2 1st Order Phase Transition

If the electroweak phase transition is predicted to be of (strong) first order, then the baryon, lepton and technibaryon violating process “freezes” slightly above the phase transition. For this reason, we have to impose two conditions; the overall charge neutrality $Q = 0$ and $Q_3 = 0$, where Q_3 is the charge associated with the T_3 isospin generator of the weak interactions. This charge has to be zero because, above the phase transition, the electroweak symmetry is not broken and therefore $Q_3 = 0$ in the Universe.

The technibaryon over baryon number density ratio is, in the same approximation as was used for the second order phase transition

$$-\frac{TB}{B} = \sigma_{DD} \frac{22 + \sigma_{\nu'}}{9(22 + 2\sigma_{DD} + \sigma_{\nu'})} \left[3 + \frac{L}{B} + \frac{1}{\sigma_{\nu'}} \frac{L'}{B} \right]. \quad (3.51)$$

T^* is expected to be larger than that of the second order case, i.e. it should be identified with the critical temperature T^c of the electroweak phase transition. This fact forces the mass of the LTB to be larger than that of the second order case to describe the whole dark matter. Our results are summarized in Fig. 3.7. As in the case of the second order phase transition, we have plotted the allowed values of the ξ parameter as function of the LTB mass, under the WMAP constraints regarding the overall density of dark matter in the Universe. ξ is, however, slightly different in this case

$$\xi \equiv \frac{L}{B} + \frac{1}{\sigma_{\nu'}} \frac{L'}{B}. \quad (3.52)$$

Using the previous example of $L' = 0$ and $L/B = -4$, one obtains an LTB mass of around 2.2 TeV.

3.3 Detection of the Neutral Technibaryon

Apart from the possibility of detecting a technibaryon in e.g. the LHC experiment it would certainly be interesting to detect the neutral technibaryon in earth based experiments for dark matter searches such as the CDMS [79, 80, 81, 82]. There are two basic ingredients affecting the detection of a cold DM object in these kinds of experiments. The first one is how large is the cross section of the object to be observed with the matter in the detector. The second has to do with the local density of DM in general and of the specific component of DM in particular. Current estimates suggest that the local density for a single component should be somewhere between 0.2-0.4 GeV/cm³. It is evident that the higher the cross section and the local density of dark matter are, the larger are the chances for the detection of the particle. The CDMS collaboration for example, can identify WIMPs by observing the recoil energy produced in elastic scattering between the WIMP and a nucleus in the detector. The expected rates of events per unit time and mass of the detector, has been calculated in several places and we refer to the review paper by Lewin and Smith [83] for a complete list of relevant

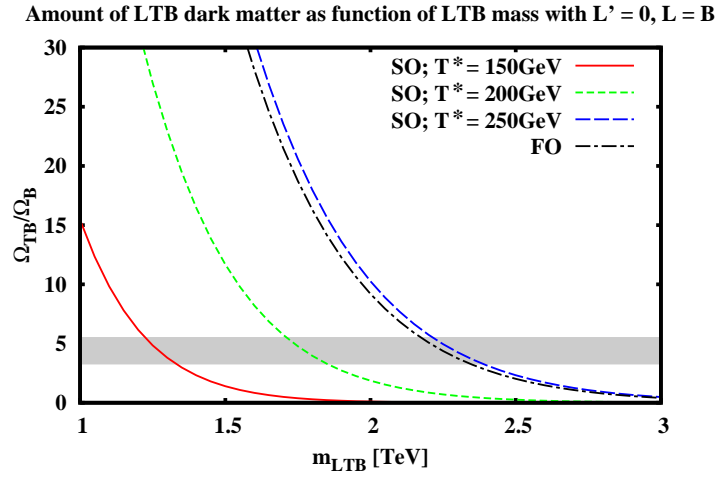


Figure 3.6: Amount of LTB dark matter as function of the mass of the LTB particle. The plot is shown for $L' = 0$ and $L = B$, for second order (SO) phase transitions with various temperatures T^* and a for first order (FO) phase transition as well.

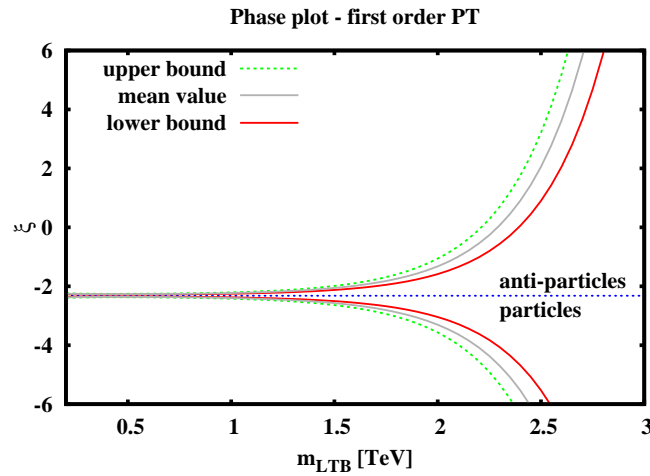


Figure 3.7: Plot representing the region of the parameters according to which the fraction of technibaryon matter density over the baryonic one takes on the values $[3.23, 5.55]$. Here we consider the case of a first order phase transition. The parameters in the plot are the mass of the LTB dark matter particle and ξ of Eq. (3.52). The dotted line separates areas of abundant particles and anti-particles.

references. The number of counts reported by the detector per unit time, mass of the detector and recoil energy is

$$\frac{dR}{dT} = \frac{R_0}{E_0 r} e^{-T/E_0 r}, \quad (3.53)$$

where T is the recoil energy of the nucleus, E_0 is the kinetic energy of the WIMP and $r = 4mM_n/(m + M_n)^2$, m and M_n being the masses of the WIMP and the nucleus, respectively. The parameter R_0 is the total rate containing the information about the cross section and is given by

$$R_0 = \frac{2}{\pi^{1/2}} \frac{N_0}{A} \frac{\rho_{dm}}{m} \sigma_0 v_0, \quad (3.54)$$

where N_0 is the Avogadro number, A is the atomic number of the nucleus of the detector, ρ_{dm} is the local dark matter density, σ_0 is the cross section for an elastic collision between the WIMP and the nucleus and v_0 is the thermal velocity of the WIMPs. One should note here that Eq. (3.53) is an approximate expression. In reality the calculation is more elaborate. For example, in principle one has to assume a Maxwell distribution for the velocities of the WIMPs up to the escape velocity for our galaxy. In addition, the effect of the motion of the earth relatively to the halo should be considered. These factors can change the expected rate. The total rate of counts can be more usefully rewritten in convenient units as

$$R_0 = \frac{503}{M_n m} \left(\frac{\sigma_0}{1\text{pb}} \right) \left(\frac{\rho_{dm}}{0.4\text{GeVcm}^{-3}} \right) \left(\frac{v_0}{230\text{kms}^{-1}} \right) \frac{\text{GeV}^2}{\text{kg.days}}. \quad (3.55)$$

Since our prospective dark matter component is a Goldstone boson, we are interested only in the spin independent elastic cross section. This is given in natural units by Ref. [84]

$$\sigma_0 = \frac{G_F^2}{2\pi} \mu^2 \bar{Y}^2 \bar{N}^2 F^2, \quad (3.56)$$

where G_F is the Fermi constant and $\bar{Y} = 2Y$. For a Dirac fermion $\bar{Y} = Y_L + Y_R$ and μ is the reduced mass of the WIMP and the nucleus target.

$$\bar{N} = N - (1 - 4 \sin^2 \theta_w) Z, \quad (3.57)$$

where N and Z are the number of neutrons and protons in the target nucleus and θ_w is the Weinberg angle. The parameter F^2 is a form factor (squared) for the target nucleus. The cross section can be written as

$$\sigma_0 = 8.431 \times 10^{-3} \frac{\mu^2}{\text{GeV}^2} \bar{Y}^2 \bar{N}^2 F^2 \text{ pb}. \quad (3.58)$$

The Ge atom has 41 neutrons and 32 protons, giving an $\bar{N} = 38.59$. Our LTB has $\bar{Y} = 1$.² Since SM neutrinos have $\bar{Y} = 1/2$, the cross section for the technibaryon will be four times larger than the one corresponding to a heavy neutrino. As we already mentioned, for typical values of the L/B ratio, in order to get the entire density for the dark matter, the mass of the technibaryon should be of the order of a TeV. The form

²We have directly computed this value for \bar{Y} using the effective Lagrangian in Ref. [1]. For a generic y we have $\bar{Y} = 2y - 1$ and it coincides with the value, one deduces by constructing the LTB wave function as follows: $\sqrt{2} |LTB\rangle = |D_L D_L\rangle - |D_R D_R\rangle$.

factor F^2 for the nucleus of Ge depends on the recoil energy T . It models the loss of coherence of the scattering for large recoil energies. For typical values of the recoil energy around 20-50 keV, one expects F^2 to be around 0.58. We estimated the nuclear form factor F using the solid sphere approximation – proper for the spin-independent WIMP interaction – which can be found in Ref. [83]. The solid sphere approximation reads

$$F^2(qr_n) = \frac{3(\sin(qr_n) - qr_n \cos(qr_n))}{(qr_n)^3}, \quad (3.59)$$

where

$$q = 6.92 \times 10^{-3} \sqrt{\frac{AT}{\text{keV}}} r_n \text{ fm}^{-1}, \quad (3.60)$$

$$r_n \simeq 1.14A^{1/3} \text{ fm}, \quad (3.61)$$

with T the recoil energy and A the atomic number. This implies that the nuclear form factor ranges from 0.72 to 0.43 when the recoil energy ranges from 20 to 50 keV.³

The number of counts that are detectable is given by

$$\text{counts} = \frac{dR}{dT} \Delta T \times \tau, \quad (3.62)$$

where τ is the exposure of the detector measured in kg.days and ΔT is the energy resolution of the detector. In the CDMS experiment, a 19.4 kg.days exposure was achieved for the Ge detectors with an energy resolution of $\Delta T = 1.5$ keV. So far no counts have been found. The 90% level of confidence would lead to 2.3 counts.

If we assume that our LTB constitutes the entire DM in the Universe, we have seen from our previous computations, that a typical value of the mass is about 2 TeV, for the second order phase transition case. Taking a recoil energy around 50 keV, $\rho_{dm} = 0.3$ GeV/cm³ and $F^2 \sim 0.43$, the number of counts predicted is around 13 which is a value few times larger than the 90% confidence value presented before. By stretching the parameters we can reduce, or even annihilate the gap, between our prediction and experimental bounds. Using still a mass around 2 TeV, but choosing a different set of inputs, i.e. $\rho_{dm} = 0.1$ GeV/cm³, $F^2 \sim 0.3$ and $T = 70$ keV, one finds around two predicted counts. Hence we would be within the 90% confidence level. Under these rather extreme conditions, one cannot yet completely exclude the possibility that our WIMP can constitute the entire DM in our Universe. Another simple way to reduce the gap between experiment and our LTB particle, if we imagine it to be a component of DM, is to increase its mass. In doing so, however, we neglect the relevant information gained in the previous sections in which we related the mass of the LTB to the fraction of DM in the Universe, it can account for.

We now take into account, in a more careful way, such a dependence on the mass of the LTB. From the previous section we learned that the general trend is that the amount of DM saturated by our LTB object decreases when increasing the mass of the LTB. In the absence of a complete computation of how DM distributes itself in the Universe we make the oversimplifying assumption that the fraction of local DM density of our LTB follows the same fraction of DM in the Universe. At this point we impose the 90% experimental constraint. Our results are reported in Fig. 3.8. In the figure we have used $F^2 \simeq 0.43$ and the thermal velocity is 230 km/s. We present both the maximal

³We may have overestimated the nuclear form factor [80]. If the physical value of F^2 is lower than the one we used then the allowed fraction of LTB-DM increases.

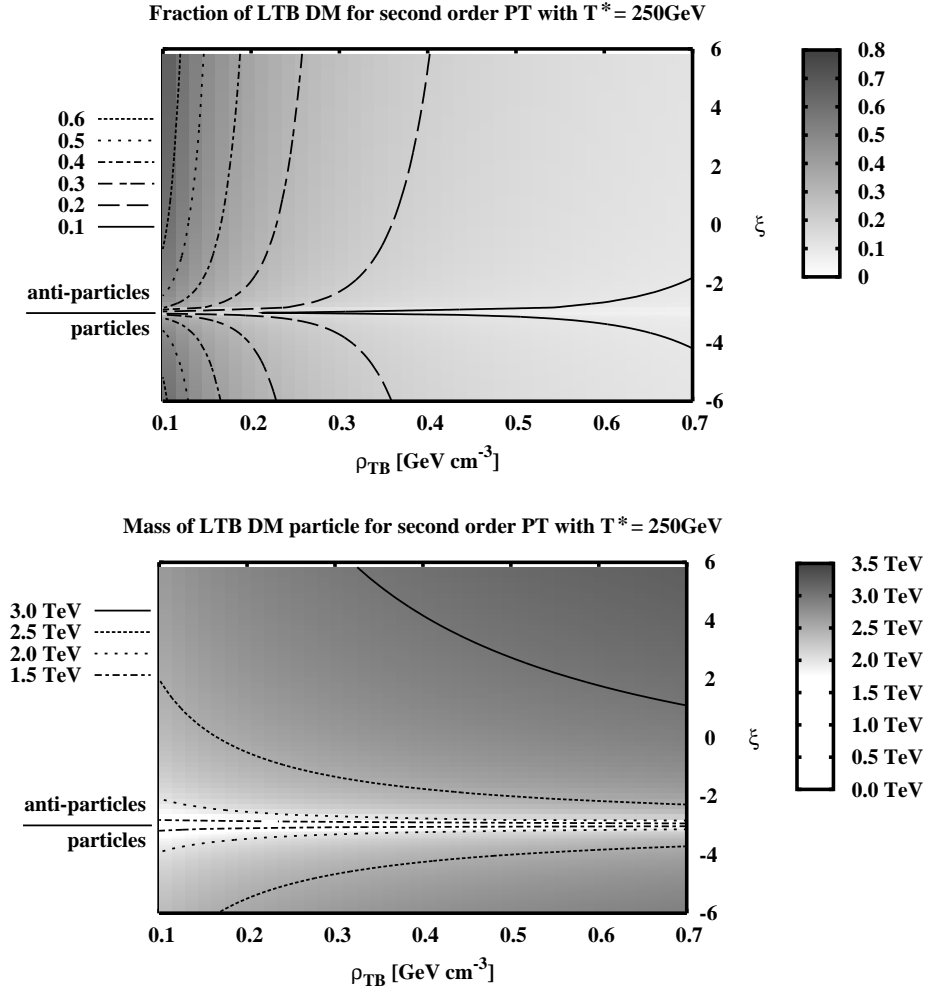


Figure 3.8: *Top Panel:* The maximal fraction of local DM density allowed by the 90% experimental constraint as function of the local DM density and the parameter ξ of Eq. (3.49). *Bottom Panel:* For the corresponding maximal fraction of local DM density currently allowed by the 90% experimental constraint as function of the local DM density and ξ , we plot the associated LTB mass. Both plots are presented with a second order phase transition with $T^* = 250\text{ GeV}$ and a recoil energy $T = 50\text{ keV}$.

fraction of local DM density determined imposing the 90% experimental constraint (Fig. 3.8) and the associated value of the LTB mass as functions of ξ . We have allowed for variations of the parameters to make our analysis more complete. Note that we have allowed the local DM density to reach, in the plots, very large values although a more modest range (i.e. up to 0.4 GeV/cm^3) is probably sufficient.

Summarizing we can say that for reasonable values of the input parameters, the 90% experimental constraint allows for a 10% to 65% of LTB-DM component in the Universe. The allowed mass for our dark matter component ranges between 1.4 and 3.3 TeV depending on the order of the associated electroweak phase transition as well as the exact value of the local DM density and the range of the experimental parameters.

Another interesting exercise one can do is to consider how much more the model is ruled out, so to speak, if the experiment enhances the equipment by being able to measure lower recoil energies. It is clear that the differential rate with respect to the recoil energy of Eq. (3.53) is exponentially dependent on the recoil energy. So the first naive answer is that it makes life exponentially harder for the model in question. But combining all the information we have gathered at this point it is also known that the fraction of DM drops exponentially as function of mass. With this at hand we make the full analysis and show the result of the mass of the LTB and the fraction of LTB DM, as function of the recoil energy which is measurable in the experiment and the ξ parameter, in Fig. 3.9. As seen from the figure, the fraction of dark matter the LTB particle can constitute, with an experiment having measurable recoil energy down to 10 keV, is less than 10%, but the corresponding masses are not that different (heavier). It is then, as expected, a point in the experimental research that really can make life hard for model builders.

We have now shown that in any case it is possible that the LTB dark matter particle only constitutes a fraction of the observed dark matter. The question to be answered at this point is: What makes the rest of the DM in the Universe? We speculate that a techni-axion, needed for the solution of the strong CP problem, could be a natural candidate (see for example Ref. [85]). In this way the two components for DM are associated to two natural and complementary extensions of the SM. An explicit model containing axions from technicolor-like dynamics has been constructed in Ref. [86].

3.4 Check of Thermal Equilibrium

It is assumed that the particles, including the LTB, are in thermal equilibrium until the point where the sphaleron process ceases to be important. Considering massless particles the temperature where the particles would decouple is found from the following inequality

$$\Gamma \gtrsim H , \quad (3.63)$$

where $\Gamma = n \langle \sigma_A |v| \rangle$ is the interaction rate and

$$H(T) \simeq 1.66 \sqrt{g_*} \frac{T^2}{M_{\text{Planck}}} , \quad (3.64)$$

with n the number density, σ_A the annihilation cross section, v the velocity of the particles, the bracket means thermally averaged, g_* the effective massless degrees of freedom and T the temperature. The freeze out temperature then is

$$T_{\text{freeze-out}} \sim (M_{\text{Planck}} G_F^2)^{-1/3} = 0.9 \text{ MeV} , \quad (3.65)$$

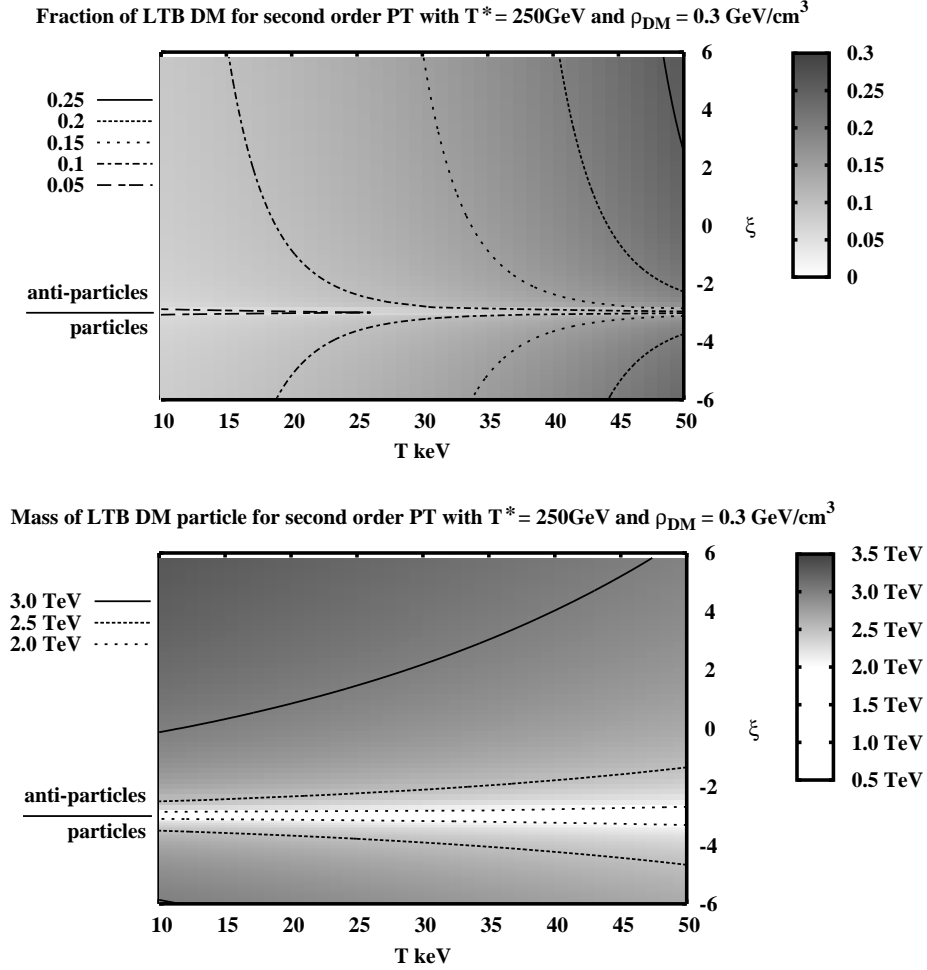


Figure 3.9: *Top Panel:* The maximal fraction of local DM density allowed by the 90% experimental constraint as function of the recoil energy measurable by the detector and the parameter ξ of Eq. (3.49). *Bottom Panel:* For the corresponding maximal fraction of local DM density currently allowed by the 90% experimental constraint as function of the recoil energy measurable by the detector and ξ , we plot the associated LTB mass. Both plots are presented with a second order phase transition with $T^* = 250 \text{ GeV}$, a recoil energy $T = 50 \text{ keV}$ and $\rho_{\text{DM}} = 0.3 \text{ GeV}/\text{cm}^3$.

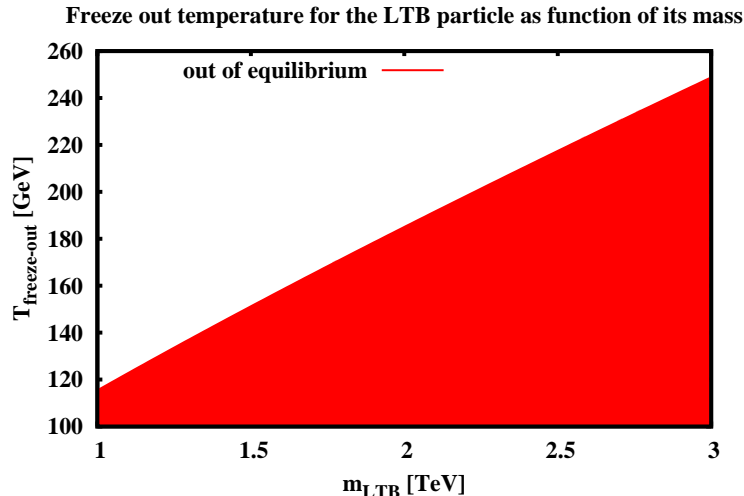


Figure 3.10: Freeze out temperature for the LTB particle as function of its mass. The filled area corresponds to the particles out of equilibrium.

where G_F is the Fermi constant. The freeze out temperature is far below the temperature of the electroweak phase transition, so thermal equilibrium is maintained.

Our LTB particle, though, cannot be considered relativistic and have a finite chemical potential different from zero. Finally the abundance is asymmetric, so the number of particles is not equal the number of antiparticles. An estimate of the constituents in the interaction rate are

$$n = gT^3 \frac{\mu}{T} g\left(\frac{m_{LTB}}{T}\right), \quad (3.66)$$

$$\langle \sigma_A |v\rangle \simeq G_F^2 m_{LTB}^2 |v|, \quad (3.67)$$

where g is the degrees of freedom for the LTB particle, the function g is that of Eq. (3.38) and m_{LTB} is the mass of the LTB particle. Taking the ratio μ/T to be constant $\sim 10^{-10}$ [71], the inequality becomes

$$m_{LTB}^2 T g\left(\frac{m_{LTB}}{T}\right) \gtrsim \frac{1.66\sqrt{g_*}}{g G_F^2 M_{\text{Planck}} |v| \frac{\mu}{T}}, \quad (3.68)$$

$g_* \sim 106$ [71], $v \sim 230$ km/h (converted to a dimensionless number) and we take $g \sim 2$. The freeze out temperature is now found, but depends on the mass of the LTB particle. The result is shown in Fig. 3.10. It is seen from the figure that for a temperature T^* of the sphaleron becoming unimportant, less than 220 GeV, the mass of the LTB then has to be relatively small in order for the calculation to be consistent.

It should be noted, that the value used to the ratio μ/T is a course estimate. If the ratio happens to be larger, then the freeze-out temperature decreases.

CHAPTER 4

Unification

There are several intriguing reasons for considering unification of the gauge forces of the SM. First, experimental values combined with one loop perturbation theory, extrapolated to very high energy, reveals that the SM gauge couplings do not unify, but they show a trend that by including some extension it might very well be plausible. Next, the quantization of electric charge is not explained in the SM and can be a relic of the breaking of a larger gauge group, e.g. $SU(5)$. One can hope to find the right mechanisms for flavor physics and connections between gauge couplings via unification in a unifying theory that is not at odds with experimental bounds. The mentioned unification into the group $SU(5)$ has severe problems with proton decay, which still is unobserved (or at a very low rate, hence e.g. physicists are here).

We are not going to make a thorough introduction to the very interesting topic of unification, but we will just introduce some pragmatic notions for computations and will have to refer to the literature. Good places to start are e.g. Refs. [87, 88].

4.1 One Loop β -function Computation

In the following, we will use the one-loop β -function to relate the coefficients of the logarithmic term in the different running coupling constants in the SM to the measured couplings at low energy (the Z mass scale). This is done by assuming unification and then extrapolating the coupling constants to the unification scale, using the running prescribed by the renormalization group equations, and then eliminating the energy scale as well as the unification scale.

The β -function is defined as follows [9]

$$t \frac{\partial \lambda}{\partial t} = \beta(\lambda(t)) \quad \Rightarrow \quad \int_{\bar{\lambda}}^{\lambda} \frac{d\lambda'}{\beta(\lambda')} = \ln t, \quad (4.1)$$

where λ is the coupling constant, t is the scale factor multiplying the momentum in the renormalization group equations and $\bar{\lambda}$ is the coupling where the scale factor $t = 1$. To one loop the β -function takes the form

$$\beta(\lambda) = \frac{b_0}{(4\pi)^2} \lambda^3, \quad (4.2)$$

where b_0 is a constant. The running coupling constant can then be integrated

$$\alpha^{-1}(t) = \frac{4\pi}{\lambda^2(t)} = C - \frac{1}{2\pi} b_0 \ln t, \quad (4.3)$$

with C an integration constant, which can be fixed by a known value of the coupling at scale M

$$\alpha^{-1}(\mu) = \alpha^{-1}(M) - \frac{1}{2\pi} b_0 \ln\left(\frac{\mu}{M}\right), \quad (4.4)$$

with μ the energy scale.

The β -function can in general be calculated to one loop with the knowledge of the group structure of the gauge theory [89]

$$\beta(\lambda) = \frac{1}{(4\pi)^2} \lambda^3 \left[\frac{2}{3} T(R_1) d(R_2) + \frac{1}{3} T(S_1) d(S_2) - \frac{11}{3} C_2(G_1) \equiv b_0 \right], \quad (4.5)$$

where $T(R_1)$ is the Casimir of the representation under which the fermion transforms and $d(R_2)$ is the dimension of the representation of the representation R_2 , where R_2 parametrizes the other gauge groups the fermion transforms under. For scalars, the same apply where the representations are denoted by $S_{1,2}$. $C_2(G_1)$ is the quadratic Casimir for the adjoint representation of the gauge group. For various group theoretical properties of Abelian and non-Abelian groups, see Appendix A.2.

The β -function coefficient b_0 for the fundamental representation of $SU(N)$ is

$$b_0 = \frac{1}{3} \sum_{f \in \text{fermions}} d_f + \frac{1}{6} \sum_{s \in \text{bosons}} d_s - \frac{11}{3} N. \quad (4.6)$$

For the two-index symmetric representation of $SU(N)$

$$b_0 = \frac{N+2}{3} \sum_{f \in \text{fermions}} d_f + \frac{N+2}{6} \sum_{s \in \text{bosons}} d_s - \frac{11}{3} N. \quad (4.7)$$

In the case of the Abelian group $U(1)$, the generator Y has to be normalized with respect to some normalization condition. The non-Abelian generators are usually already normalized as

$$\text{Tr} \{ T^a T^b \} = \frac{1}{2} \delta^{ab}. \quad (4.8)$$

One condition commonly used is to set the trace of the $U(1)$ of hypercharge equal to the trace of the isospin generator T_3

$$\text{Tr} \tilde{Y}^2 \equiv \text{Tr} cY^2 = \text{Tr}(T^3)^2. \quad (4.9)$$

The reason why it is necessary to normalize the generator correctly, is that they all have to be embedded into a larger framework in the unified theory and the hypercharge generator can be multiplied by a constant c while the coupling g' is divided by c and the physics at the Lagrangian level is still the same.

The β -function coefficient in the $U(1)$ case then becomes

$$b_0 = \frac{2}{3} \sum_{f \in \text{fermions}} \tilde{Y}_f^2 d_f + \frac{1}{3} \sum_{s \in \text{bosons}} \tilde{Y}_s^2 d_s, \quad (4.10)$$

where \tilde{Y} is the normalized hypercharge generator.

Assuming unification, we can write down Eq. (4.4) for each gauge coupling in the SM

$$\alpha_1^{-1}(\mu) = \alpha_U^{-1} - \frac{1}{2\pi} b_0^1 \ln \left(\frac{\mu}{M_U} \right), \quad (4.11)$$

$$\alpha_2^{-1}(\mu) = \alpha_U^{-1} - \frac{1}{2\pi} b_0^2 \ln \left(\frac{\mu}{M_U} \right), \quad (4.12)$$

$$\alpha_3^{-1}(\mu) = \alpha_U^{-1} - \frac{1}{2\pi} b_0^3 \ln \left(\frac{\mu}{M_U} \right), \quad (4.13)$$

where α_U is the coupling constant at the unification scale. Eliminating the α_U and the logarithmic factor, we get the following expression

$$\frac{\alpha_2^{-1}(M_Z) - \alpha_3^{-1}(M_Z)}{\alpha_1^{-1}(M_Z) - \alpha_2^{-1}(M_Z)} = \frac{b_0^2 - b_0^3}{b_0^1 - b_0^2}, \quad (4.14)$$

where the indices 1, 2, 3 denote $SU(3)_c$, $SU(2)_L$ and $U(1)_Y$, respectively. In order to compare with experimental data, we need to relate the couplings of the gauge forces to the electroweak parameters

$$\alpha_1^{-1}(M_Z) = \frac{4\pi c}{g^2} = c \frac{1 - s_Z^2}{\alpha_{QED}(M_Z)} \quad (4.15)$$

$$\alpha_2^{-1}(M_Z) = \frac{s_Z^2}{\alpha_{QED}(M_Z)}, \quad (4.16)$$

where $\alpha_{QED}(M_Z)$ is the QED fine structure constant evaluated at the Z mass.

Evaluating the normalization condition for the (one family)¹ SM, we get

$$c \frac{10}{3} = 2 \quad \Rightarrow \quad c = \frac{3}{5}. \quad (4.17)$$

Thus the hypercharge generator is

$$\tilde{Y} = \sqrt{\frac{3}{5}} Y. \quad (4.18)$$

The left-hand-side (lhs) of Eq. (4.14) can be computed with the experimental values and one obtains ~ 0.72 using the data from the particle data group (PDG), see Appendix A.3. The rhs. is then the prediction by the theory, and if it is the exact value of that of the lhs., the model predicts unification.

One can amuse oneself with the trivial calculations of the one loop β -function coefficients

$$b_0^1 = \frac{4N_g}{3} + \frac{1}{10} = \frac{41}{10}, \quad (4.19)$$

$$b_0^2 = \frac{4N_g}{3} + \frac{1}{6} - \frac{22}{3} = -\frac{19}{6}, \quad (4.20)$$

$$b_0^3 = \frac{4N_g}{3} - \frac{11N_c}{3} = -7, \quad (4.21)$$

¹Taking into account all three families will just be a factor of 3 on each side of the equation and thus will not change c .

where N_g is the number of SM generations and N_c is the number of QCD colors. The rhs. of Eq. (4.14) can then be evaluated to be $115/218 \sim 0.53$, which is quite off with respect to the experimental value (the lhs.).

Repeating the calculation for the $SU(2)$ -Adj. model with a generic choice of the hypercharge parameter y , we first have to take care of the normalization of the hypercharge generator. In order to keep everything clear with respect to the normalizations at different scales, we use the running coupling constants α_i for the SM particle content, where

$$\alpha_i(\mu), \quad \mu \in [M_Z, \epsilon M_Z], \quad 1 < \epsilon \ll \frac{M_U}{M_Z}, \quad (4.22)$$

with M_U being the unification scale. In the oversimplified approximation, we imagine that all the new particles are added to the theory at scale ϵM_Z . For the total particle content which is the SM and the technicolor particles, we denote the running couplings $\tilde{\alpha}_i$

$$\tilde{\alpha}_i(\mu), \quad \mu \in [\epsilon M_Z, M_U]. \quad (4.23)$$

For the hypercharge coupling, the normalization constant c will in general differ from that of the SM normalized one. Playing the same game as before, we can write down a relation between the β -function coefficients \tilde{b}_0^i of the running coupling constants for the full particle content and the running coupling constants

$$\frac{\tilde{\alpha}_2^{-1}(\epsilon M_Z) - \tilde{\alpha}_3^{-1}(\epsilon M_Z)}{\tilde{\alpha}_1^{-1}(\epsilon M_Z) - \tilde{\alpha}_2^{-1}(\epsilon M_Z)} = \frac{\tilde{b}_0^2 - \tilde{b}_0^3}{\tilde{b}_0^1 - \tilde{b}_0^2}. \quad (4.24)$$

Using that

$$\alpha_i(\epsilon M_Z) = \tilde{\alpha}_i(\epsilon M_Z), \quad (4.25)$$

as well as Eqs. (4.11-4.13) with the unification scale replaced by the Z mass scale (and the fact that the couplings do not unify at the Z mass scale), we obtain

$$\frac{\alpha_2^{-1}(M_Z) - \frac{b_0^2}{2\pi} \ln \epsilon - \alpha_3^{-1}(M_Z) + \frac{b_0^3}{2\pi} \ln \epsilon}{\alpha_1^{-1}(M_Z) - \frac{b_0^1}{2\pi} \ln \epsilon - \alpha_2^{-1}(M_Z) + \frac{b_0^2}{2\pi} \ln \epsilon} = \frac{\tilde{b}_0^2 - \tilde{b}_0^3}{\tilde{b}_0^1 - \tilde{b}_0^2}. \quad (4.26)$$

Taking for simplicity (and to fairly good approximation) the limit of $\epsilon \rightarrow 1$, which is the same as inserting all the new particles just after the Z mass scale, the relation simplifies to

$$\frac{\alpha_2^{-1}(M_Z) - \alpha_3^{-1}(M_Z)}{\alpha_1^{-1}(M_Z) - \alpha_2^{-1}(M_Z)} = \frac{\tilde{b}_0^2 - \tilde{b}_0^3}{\tilde{b}_0^1 - \tilde{b}_0^2}, \quad (4.27)$$

where we identify the lhs. as that of Eq. (4.14). We understand this because there is not yet added particles. The rhs. of Eq. (4.27), though, contains the coefficients of the logarithmic terms, all the way up to the unification scale M_U and includes all the particles. Computing the normalization constant for the hypercharge generator for the $\tilde{\alpha}_1$ coupling constant, we get

$$\begin{aligned} c \left(\frac{10N_g}{3} + \frac{1}{4} (2 + N_{tc}(N_{tc} + 1) + 2(18 + N_{tc}(N_{tc} + 1))y^2) \right) &= 2N_g + 2, \\ \Rightarrow c &= \frac{24(1 + N_g)}{40N_g + 3(2 + N_{tc}(N_{tc} + 1) + 2(18 + N_{tc}(N_{tc} + 1))y^2)}. \end{aligned} \quad (4.28)$$

With this at hand it is easy to write down the β -function coefficients of the technicolor model, here for generic number of technicolors N_{tc}

$$\tilde{b}_0^1 = \frac{4(N_g + 1)}{3}, \quad (4.29)$$

$$\tilde{b}_0^2 = \frac{4N_g}{3} + \frac{1}{6}(2 + N_{tc}(N_{tc} + 1)) - \frac{22}{3}, \quad (4.30)$$

$$\tilde{b}_0^3 = \frac{4N_g}{3} - \frac{11N_c}{3}, \quad (4.31)$$

$$\tilde{b}_0^4 = \frac{2}{3}(N_{tc} + 2)N_f - \frac{11N_{tc}}{3}, \quad (4.32)$$

where N_f is the number of techniflavors, which is two in the case of the minimal one doublet case. The index 4 refers to the technicolor force. This is a remarkable result. All the way the computation is completely generic. The hypercharge parameter y has not been specified, but still it has vanished from the β -function coefficients. There is a simple explanation to this. We have only fermions (and gauge bosons), but no scalars in the theory. Thus, the β -function coefficient \tilde{b}_0^1 is simply

$$\tilde{b}_0^1 = \frac{2}{3}\text{Tr}\tilde{Y}_f^2 = \frac{2}{3}\text{Tr}(T^3)^2 = \frac{2}{3}(2N_g + 2), \quad (4.33)$$

which shows consistency, as it is the same result as that of Eq. (4.29). This, however, would not necessarily be the case if the theory had both fermions and scalars, as they are weighted differently in the β -function coefficient, but not in the normalization of the hypercharge generator.

In the case of three QCD colors, two technicolors and one doublet of techniquarks, the coefficients simplify to

$$b_0^1 = \frac{16}{3}, \quad b_0^2 = -2, \quad b_0^3 = -7, \quad b_0^4 = -2. \quad (4.34)$$

It is then straightforward to check unification of the model and one obtains the remarkable result $15/22 \sim 0.68$ for the rhs. of Eq. (4.27), which is much better than that of the SM. It should be noted, that this model (the $SU(2)$ -Adj.) is not a full theory explaining all the problems of Section 2.1.4. Therefore it is not known which contributions the extended technicolor (or any equivalent extension of the model) will make. So if a small correction is added to the running of the gauge couplings, they might very well unify.

The couplings of the pure SM and the SM with the $SU(2)$ -Adj. model as an extension, are shown in Figs. 4.1 and 4.2, respectively. An interesting point is observed from Fig. 4.2 (but also from Eq. (4.34)) that the slope of the techniforce is such, that unification of all four gauge forces in one point is not possible, if the electroweak symmetry has to break before chiral symmetry in QCD (assuming that CSB occurs when the gauge force becomes strong).

It is interesting to see how good the approximation of taking $\epsilon \rightarrow 1$ is, which is the same as inserting the new particles *just* after the Z mass scale. The lhs. of Eq. (4.26) changes with respect to the lhs. of Eq. (4.14), when moving ϵ away from 1. Increasing ϵ to 50, which corresponds to inserting the new particles at fifty times the Z mass scale implies a monotonic increase in the value of the lhs. of Eq. (4.26) to below the 1 percent level, so the approximation of $\epsilon \rightarrow 1$ can indeed be considered quite good.

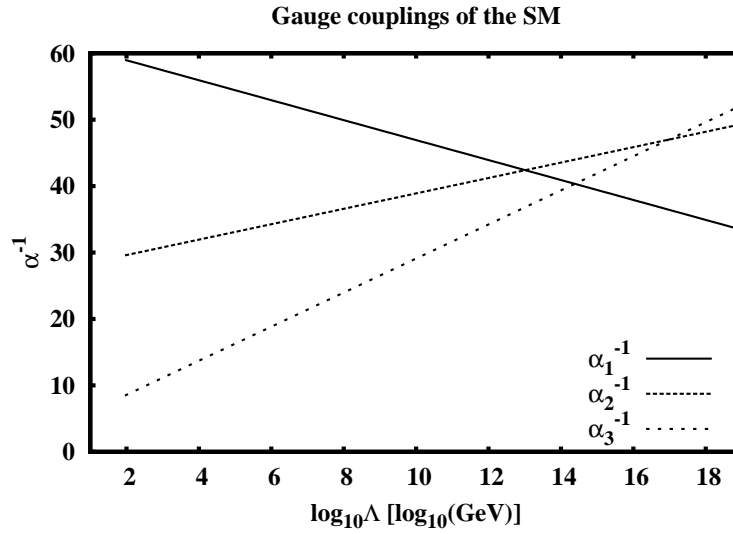


Figure 4.1: Extrapolation of the gauge couplings in the SM. A trend of unification is observed, but it is far from exact.

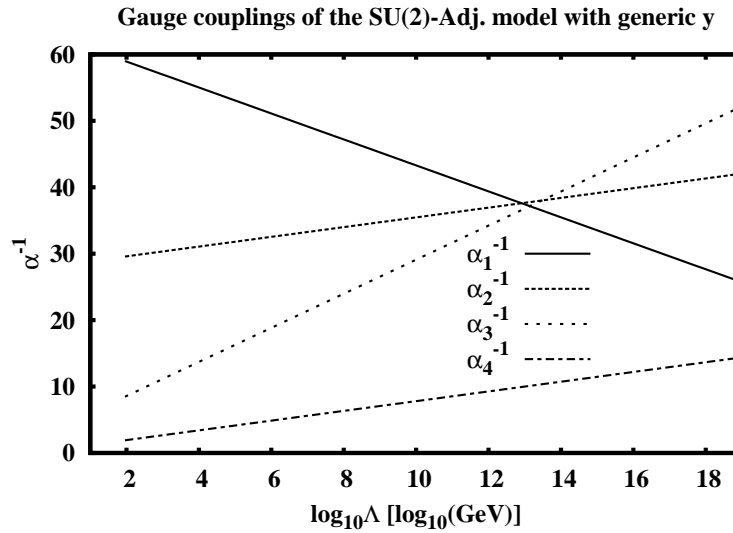


Figure 4.2: Extrapolation of the gauge couplings in the $SU(2)$ -Adj. model. It is seen that the gauge couplings of the SM do almost unify (but as calculated above, it is still not exact, but far better than in the pure SM case). The gauge coupling value of the techniforce at the Z mass is taken to be the critical coupling of Eq. (2.46).

CHAPTER 5

Competing Models

It is out of the scope of this thesis to make a review of all the competing models, so in the lack of space we will just mention a few of them and refer to the literature.

It is already mentioned in the introduction that there are (at least) three different methods to cure the naturalness problem of the SM Higgs boson (see Section 1.2).

Of recent works in the technicolor field, it is worth to mention Christensen and Shrock's extension of technicolor with two ETC groups [90]. Hong and Yee have made a holographic estimate of the oblique corrections for walking technicolor [91]. In the line of the holographic approach, Hirn and Sanz have shown that a negative S parameter in technicolor is possible [92]. Davoudiasl has considered a cosmological scenario with a techni-axion [85]. Lane has considered low energy searches in existing experimental data sets for technicolor (in the Technicolor Straw Man framework) [93], but also Feligioni has made work in this direction [94]. Recent considerations in the direction of topcolor assisted technicolor models have been made, see Refs. [95, 96]. But this is just a few of the recent works.

A very popular model, in the supersymmetric scenario, is the minimal supersymmetric SM (MSSM). As already explained, it solves the naturalness problem by cancellation of quadratic divergences in the quantum corrections between the Higgs bosons (there are usually two doublets, in order to make the higgsinos anomaly free) and the higgsinos. This is in some way the same as saying that we want to believe in an extrapolation of the SM up to the Planck scale (or GUT scale), which may be naive but might as well be nature (and very good for the string theory community). Among the advantages of the MSSM is that everything is perturbative and calculable. This fact has made many theorists make a great effort exploring signatures and thus it is a model where the experimentalist really know what to look for (which in the end is how physics is determined!). This is a problem with strongly interacting theories; it is much harder to tell exactly what are the observables seen at the collider experiment. The MSSM also has some candidates for dark matter, which typically is a neutralino WIMP. But there are still problems left in the MSSM: Flavor physics, the μ problem (which in short is a new hierarchy problem of the model), the strong CP problem (which is problematic as an axion is not directly compatible) and finding a mechanism to softly break supersymmetry. For references, a good place to start is in Refs. [97, 98, 99, 58]. An introduction to supersymmetric dark matter candidates can be found in e.g. Ref. [73].

In the little Higgs models, the Higgs boson is a pseudo Goldstone boson and its mass is protected from one loop quadratic divergences by approximate global symmetries. The models rely on a *collective* symmetry breaking in which there is only *little*

or no fine tuning necessary. There are different variants as the Minimal Moose and the Littlest Higgs. In this scenario typical problems still are to establish their phenomenological naturalness. Interesting further reading can be found in Refs. [100, 101].

CHAPTER 6

Conclusions and Outlook

We have introduced some of the problems in particle physics and motivated why especially electroweak symmetry breaking is an interesting topic to study with respect to the “guarantee” of experimental discovery of whatever the new physics may be. Next, we have introduced technicolor in basics, the problems with technicolor and the common notions in this field and finally the Sannino-Tuominen model, which solves some of the phenomenological problems.

Then we move on and investigate the specific $SU(2)$ -Adj. model more in depth and construct effective theories [1] and make brief considerations on the signatures. We compute the Feynman rules for the linearly realized effective theory, which can be found in Appendix C. As it is seen in many places in modern particle physics, cosmological constraints, and here we mean constraints on dark matter, can be used as a supplementary guideline for the model in question. We thus construct a dark matter candidate/component, compute what would be the relic abundance and consider the constraints of direct detection from earth based experiments [2]. We consider both the case of a first order electroweak phase transition and a second order one. We find, that is plausible that our LTB dark matter candidate can constitute the whole amount of the observed dark matter, but depending on the parameter ξ , which is a weighted sum of the ratios of lepton and *new* lepton to baryon densities and also what is the exact *local* density of dark matter in the halo. We then make a check of the thermal equilibrium for the technibaryons and find that their masses have to be relatively low or the temperature, where the sphaleron process becomes unimportant has to be relatively high, in order for the computation to be completely valid. Finally the problem of unification is considered and we have shown that it might be plausible to have unification within the model, if we take into account that the model is not complete, in the sense that an extension for mass generation and flavor physics has to be incorporated.

This leads to the question of where to go next. Flavor physics and a mass generation mechanism is one thing that would be interesting to investigate. As already mentioned, it is an ongoing project with Fabio Maltoni and Francesco Sannino of implementing the model into a software called MadGraph for phenomenological computations. Another future project which we have already started with Thomas Rytov and Francesco Sannino, is to use unification as a guideline to select (and discard) technicolor models in “all” higher dimensional representations, with or without supersymmetry.

A further idea could be to make the $SU(2)$ -Adj. model $\mathcal{N} = 4$ supersymmetric at some higher scale. Other suggestions could be extra dimensions; e.g. in the line of the holographic approach, which is seen in the literature.

Conventions and Identities

We use the mostly negative metric which is $\text{diag}(1, -1, -1, -1)$ and in general the conventions of Wess and Bagger [58].

A.1 Identities for the Weinberg Angle

$$g^2 \cos^2 \theta_w = (g^2 + g'^2)(1 + \sin^4 \theta_w - 2 \sin^2 \theta_w) \quad (\text{A.1})$$

$$g'^2 \sin^2 \theta_w = (g^2 + g'^2) \sin^4 \theta_w \quad (\text{A.2})$$

$$gg' \sin 2\theta_w = 2(g^2 + g'^2)(\sin^2 \theta_w - \sin^4 \theta_w) \quad (\text{A.3})$$

$$g^2 \sin^2 \theta_w = e^2 \quad (\text{A.4})$$

$$g'^2 \cos^2 \theta_w = e^2 \quad (\text{A.5})$$

$$gg' \sin 2\theta_w = 2e^2 \quad (\text{A.6})$$

$$g^2 \sin \theta_w = g^2 \sec \theta_w (1 - \sin^2 \theta_w) \quad (\text{A.7})$$

$$gg' \sin \theta_w = g^2 \sec \theta_w \sin^2 \theta_w \quad (\text{A.8})$$

$$gg' \cos 2\theta_w = eg \sec \theta_w (1 - 2 \sin^2 \theta_w) \quad (\text{A.9})$$

$$g^2 \sin 2\theta_w = 2eg \sec \theta_w (1 - \sin^2 \theta_w) \quad (\text{A.10})$$

$$g'^2 \sin 2\theta_w = 2eg \sec \theta_w \sin^2 \theta_w \quad (\text{A.11})$$

A.2 Properties for Unitary Groups

$SU(N)$:

$$C_2(\square) = \frac{N^2 - 1}{2N} \quad (\text{A.12})$$

$$d(\square) = N \quad (\text{A.13})$$

$$r(\square) = N^2 - 1 \quad (\text{A.14})$$

$$T(\square) = \frac{C_2(\square)d(\square)}{r} = \frac{1}{2} \quad (\text{A.15})$$

$$C_2(\text{Adj}) = N \quad (\text{A.16})$$

$$C_2(\square\square) = \frac{(N+2)(N-1)}{N} \quad (\text{A.17})$$

$$d(\square\square) = \frac{N}{2}(N+1) \quad (\text{A.18})$$

$$T(\square\square) = \frac{C_2(\square\square)d(\square\square)}{r} = \frac{N+2}{2}, \quad (\text{A.19})$$

where r is the number of generators, \square is the fundamental representation, Adj. is the adjoint representation and $\square\square$ is the two-index symmetric representation.

$U(1)$:

$$C_2(\square) = \tilde{Y}^2 \quad (\text{A.20})$$

$$T(\square) = \tilde{Y}^2 \quad (\text{A.21})$$

$$d(\square) = 1 \quad (\text{A.22})$$

$$C_2(\text{adj}) = 0, \quad (\text{A.23})$$

where \tilde{Y} is the normalized hypercharge.

A.3 Measured Electroweak Data

From the particle data group we obtain the following electroweak data

$$M_Z = 91.1876 \text{ GeV} \quad (\text{A.24})$$

$$\alpha_s(M_Z) = 0.1176(20) \quad (\text{A.25})$$

$$\alpha_{QED}^{-1}(M_Z) = 127.918 \quad (\text{A.26})$$

$$\sin^2(\theta_w) \equiv s_Z^2 = 0.23122(15) \quad (\text{A.27})$$

APPENDIX \mathfrak{B}

Generators

It is convenient to use the following representation of $SU(4)$

$$S^a = \begin{pmatrix} \mathbf{A} & \mathbf{B} \\ \mathbf{B}^\dagger & -\mathbf{A}^T \end{pmatrix}, \quad X^i = \begin{pmatrix} \mathbf{C} & \mathbf{D} \\ \mathbf{D}^\dagger & \mathbf{C}^T \end{pmatrix}, \quad (\text{B.1})$$

where A is hermitian, C is hermitian and traceless, $B = -B^T$ and $D = D^T$. The S are also a representation of the $SO(4)$ generators, and thus leave the vacuum invariant $S^a E + E S^a = 0$. Explicitly, the generators read

$$S^a = \frac{1}{2\sqrt{2}} \begin{pmatrix} \tau^a & \mathbf{0} \\ \mathbf{0} & -\tau^{aT} \end{pmatrix}, \quad a = 1, \dots, 4, \quad (\text{B.2})$$

where $a = 1, 2, 3$ are the Pauli matrices and $\tau^4 = \mathbb{1}$. These are the generators for $SU_V(2) \times U_V(1)$.

$$S^a = \frac{1}{2\sqrt{2}} \begin{pmatrix} \mathbf{0} & \mathbf{B}^a \\ \mathbf{B}^{a\dagger} & \mathbf{0} \end{pmatrix}, \quad a = 5, 6, \quad (\text{B.3})$$

with

$$B^5 = \tau^2, \quad B^6 = i\tau^2. \quad (\text{B.4})$$

The rest of the generators which do not leave the vacuum invariant are

$$X^i = \frac{1}{2\sqrt{2}} \begin{pmatrix} \tau^i & \mathbf{0} \\ \mathbf{0} & \tau^{iT} \end{pmatrix}, \quad i = 1, 2, 3, \quad (\text{B.5})$$

and

$$X^i = \frac{1}{2\sqrt{2}} \begin{pmatrix} \mathbf{0} & \mathbf{D}^i \\ \mathbf{D}^{i\dagger} & \mathbf{0} \end{pmatrix}, \quad i = 4, \dots, 9, \quad (\text{B.6})$$

with

$$\begin{aligned} D^4 &= \mathbb{1}, & D^6 &= \tau^3, & D^8 &= \tau^1, \\ D^5 &= i\mathbb{1}, & D^7 &= i\tau^3, & D^9 &= i\tau^1. \end{aligned} \quad (\text{B.7})$$

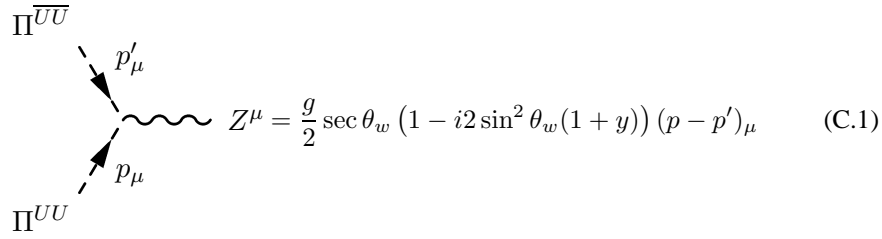
The generators are normalized as follows

$$\text{Tr} [S^a S^b] = \text{Tr} [X^a X^b] = \frac{1}{2} \delta^{ab}, \quad \text{Tr} [X^i S^a] = 0. \quad (\text{B.8})$$

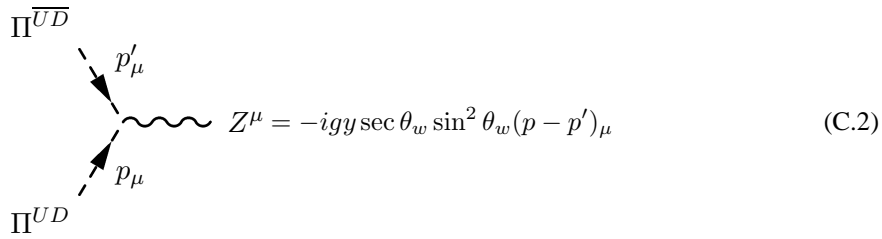
APPENDIX \mathcal{E}

Feynman Rules for the $SU(2)$ -Adj. Model

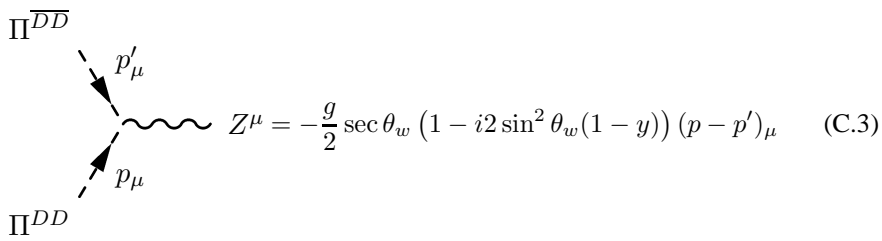
The convention used here is that the Goldstone bosons of the theory are incoming states so it holds from left to right, that the technibaryon number is conserved (zero). The gauge bosons are outgoing states.



$$\begin{array}{c} \Pi^{\overline{UU}} \\ \swarrow p'_\mu \\ \text{---} \\ \searrow p_\mu \\ \Pi^{UU} \end{array} \quad Z^\mu = \frac{g}{2} \sec \theta_w (1 - i2 \sin^2 \theta_w (1 + y)) (p - p')_\mu \quad (\text{C.1})$$



$$\begin{array}{c} \Pi^{\overline{UD}} \\ \swarrow p'_\mu \\ \text{---} \\ \searrow p_\mu \\ \Pi^{UD} \end{array} \quad Z^\mu = -igy \sec \theta_w \sin^2 \theta_w (p - p')_\mu \quad (\text{C.2})$$



$$\begin{array}{c} \Pi^{\overline{DD}} \\ \swarrow p'_\mu \\ \text{---} \\ \searrow p_\mu \\ \Pi^{DD} \end{array} \quad Z^\mu = -\frac{g}{2} \sec \theta_w (1 - i2 \sin^2 \theta_w (1 - y)) (p - p')_\mu \quad (\text{C.3})$$

$$\begin{array}{c} \sigma \\ \swarrow p'_\mu \\ \text{---} \\ \searrow p_\mu \\ \Pi^0 \end{array} \quad Z^\mu = \frac{ig}{2} \sec \theta_w (p - p')_\mu \quad (\text{C.4})$$

$$\begin{array}{c} \Pi^+ \\ \swarrow p'_\mu \\ \text{---} \\ \searrow p_\mu \\ \Pi^- \end{array} \quad Z^\mu = ig \sec \theta_w \sin^2 \theta_w (p - p')_\mu \quad (\text{C.5})$$

$$\begin{array}{c} \Pi^{\overline{UU}} \\ \swarrow p'_\mu \\ \text{---} \\ \searrow p_\mu \\ \Pi^{UU} \end{array} \quad A^\mu = e(1 + y)(p - p')_\mu \quad (\text{C.6})$$

$$\begin{array}{c} \Pi^{\overline{UD}} \\ \swarrow p'_\mu \\ \text{---} \\ \searrow p_\mu \\ \Pi^{UD} \end{array} \quad A^\mu = ey(p - p')_\mu \quad (\text{C.7})$$

$$\begin{array}{c} \Pi^{\overline{DD}} \\ \swarrow p'_\mu \\ \text{---} \\ \searrow p_\mu \\ \Pi^{DD} \end{array} \quad A^\mu = -e(1 - y)(p - p')_\mu \quad (\text{C.8})$$

$$\begin{array}{c} \Pi^+ \\ \swarrow p'_\mu \\ \text{---} \\ \searrow p_\mu \\ \Pi^- \end{array} \quad A^\mu = -e(p - p')_\mu \quad (\text{C.9})$$

$$W^{-\mu} = -\frac{ig}{2}(p-p')_{\mu} \quad (C.16)$$

$$W^{-\mu} = \frac{g}{2}(p-p')_{\mu} \quad (C.17)$$

$$= -2g^2 \quad (C.18)$$

$$= -2g^2 \quad (C.19)$$

$$= -\frac{g^2}{2} \quad (C.20)$$

$$= -g^2 \quad (C.21)$$

$$= -\frac{g^2}{2} \quad (\text{C.22})$$

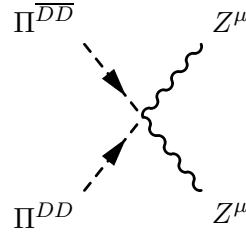
$$= -\frac{g^2}{2} \quad (\text{C.23})$$

$$= -\frac{g^2}{2} \quad (\text{C.24})$$

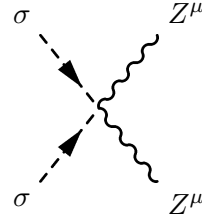
$$= -\frac{g^2}{2} \quad (\text{C.25})$$

$$= -2(g^2 + g'^2) \left(4 - \frac{1}{2} \sin^2 \theta_w (4 + y) + 2 \sin^4 \theta_w (4 + 5y + 4y^2) \right) \quad (\text{C.26})$$

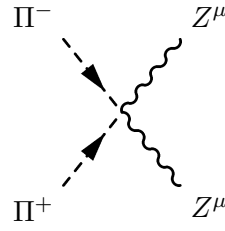
$$= -16(g^2 + g'^2) y^2 \sin^4 \theta_w \quad (\text{C.27})$$



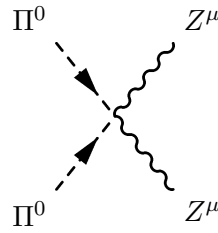
$$= -2(g^2 + g'^2) \left(4 - \frac{1}{2} \sin^2 \theta_w (4 - y) + 2 \sin^4 \theta_w (4 - 5y + 4y^2) \right) \quad (\text{C.28})$$



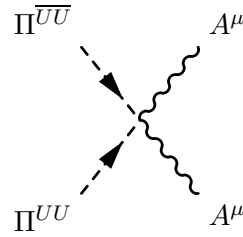
$$= -4(g^2 + g'^2) \left(1 - \frac{3}{2} \sin^2 \theta_w + \frac{3}{2} \sin^4 \theta_w \right) \quad (\text{C.29})$$



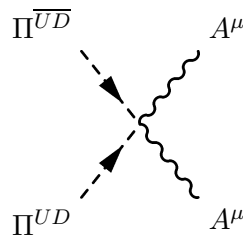
$$= -2(g^2 + g'^2) (2 - 5 \sin^2 \theta_w + 5 \sin^4 \theta_w) \quad (\text{C.30})$$



$$= -4(g^2 + g'^2) \left(1 - \frac{3}{2} \sin^2 \theta_w + \frac{3}{2} \sin^4 \theta_w \right) \quad (\text{C.31})$$



$$= -4e^2 (4 + 5y + 4y^2) \quad (\text{C.32})$$



$$= -16y^2 e^2 \quad (\text{C.33})$$

$$= -4e^2 (4 - 5y + 4y^2) \quad (\text{C.34})$$

$$= -6e^2 \quad (\text{C.35})$$

$$= -10e^2 \quad (\text{C.36})$$

$$= -6e^2 \quad (\text{C.37})$$

$$= g^2 \sec \theta_w (-1 + \sin^2 \theta_w (y + 1)) \quad (\text{C.38})$$

$$= g^2 \sec \theta_w (1 + \sin^2 \theta_w (y - 1)) \quad (\text{C.39})$$

$$= -\frac{ig^2}{2} \sec \theta_w \sin^2 \theta_w \quad (\text{C.40})$$

$$= -\frac{g^2}{2} \sec \theta_w \sin^2 \theta_w \quad (\text{C.41})$$

$$= g^2 \sec \theta_w (-1 + \sin^2 \theta_w (y + 1)) \quad (\text{C.42})$$

$$= g^2 \sec \theta_w (1 + \sin^2 \theta_w (y - 1)) \quad (\text{C.43})$$

$$= \frac{ig^2}{2} \sec \theta_w \sin^2 \theta_w \quad (\text{C.44})$$

$$= -\frac{g^2}{2} \sec \theta_w \sin^2 \theta_w \quad (\text{C.45})$$

$$= -\frac{i}{2}eg \quad (\text{C.52})$$

$$= \frac{1}{2}eg \quad (\text{C.53})$$

$$= -eg \sec \theta_w (2 + y - 8 \sin^2 \theta_w (2 + 3y + 2y^2)) \quad (\text{C.54})$$

$$= -4egy^2 \sec \theta_w \sin^2 \theta_w \quad (\text{C.55})$$

$$= -eg \sec \theta_w (2 - y - 8 \sin^2 \theta_w (2 - 3y + 2y^2)) \quad (\text{C.56})$$

$$= -\frac{1}{2}eg \sec \theta_w (1 - 2 \sin^2 \theta_w) \quad (\text{C.57})$$

$$= -\frac{3}{2}eg \sec \theta_w (1 - 2 \sin^2 \theta_w) \quad (\text{C.58})$$

$$= -\frac{1}{2}eg \sec \theta_w (1 - 2 \sin^2 \theta_w) \quad (\text{C.59})$$

$$= -6(\lambda + \tilde{\lambda}) \quad (\text{C.60})$$

$$= -4(\lambda + \tilde{\lambda}) \quad (\text{C.61})$$

$$= -6(\lambda + \tilde{\lambda}) \quad (\text{C.62})$$

$$= -2 \left((1 + \delta_{ij})\lambda + 2(1 + \delta_{ij}(\delta_{iUU} + \delta_{iDD})) \right. \\ \left. \times (1 - \delta_{iUU}\delta_{jDD} - \delta_{iDD}\delta_{jUU})\tilde{\lambda} \right) \quad (\text{C.63})$$

with $i, j = UU, UD, DD$

$$\begin{array}{ccc}
 \Pi^{\bar{i}} & & \Pi^+ \\
 \diagdown & & \diagup \\
 & \times & \\
 \diagup & & \diagdown \\
 \Pi^i & & \Pi^-
 \end{array}
 = -2 \left(\lambda + 2 \left(1 + \frac{3}{2} \delta_{iUD} \right) \tilde{\lambda} \right)
 \quad \text{(C.64)}$$

with $i = UU, UD, DD$

$$\begin{array}{ccc}
 \Pi^{\bar{i}}, \Pi^+ & & \sigma \\
 \diagdown & & \diagup \\
 & \times & \\
 \diagup & & \diagdown \\
 \Pi^i, \Pi^- & & \sigma
 \end{array}
 = -2(\lambda + \tilde{\lambda})
 \quad \text{(C.65)}$$

with $i = UU, UD, DD$

$$\begin{array}{ccc}
 \Pi^{\bar{i}}, \Pi^+, \sigma & & \Pi^0 \\
 \diagdown & & \diagup \\
 & \times & \\
 \diagup & & \diagdown \\
 \Pi^i, \Pi^-, \sigma & & \Pi^0
 \end{array}
 = -2 \left(\lambda + (1 + 2(\delta_{iUU} + \delta_{iDD})) \tilde{\lambda} \right)
 \quad \text{(C.66)}$$

with $i = UU, UD, DD$

$$\begin{array}{ccc}
 \Pi^{\overline{UU}} & & \Pi^{\overline{UD}} \\
 \diagdown & & \diagup \\
 & \times & \\
 \diagup & & \diagdown \\
 \Pi^{UD} & & \Pi^{DD}
 \end{array}
 = -4\tilde{\lambda}
 \quad \text{(C.67)}$$

$$\begin{array}{ccc}
 \Pi^{DD} & & \Pi^{UU} \\
 \diagdown & & \diagup \\
 & \times & \\
 \diagup & & \diagdown \\
 \Pi^+ & & \Pi^-
 \end{array}
 = -4\tilde{\lambda}
 \quad \text{(C.68)}$$

$$\begin{array}{ccc}
 \Pi^{DD} & & \Pi^{UD} \\
 \diagdown & & \diagup \\
 & \times & \\
 \diagup & & \diagdown \\
 \Pi^+ & & \Pi^0
 \end{array}
 = -2\tilde{\lambda}
 \quad \text{(C.69)}$$

$$\begin{array}{ccc}
 \Pi^{UU} & & \Pi^{UD} \\
 \swarrow \text{---} & & \nwarrow \text{---} \\
 & & \text{---} \\
 \searrow \text{---} & & \swarrow \text{---} \\
 \Pi^{-} & & \Pi^0
 \end{array} = -2\tilde{\lambda} \tag{C.70}$$

$$\begin{array}{ccc}
 & & \nu_e \\
 & & \nearrow \\
 \Pi^0, \sigma \text{ ---} & & \text{---} \\
 & & \searrow \\
 & & \bar{\nu}_e
 \end{array} = \begin{cases} iY_{\text{lepton-U}} & \text{for } \Pi^0 \\ -Y_{\text{lepton-U}} & \text{for } \sigma \end{cases} \tag{C.71}$$

$$\begin{array}{ccc}
 & & e^{-} \\
 & & \nearrow \\
 \Pi^{-} \text{ ---} & & \text{---} \\
 & & \searrow \\
 & & \bar{\nu}_e
 \end{array} = i\sqrt{2}Y_{\text{lepton-U}} \tag{C.72}$$

$$\begin{array}{ccc}
 & & e^{-} \\
 & & \nearrow \\
 \Pi^0, \sigma \text{ ---} & & \text{---} \\
 & & \searrow \\
 & & e^{+}
 \end{array} = \begin{cases} -iY_{\text{lepton-D}} & \text{for } \Pi^0 \\ -Y_{\text{lepton-D}} & \text{for } \sigma \end{cases} \tag{C.73}$$

$$\begin{array}{ccc}
 & & \nu_e \\
 & & \nearrow \\
 \Pi^{+} \text{ ---} & & \text{---} \\
 & & \searrow \\
 & & e^{+}
 \end{array} = i\sqrt{2}Y_{\text{lepton-D}} \tag{C.74}$$

$$\begin{array}{ccc}
 & & u \\
 & & \nearrow \\
 \Pi^0, \sigma \text{ ---} & & \text{---} \\
 & & \searrow \\
 & & \bar{u}
 \end{array} = \begin{cases} iY_{\text{quark-U}} & \text{for } \Pi^0 \\ -Y_{\text{quark-U}} & \text{for } \sigma \end{cases} \tag{C.75}$$

Bibliography

- [1] Sven Bjarke Gudnason, Chris Kouvaris, and Francesco Sannino. Towards working technicolor: Effective theories and dark matter. *Phys. Rev.*, D73:115003, 2006, hep-ph/0603014.
- [2] Sven Bjarke Gudnason, Chris Kouvaris, and Francesco Sannino. Dark matter from new technicolor theories. 2006, hep-ph/0608055.
- [3] Precision electroweak measurements on the z resonance. *Phys. Rept.*, 427:257, 2006, hep-ex/0509008.
- [4] Francesco Sannino and Kimmo Tuominen. Techniorientifold. *Phys. Rev.*, D71:051901, 2005, hep-ph/0405209.
- [5] F. Sannino. Dynamical breaking of the electroweak theory. 2006, hep-ph/0606128.
- [6] Massimo Persic, Paolo Salucci, and Fulvio Stel. The universal rotation curve of spiral galaxies: 1. the dark matter connection. *Mon. Not. Roy. Astron. Soc.*, 281:27, 1996, astro-ph/9506004.
- [7] Douglas Scott and George Smoot. Cosmic microwave background mini-review. 2006, astro-ph/0601307.
- [8] D. N. Spergel et al. Wilkinson microwave anisotropy probe (wmap) three year results: Implications for cosmology. 2006, astro-ph/0603449.
- [9] Michael E. Peskin and D. V. Schroeder. An introduction to quantum field theory. Reading, USA: Addison-Wesley (1995) 842 p.
- [10] Laura Reina. Tasi 2004 lecture notes: Higgs boson physics. 2005, hep-ph/0512377.
- [11] Michael S. Chanowitz and Mary K. Gaillard. The tev physics of strongly interacting w 's and z 's. *Nucl. Phys.*, B261:379, 1985.
- [12] John M. Cornwall, David N. Levin, and George Tiktopoulos. Derivation of gauge invariance from high-energy unitarity bounds on the s - matrix. *Phys. Rev.*, D10:1145, 1974.
- [13] G. J. Gounaris, R. Kogerler, and H. Neufeld. On the relationship between longitudinally polarized vector bosons and their unphysical scalar partners. *Phys. Rev.*, D34:3257, 1986.

-
- [14] S. L. Glashow. Partial symmetries of weak interactions. *Nucl. Phys.*, 22:579–588, 1961.
- [15] Benjamin W. Lee, C. Quigg, and H. B. Thacker. Weak interactions at very high-energies: The role of the higgs boson mass. *Phys. Rev.*, D16:1519, 1977.
- [16] Benjamin W. Lee, C. Quigg, and H. B. Thacker. The strength of weak interactions at very high-energies and the higgs boson mass. *Phys. Rev. Lett.*, 38:883, 1977.
- [17] G. F. Giudice and A. Romanino. Split supersymmetry. *Nucl. Phys.*, B699:65–89, 2004, hep-ph/0406088.
- [18] Roger F. Dashen and Herbert Neuberger. How to get an upper bound on the higgs mass. *Phys. Rev. Lett.*, 50:1897, 1983.
- [19] Julius Kuti, Lee Lin, and Yue Shen. Upper bound on the higgs mass in the standard model. *Phys. Rev. Lett.*, 61:678, 1988.
- [20] Anna Hasenfratz, Karl Jansen, Christian B. Lang, Thomas Neuhaus, and Hiroshi Yoneyama. The triviality bound of the four component ϕ^4 model. *Phys. Lett.*, B199:531, 1987.
- [21] Dimitris Kominis and R. Sekhar Chivukula. Triviality bounds in two doublet models. *Phys. Lett.*, B304:152–158, 1993, hep-ph/9301222.
- [22] Christopher T. Hill and Elizabeth H. Simmons. Strong dynamics and electroweak symmetry breaking. *Phys. Rept.*, 381:235–402, 2003, hep-ph/0203079.
- [23] Michael S. Chanowitz. Electroweak symmetry breaking: Unitarity, dynamics, experimental prospects. *Ann. Rev. Nucl. Part. Sci.*, 38:323–420, 1988.
- [24] Edward Farhi and Leonard Susskind. Technicolor. *Phys. Rept.*, 74:277, 1981.
- [25] Romesh K. Kaul. Technicolor. *Rev. Mod. Phys.*, 55:449, 1983.
- [26] Kenneth Lane. Two lectures on technicolor. 2002, hep-ph/0202255.
- [27] R. Sekhar Chivukula. Technicolor and compositeness. 2000, hep-ph/0011264.
- [28] Steven Weinberg. Implications of dynamical symmetry breaking: An addendum. *Phys. Rev.*, D19:1277–1280, 1979.
- [29] Elliott D. Bloom and Frederick J. Gilman. Scaling and the behavior of nucleon resonances in inelastic electron - nucleon scattering. *Phys. Rev.*, D4:2901, 1971.
- [30] Estia Eichten and Kenneth D. Lane. Dynamical breaking of weak interaction symmetries. *Phys. Lett.*, B90:125–130, 1980.
- [31] Savas Dimopoulos and Leonard Susskind. Mass without scalars. *Nucl. Phys.*, B155:237–252, 1979.
- [32] E. Farhi and Leonard Susskind. A technicolored g.u.t. *Phys. Rev.*, D20:3404–3411, 1979.
- [33] Steven Weinberg. Phenomenological lagrangians. *Physica*, A96:327, 1979.

- [34] Michael E. Peskin and Tatsu Takeuchi. Estimation of oblique electroweak corrections. *Phys. Rev.*, D46:381–409, 1992.
- [35] Michael E. Peskin and Tatsu Takeuchi. A new constraint on a strongly interacting higgs sector. *Phys. Rev. Lett.*, 65:964–967, 1990.
- [36] Koichi Yamawaki, Masako Bando, and Ken-iti Matumoto. Scale invariant technicolor model and a technidilaton. *Phys. Rev. Lett.*, 56:1335, 1986.
- [37] Bob Holdom. Technicolor. *Phys. Lett.*, B150:301, 1985.
- [38] Bob Holdom. Raising the sideways scale. *Phys. Rev.*, D24:1441, 1981.
- [39] Thomas W. Appelquist, Dimitra Karabali, and L. C. R. Wijewardhana. Chiral hierarchies and the flavor changing neutral current problem in technicolor. *Phys. Rev. Lett.*, 57:957, 1986.
- [40] Heinz Pagels. Departures from chiral symmetry: A review. *Phys. Rept.*, 16:219, 1975.
- [41] Reijiro Fukuda and Taichiro Kugo. Schwinger-dyson equation for massless vector theory and absence of fermion pole. *Nucl. Phys.*, B117:250, 1976.
- [42] Andrew G. Cohen and Howard Georgi. Walking beyond the rainbow. *Nucl. Phys.*, B314:7, 1989.
- [43] Thomas Appelquist, Kenneth D. Lane, and Uma Mahanta. On the ladder approximation for spontaneous chiral symmetry breaking. *Phys. Rev. Lett.*, 61:1553, 1988.
- [44] Thomas Appelquist, Anuradha Ratnaweera, John Terning, and L. C. R. Wijewardhana. The phase structure of an $su(n)$ gauge theory with $n(f)$ flavors. *Phys. Rev.*, D58:105017, 1998, hep-ph/9806472.
- [45] R. Sekhar Chivukula, Stephen B. Selipsky, and Elizabeth H. Simmons. Nonoblique effects in the $z b$ anti- b vertex from etc dynamics. *Phys. Rev. Lett.*, 69:575–577, 1992, hep-ph/9204214.
- [46] Ernest Ma. Quarks with charm and color: A new model of their strong and weak interactions. *Phys. Lett.*, B58:442, 1975.
- [47] William J. Marciano. Exotic new quarks and dynamical symmetry breaking. *Phys. Rev.*, D21:2425, 1980.
- [48] Deog Ki Hong, Stephen D. H. Hsu, and Francesco Sannino. Composite higgs from higher representations. *Phys. Lett.*, B597:89–93, 2004, hep-ph/0406200.
- [49] Dennis D. Dietrich, Francesco Sannino, and Kimmo Tuominen. Light composite higgs from higher representations versus electroweak precision measurements: Predictions for lhc. *Phys. Rev.*, D72:055001, 2005, hep-ph/0505059.
- [50] Dennis D. Dietrich, Francesco Sannino, and Kimmo Tuominen. Light composite higgs and precision electroweak measurements on the z resonance: An update. *Phys. Rev.*, D73:037701, 2006, hep-ph/0510217.

- [51] N. Evans and F. Sannino. Minimal walking technicolour, the top mass and precision electroweak measurements. 2005, hep-ph/0512080.
- [52] A. Armoni, M. Shifman, and G. Veneziano. Exact results in non-supersymmetric large n orientifold field theories. *Nucl. Phys.*, B667:170–182, 2003, hep-th/0302163.
- [53] A. Armoni, M. Shifman, and G. Veneziano. Susy relics in one-flavor qcd from a new $1/n$ expansion. *Phys. Rev. Lett.*, 91:191601, 2003, hep-th/0307097.
- [54] Raman Sundrum and Stephen D. H. Hsu. Walking technicolor and electroweak radiative corrections. *Nucl. Phys.*, B391:127–146, 1993, hep-ph/9206225.
- [55] Thomas Appelquist and Francesco Sannino. The physical spectrum of conformal $su(n)$ gauge theories. *Phys. Rev.*, D59:067702, 1999, hep-ph/9806409.
- [56] Edward Witten. An $su(2)$ anomaly. *Phys. Lett.*, B117:324–328, 1982.
- [57] F. Sannino and M. Shifman. Effective lagrangians for orientifold theories. *Phys. Rev.*, D69:125004, 2004, hep-th/0309252.
- [58] J. Wess and J. Bagger. Supersymmetry and supergravity. Princeton, USA: Univ. Pr. (1992) 259 p.
- [59] Alfonso R. Zerwekh. Associate higgs and gauge boson production at hadron colliders in a model with vector resonances. *Eur. Phys. J.*, C46:791–795, 2006, hep-ph/0512261.
- [60] Thomas Appelquist, P. S. Rodrigues da Silva, and Francesco Sannino. Enhanced global symmetries and the chiral phase transition. *Phys. Rev.*, D60:116007, 1999, hep-ph/9906555.
- [61] Fabio Maltoni and Tim Stelzer. Madevent: Automatic event generation with madgraph. *JHEP*, 02:027, 2003, hep-ph/0208156.
- [62] T. Stelzer and W. F. Long. Automatic generation of tree level helicity amplitudes. *Comput. Phys. Commun.*, 81:357–371, 1994, hep-ph/9401258.
- [63] H. Murayama, I. Watanabe, and K. Hagiwara. Helas: Helicity amplitude subroutines for feynman diagram evaluations. KEK-91-11.
- [64] C. M. Carollo, P. T. de Zeeuw, R. P. van der Marel, I. J. Danziger, and E. E. Qian. Dark matter in elliptical galaxies. *Astrophys. J.*, 441:L25, 1995, astro-ph/9501046.
- [65] Annamaria Borriello, Paolo Salucci, and Luigi Danese. The fundamental plane of ellipticals: I. the dark matter connection. *Mon. Not. Roy. Astron. Soc.*, 341:1109, 2003, astro-ph/0208268.
- [66] J. C. Mather, D. J. Fixsen, R. A. Shafer, C. Mosier, and D. T. Wilkinson. Calibrator design for the coBE far infrared absolute spectrophotometer (firas). *Astrophys. J.*, 512:511–520, 1999, astro-ph/9810373.
- [67] Adam G. Riess et al. Observational evidence from supernovae for an accelerating universe and a cosmological constant. *Astron. J.*, 116:1009–1038, 1998, astro-ph/9805201.

- [68] Keith A. Olive. Inflation. *Phys. Rept.*, 190:307–403, 1990.
- [69] Edwin L. Turner, Jeremiah P. Ostriker, and III Gott, J. Richard. The statistics of gravitational lenses: The distributions of image angular separations and lens redshifts. *Astrophys. J.*, 284:1–22, 1984.
- [70] Simon D. M. White, C. S. Frenk, and M. Davis. Clustering in a neutrino-dominated universe. *Astrophys. J.*, 274:L1–L5, 1983.
- [71] E. W. Kolb and Michael S. Turner. The early universe. *Front. Phys.*, 69:1–547, 1990.
- [72] S. Dodelson. Modern cosmology. Amsterdam, Netherlands: Academic Pr. (2003) 440 p.
- [73] Keith A. Olive. Dark matter. 2003, astro-ph/0301505.
- [74] S. Nussinov. Technocosmology: Could a technibaryon excess provide a 'natural' missing mass candidate? *Phys. Lett.*, B165:55, 1985.
- [75] Stephen M. Barr, R. Sekhar Chivukula, and Edward Farhi. Electroweak fermion number violation and the production of stable particles in the early universe. *Phys. Lett.*, B241:387–391, 1990.
- [76] V. A. Kuzmin, V. A. Rubakov, and M. E. Shaposhnikov. On the anomalous electroweak baryon number nonconservation in the early universe. *Phys. Lett.*, B155:36, 1985.
- [77] F. R. Klinkhamer and N. S. Manton. A saddle point solution in the weinberg-salam theory. *Phys. Rev.*, D30:2212, 1984.
- [78] Jeffrey A. Harvey and Michael S. Turner. Cosmological baryon and lepton number in the presence of electroweak fermion number violation. *Phys. Rev.*, D42:3344–3349, 1990.
- [79] D. S. Akerib et al. First results from the cryogenic dark matter search in the soudan underground lab. *Phys. Rev. Lett.*, 93:211301, 2004, astro-ph/0405033.
- [80] Vuk Mandic. First results from the cryogenic dark matter search experiment at the deep site. FERMILAB-THESIS-2004-53.
- [81] Gen-sheng Wang. The cryogenic dark matter search and background rejection with event position information. FERMILAB-THESIS-2005-09.
- [82] D. S. Akerib et al. Limits on spin-independent wimp nucleon interactions from the two-tower run of the cryogenic dark matter search. *Phys. Rev. Lett.*, 96:011302, 2006, astro-ph/0509259.
- [83] J. D. Lewin and P. F. Smith. Review of mathematics, numerical factors, and corrections for dark matter experiments based on elastic nuclear recoil. *Astropart. Phys.*, 6:87–112, 1996.
- [84] Mark W. Goodman and Edward Witten. Detectability of certain dark-matter candidates. *Phys. Rev.*, D31:3059, 1985.

- [85] Hooman Davoudiasl. Cosmology with light axions from technicolor. 2006, hep-ph/0607111.
- [86] S. D. H. Hsu and F. Sannino. New solutions to the strong cp problem. *Phys. Lett.*, B605:369–375, 2005, hep-ph/0408319.
- [87] Graham G. Ross. Grand unified theories. Reading, Usa: Benjamin/cummings (1984) 497 P. (Frontiers In Physics, 60).
- [88] Paul Langacker. Grand unified theories and proton decay. *Phys. Rept.*, 72:185, 1981.
- [89] D. R. T. Jones. The two loop beta function for a $g(1) \times g(2)$ gauge theory. *Phys. Rev.*, D25:581, 1982.
- [90] Neil D. Christensen and Robert Shrock. Extended technicolor models with two etc groups. *Phys. Rev.*, D74:015004, 2006, hep-ph/0603149.
- [91] Deog Ki Hong and Ho-Ung Yee. Holographic estimate of oblique corrections for technicolor. 2006, hep-ph/0602177.
- [92] Johannes Hirn and Veronica Sanz. A negative s parameter from holographic technicolor. 2006, hep-ph/0606086.
- [93] Kenneth Lane. Search for low-scale technicolor at the tevatron. 2006, hep-ph/0605119.
- [94] L. Feligioni. Searches for technicolor particles at d0. *Int. J. Mod. Phys.*, A20:3302–3304, 2005.
- [95] Gang Lv, Jinshu Huang, and Gongru Lu. Corrections to the process $e^+ e^- \rightarrow \bar{c} b$ anti-b in the topcolor assisted technicolor model. *Phys. Rev.*, D73:015008, 2006.
- [96] Xuelei Wang, Qingpeng Qiao, and Qiaoli Zhang. $H(tc)$ π^0 and $\pi^+ \pi^-$ pair production at the planned $e^+ e^-$ colliders in the topcolor-assisted technicolor model. *Phys. Rev.*, D71:095012, 2005.
- [97] Stephen P. Martin. A supersymmetry primer. 1997, hep-ph/9709356.
- [98] Ian J. R. Aitchison. Supersymmetry and the mssm: An elementary introduction. 2005, hep-ph/0505105.
- [99] Jose Miguel Figueroa-O’Farrill. Busstepp lectures on supersymmetry. 2001, hep-th/0109172.
- [100] Martin Schmaltz and David Tucker-Smith. Little higgs review. *Ann. Rev. Nucl. Part. Sci.*, 55:229–270, 2005, hep-ph/0502182.
- [101] David B. Kaplan and Howard Georgi. $Su(2) \times u(1)$ breaking by vacuum misalignment. *Phys. Lett.*, B136:183, 1984.